

Secondary metabolites in the interaction of *Aspergillus fumigatus* and *Pseudomonas aeruginosa* in cystic fibrosis sputum

Dissertation

To fulfil the requirements for the degree of
“doctor rerum naturalium” (Dr. rer. nat.)

Submitted to the Council of the Faculty of Biological Sciences of the Friedrich Schiller
University in Jena

by Michal Flak, BSc. (Hons), MSc.
born on the 11th May 1991 in Martin, Slovakia

Jena, June 2020

Diese Arbeit wurde am Leibniz-Institut für Naturstoff-Forschung und Infektionsbiologie e.V., Hans-Knöll-Institut Jena, in der Abteilung Molekulare und Angewandte Mikrobiologie – Lehrstuhl für Mikrobiologie und Molekulare Biologie, Friedrich-Schiller-Universität Jena, unter Leitung von Prof. Dr. Axel A. Brakhage angefertigt.

Gutachter 1: Prof. Dr. Axel A. Brakhage, Friedrich-Schiller-Universität Jena

Gutachter 2: Prof. Dr. Erika Kothe, Friedrich-Schiller-Universität Jena

Gutachter 3: Prof. Dr. Bodo Philipp, Universität Münster

Datum der öffentlichen Verteidigung: 22. Oktober 2020

Table of contents

Table of contents	II
Summary	VI
Zusammenfassung	VIII
A Introduction	1
1 Ecology of cystic fibrosis lung	1
2 Aspergillus fumigatus	3
2.1 A. fumigatus infection in cystic fibrosis	3
2.1.1 Secondary metabolism of A. fumigatus	4
2.1.2 Secondary metabolism and environmental iron acquisition by A. fumigatus	6
2.2.2 Isonitrile-containing secondary metabolites from A. fumigatus and other fungi	6
3 Pseudomonas aeruginosa	7
3.1 Secondary metabolism in P. aeruginosa	8
3.1.1 P. aeruginosa secondary metabolism and iron acquisition	8
3.1.2 Cyanide production in P. aeruginosa	10
4 Aspergillus - Pseudomonas interaction	12
5 Aim of this study: Studying interactions relevant to cystic fibrosis	15
B Materials and Methods	16
1 Strains and Materials	16
1.1 Bacterial strains	16
1.2 Fungal strains	16
1.3 Plasmids	17
1.4 Oligonucleotides	17
1.4.1 PCR primers	17
1.4.2 qRT-PCR primers	18
1.5 Standard media and supplements	19
2 Cultivation methods	22
2.1 Axenic culture conditions	22
2.1.1 Cultivation of Escherichia coli	22
2.1.2 Cultivation of Pseudomonas aeruginosa	22
2.1.3 Cultivation of Aspergillus fumigatus	23
2.2 Co-cultivation conditions	23

2.3 Cell count determination	23
2.4 Biomass measurement	23
3 Molecular biology methods	24
3.1 Nucleic acid isolation	24
3.1.1 Isolation of genomic DNA	24
3.1.2 Isolation of RNA from <i>A. fumigatus</i>	24
3.1.3 Isolation of plasmids from <i>E. coli</i>	25
3.1.4 Isolation of DNA fragments from agarose gel	25
3.2 Manipulation of nucleic acids	25
3.2.1 DNA restriction digestion	25
3.2.2 Cloning and DNA assembly	25
3.2.3 Polymerase chain reaction (PCR)	26
3.2.4 Agarose gel electrophoresis	26
3.2.5 First-strand complementary DNA (cDNA) synthesis	26
3.2.6 qRT-PCR analysis	26
3.3 Transfer of nucleic acids on membranes	27
3.3.1 Southern blot analysis	27
3.3.2 Southern blot probe generation	28
3.4 Transformation of cells with nucleic acids	28
3.4.1 Transformation of <i>E. coli</i>	28
3.4.2 Transformation of <i>P. aeruginosa</i>	28
3.4.3 Transformation of <i>A. fumigatus</i>	29
4 Biochemical and analytical methods	29
4.1 Protein isolation from co-cultivation supernatant	29
4.2 Measurement of cyanide concentrations in cultures	30
4.3 Extraction of secondary metabolites	30
4.3.1 Extraction and purification of triacetylfusarinine C	31
4.4 LC-MS analysis of extracted microbial secondary metabolites	31
4.4.1 HPLC-HRESI-MS analysis	32
4.5 MALDI-TOF-IMS analysis	32
4.6 Radioactive labelling and siderophore internalisation measurement	32
5 Microscopy	33
C Results	34

1 Establishment of a cystic fibrosis sputum-mimicking in vitro model of co-cultivation	34
1.1 Microbiological analysis of <i>A. fumigatus</i> under cystic fibrosis sputum-mimicking conditions	34
1.1.1 SCFM2 is suitable for cultivation of <i>A. fumigatus</i> and <i>P. aeruginosa</i> monocultures	34
1.1.2 SCFM2 supports a balanced growth of <i>A. fumigatus</i> and <i>P. aeruginosa</i> in co-cultivation	36
1.2 The adherence of <i>P. aeruginosa</i> onto <i>A. fumigatus</i> is passive and does not support further colonisation	38
1.3 Hypoxic conditions favour <i>P. aeruginosa</i> growth in static culture	38
2 Transcriptome analysis of <i>A. fumigatus</i> and <i>P. aeruginosa</i> interaction	39
3 Secondary metabolism of <i>A. fumigatus</i> confronted with <i>P. aeruginosa</i>	44
3.1 <i>A. fumigatus</i> CF10 produces a xanthocillin derivative in co-culture with <i>P. aeruginosa</i>	47
3.1.1 BU-4704 and BU-4704B are produced by an uncharacterised gene cluster of <i>A. fumigatus</i>	49
3.2 <i>A. fumigatus</i> CF10 harbours a non-functional PKS cluster	54
3.3 MALDI-IMS analysis	54
4 Fungal and bacterial siderophores in the interaction	58
4.1 <i>A. fumigatus</i> does not disrupt quorum sensing of <i>P. aeruginosa</i>	58
4.2 <i>P. aeruginosa</i> is likely capable of using TAFC as a xenosiderophore	59
4.2.1 Radioactive labelling of TAFC indicates internalisation of the siderophore by <i>P. aeruginosa</i>	60
5 LC-MS-based secretome analysis of <i>A. fumigatus</i> and <i>P. aeruginosa</i> co-culture	62
5.1 <i>A. fumigatus</i> produces a putative cyanide hydratase in co-cultivation with <i>P. aeruginosa</i>	67
5.1.1 The expression of <i>chtA</i> is contingent on the presence of cyanide	69
5.1.2 <i>AfCHT</i> is essential for growth in presence of cyanide and rapidly detoxifies exogenous KCN	69
5.1.3 Cyanide detoxication during co-cultivation with <i>P. aeruginosa</i>	71
6 Mutual detoxication of <i>A. fumigatus</i> and <i>P. aeruginosa</i>	73
C Discussion	75
1 Studying the ecology of microbial interactions relevant to human infections	75
1.1 The effects of growth media and mimicking host environment	76
2 Fungal cell wall remodelling in response to co-cultivation with <i>P. aeruginosa</i>	78

3 Secondary metabolism in the interaction of <i>A. fumigatus</i> and <i>P. aeruginosa</i>	79
3.1 Secondary metabolites of <i>P. aeruginosa</i>	79
3.2 Secondary metabolites of <i>A. fumigatus</i>	81
3.2.1 Interaction of <i>A. fumigatus</i> with <i>P. aeruginosa</i> induces the production of isonitrilated compounds in the fungus	82
4 Siderophore piracy of <i>P. aeruginosa</i> extends to fungal siderophores	83
5 Bacterial cyanogenesis and fungal cyanide degradation	84
6 Mutual detoxication - achieving balance between <i>A. fumigatus</i> and <i>P. aeruginosa</i>	85
References	88
List of Tables	110
List of figures	111
Abbreviations	113
Curriculum vitae	115
Scientific publications	116
Acknowledgements	117
Ehrenwörtliche Erklärung	118

Summary

Aspergillus fumigatus and *Pseudomonas aeruginosa* are the most persistent fungal and bacterial pathogens, respectively, commonly co-isolated from the expectorated sputum of cystic fibrosis (CF) patients. Co-colonisation by both microbes has been associated with a worse clinical outcome and a poorer prognosis for CF patients. The recent years have seen multiple attempts at characterising the interactions between the bacterial species and the fungus. While several mechanisms of mutual inhibition have been proposed in published literature, the interaction models have been based on conventional cultivation strategies, and have thus fallen short of appropriately acknowledging the particular nutritional environment, in which the interaction takes place.

In the present study, I have developed a model of the interaction that imitates the native conditions of a cystic fibrosis lung more closely. Using the defined complex synthetic cystic fibrosis sputum medium (SCFM2), I have established cultivation conditions that mimic to a certain extent the growth conditions inside the lung, and, at the same time, do not provide a selective advantage to one of the microorganisms over the other. On SCFM2 agar plates, radial growth of *A. fumigatus* and *P. aeruginosa* colonies were comparable, and any initial inhibition in the confrontation zone was quickly overcome by the advancing biomass, resulting in combined growth. Although SCFM2 does not support sporulation and biomass formation of *A. fumigatus* to the same extent as *Aspergillus* minimal medium, the synthetic sputum was deemed to be a suitable approximation of human CF sputum. During co-cultivation in SCFM2, *P. aeruginosa* attached to *A. fumigatus* passively, as observed previously in AMM, and remained immobile, showing no trophic tendencies.

A transcriptome analysis of *A. fumigatus* confronted with *P. aeruginosa* for 24 hours revealed an upregulation of transmembrane transport, as well as iron acquisition and metabolism genes, hinting at environmental iron deficiency. Conversely, multiple biosynthetic gene clusters were downregulated, suggesting an attenuation of secondary metabolism in the fungus. These included mycotoxins such as gliotoxin, fumagillin, pseurotins, helvolic acid, or fumitremorgins. The finding was further supported by an HPLC-MS analysis, which showed a decrease in abundance or complete absence of these compounds in co-culture, as opposed to axenic fungal culture. The apparent dysregulation of secondary metabolism in *P. aeruginosa* co-culture was surprising, given that multiple mycotoxins produced by *A. fumigatus* exhibit antibacterial properties.

Furthermore, the differential regulation of numerous genes involved in polysaccharide metabolism suggested that the interaction with *P. aeruginosa* incites a cell wall restructuring in the fungus.

The interaction of microbes has previously been reported as an elicitor of secondary metabolite production. The CF isolate *A. fumigatus* CF10 produced two isonitrilated dityrosine peptides, BU-4704 and BU-4704B, in interaction with *P. aeruginosa*. Due to the structural similarity of BU-4704 to a precursor of paerucumarin, a pseudomonadal metabolite, whose biosynthesis has been elucidated, the biosynthetic gene cluster producing the peptides was identified. The backbone enzyme of the cluster is a non-ribosomal peptide synthetase (NRPS), containing an isonitrile synthase domain (NRPS-ICS), responsible for the conversion of tyrosine amino groups into nitrile moieties. A deletion mutant lacking the NRPS-ICS gene did not produce BU-4704 and its congener, but did not show altered fitness in co-culture with *P. aeruginosa*. This finding

strongly suggests that while the production of the compounds is elicited by the presence of the bacterium, the metabolites themselves do not play an inhibitory role, conferring a selective advantage upon *A. fumigatus*. The co-cultivation also leads to a transcriptional activation of a heretofore uncharacterised polyketide synthase (PKS) biosynthetic gene cluster. However, no compound produced by the fungus in co-culture could be attributed to the cluster, nor did the secondary metabolic profile of the culture extract change when the PKS gene was deleted. I therefore concluded that the cluster is either dysfunctional, or the tested conditions were insufficient to elicit the biosynthesis of the cluster product.

Matrix-assisted laser desorption ionisation imaging mass spectrometry (MALDI-IMS) of the microorganisms in co-cultivation revealed that the bacterium deploys a different set of rhamnolipid biosurfactants when exposed to *A. fumigatus* than in monoculture. A decrease in the abundance of pyoverdine, the high-affinity siderophore of *P. aeruginosa*, in co-cultivation with the fungus provided a strong hint that *P. aeruginosa* can pirate the fungal siderophore triacetylfusarinine C (TAFC) and use it as a sole source of iron. The hypothesis was further tested by radioactive labelling of the TAFC molecule with ⁶⁸Ga; the results strongly indicated that the labelled siderophore was internalised by the bacterium, and further testing is warranted to unequivocally confirm the proposed process.

An analysis of the total secreted proteins present in the culture supernatant of *A. fumigatus* and *P. aeruginosa* co-cultivation revealed the presence of a fungal cyanide hydratase, an enzyme which detoxifies cyanide into formamide. The expression of the encoding *chtA* gene was activated specifically by the presence of cyanide, rather than the bacterium. The protein product was essential for growth of the fungus in presence of cyanide. Under a narrow set of conditions, *P. aeruginosa* is known to be cyanogenic. I hypothesise that these conditions were present during the cultivation before the secretome analysis; however, the conditions could not be replicated to a satisfactory extent and the levels of cyanide in *P. aeruginosa* monocultures and cultures grown in SCFM2 could not be measured. Therefore, implicit evidence is given that when pseudomonadal cyanogenesis occurs in CF lung in presence of *A. fumigatus*, the fungus is capable of degrading the toxin.

Finally, antiproliferative activity testing of the extracts of respective axenic cultures and co-cultures of both organisms grown in synthetic sputum showed that, counter-intuitively, fungal monoculture extracts inhibit the proliferation of pulmonary epithelia more than the extracts of the co-cultures or *P. aeruginosa* alone. Summarily, the results presented here indicate that rather than engaging in extreme antagonistic behaviour, *A. fumigatus* and *P. aeruginosa* co-occurring in the human CF lung achieve a delicate balance, detoxifying each other's secreted secondary metabolic potential.

Zusammenfassung

Aspergillus fumigatus und *Pseudomonas aeruginosa* sind die häufigsten Pilz- bzw. bakteriellen Erreger, die gemeinsam aus ausgehustetem Sputum von Mukoviszidose (cystische Fibrose, CF) -Patienten isoliert werden. Die gemeinsame Besiedelung durch beide Mikroorganismen wird mit einem erschwerten klinischen Verlauf und einer schlechteren Prognose für CF-Patienten in Verbindung gebracht. In den letzten Jahren wurden viele Versuche unternommen, die Interaktionen zwischen Bakterium und Pilz zu charakterisieren. Mehrere Mechanismen der gegenseitigen Hemmung wurden veröffentlicht, aber die Versuchsmodelle basierten stets auf konventionellen Kultivierungsstrategien und die besonderen Umweltbedingungen, in denen die Interaktionen stattfinden, wurden daher wenig berücksichtigt.

In dieser Studie habe ich ein Interaktionsmodell entwickelt, das den Nährstoff-Bedingungen einer Lunge von Mukoviszidose-Patienten stärker ähnelt. Durch die Verwendung eines definierten komplexen synthetischen Cystische Fibrose Sputum-Mediums (SCFM2) habe ich Kultivierungsbedingungen geschaffen, welche die Wachstumsbedingungen in der Lunge realistisch repräsentieren und gleichzeitig keines der beiden Mikroorganismen selektiv bevorzugt. Auf SCFM2-Agarplatten war das radiale Wachstum von *A. fumigatus* und *P. aeruginosa* vergleichbar und anfängliche Wachstumshemmungen in der Übergangszone waren schnell durch die sich ausbreitende Biomasse überwachsen und führten zu gemeinschaftlichem Wachstum. Obwohl SCFM2 weder die Sporulierung noch die Biomassebildung von *A. fumigatus* im gleichen Ausmaß förderte wie *Aspergillus* Minimal Medium, kann das synthetische SCFM2-Sputum als das geeignetere Medium betrachtet werden, um die Bedingungen des humanen CF-Sputum zu simulieren. Während der Ko-Kultivierung in SCFM2, war *P. aeruginosa* - wie schon früher gezeigt - passiv an *A. fumigatus* gebunden und blieb unbeweglich.

Eine Transkriptomanalyse von *A. fumigatus* nach 24-stündiger Ko-Kultur mit *P. aeruginosa*, zeigte eine Hochregulierung von Genen, die sowohl für den Transmembrantransport als auch für Eisenaufnahme und Stoffwechsel verantwortlich sind. Dieser Befund deutet auf einen Eisenmangel während der Ko-Kultivierung. Umgekehrt waren mehrere Gencluster für Sekundärmetabolite herabreguliert, was auf eine Herabsetzung des sekundären Metabolismus im Pilz hinweist. Darunter waren Mykotoxine wie Gliotoxin, Fumagillin, Pseurotin, Helvolinsäure und Fumitremorgine. Das Ergebnis wurde zusätzlich durch eine HPLC-MS-Analyse gestützt, die im Gegensatz zur Monokultur eine Reduktion oder völlige Abwesenheit dieser Komponenten in Ko-Kulturen nachwies. Die offensichtlich veränderte Regulation des Sekundärmetabolismus in der *P. aeruginosa* Ko-Kultur war überraschend, da mehrere Mykotoxine, die von *A. fumigatus* produziert werden, antibakterielle Eigenschaften besitzen. Zusätzlich weist eine veränderte Regulation zahlreicher Gene, die in den Polysaccharid Stoffwechsel involviert sind, darauf hin, dass die Interaktion mit *P. aeruginosa* eine Zellwandumstrukturierung im Pilz auslöst.

Frühere Arbeiten zeigten, dass die Interaktion von Mikroorganismen die Produktion von Sekundärmetaboliten anregen kann. Das klinische CF-Isolat *A. fumigatus* CF10 produzierte während der Interaktion mit *P. aeruginosa* zwei isonitrilierte Dityrosin-Peptide, BU-4704 und BU-4704B. Aufgrund der strukturellen Ähnlichkeit von BU-4704 mit einem Vorprodukt von Paerucumarin, einem Metaboliten von *Pseudomonas*, dessen Biosynthese aufgeklärt ist, wurde das Biosynthese-Gencluster für die Peptide identifiziert. Das Hauptenzym des Genclusters ist eine nicht-ribosomale Peptidsynthetase (NRPS), die eine Isonitrilsynthase-Domäne (NRPS-ICS) enthält, welche für die Umwandlung von Tyrosinaminogruppen in Nitrileinheiten zuständig ist.

Eine Deletionsmutante, deren NRPS-ICS Gen fehlt, produzierte zwar kein BU-4704 und Derivate, wies jedoch trotzdem keine veränderte Fitness in Ko-Kultur mit *P. aeruginosa* auf. Diese Beobachtung weist darauf hin, dass die Metabolite selbst keine hemmende Rolle spielen und somit *A. fumigatus* keinen Selektionsvorteil bieten, auch wenn die Produktion der Stoffe in Anwesenheit der Bakterien induziert wird. Die Ko-Kultivierung führte außerdem zur transkriptionellen Aktivierung eines bisher uncharakterisierten Polyketid-Synthase (PKS) Biosynthese-Genclusters. Jedoch konnte keine Verbindung, die vom Pilz in Ko-Kultur produziert wurde, dem Gencluster zugeordnet werden und das Profil der Sekundärmetabolite war in Kulturextrakten von Pilzen mit deletiertem PKS-Gen unverändert. Diese Ergebnisse erlauben die Schlussfolgerung, dass das Gencluster entweder nicht funktionell war oder die verwendeten Versuchsbedingungen nicht die Biosynthese induzierten.

Analysen mit MALDI-IMS (Matrix-assisted laser desorption ionisation imaging mass spectrometry) mit Mikroorganismen in Ko-Kultur zeigten, dass das Bakterium in Ko-Kultur mit *A. fumigatus* andere Rhamnolipid-Biotenside ausschüttet als in Monokultur. Eine Reduktion der Menge an Pyoverdine, dem hochaffinen Siderophor von *P. aeruginosa*, in Ko-Kultur mit dem Pilz führte zu der Annahme, dass *P. aeruginosa* das Pilzsiderophor Triacetyl-Fusarinin C (TAFC) als alleinige Eisenquelle verwenden kann. Die Hypothese wurde durch radioaktive Markierung des TAFC-Moleküls mit ⁶⁸Ga überprüft; die Ergebnisse ergaben einen starken Hinweis darauf, dass das markierte Siderophor vom Bakterium aufgenommen wurde. Allerdings sind weitere Tests nötig, um diese starken Indizien zu bestätigen.

Die Analyse aller sekretierten Proteine in Überständen von Mischkulturen von *A. fumigatus* und *P. aeruginosa* führte zur Identifikation einer pilzlichen Cyanid-Hydratase. Dieses Enzym wandelt giftiges Cyanid in harmloses Formamid um. Die Expression des kodierenden *chtA*-Gens wurde in Anwesenheit von Cyanid aktiviert, nicht jedoch in Anwesenheit des Bakteriums. Bei Anwesenheit von Cyanid war das Protein für das Pilzwachstum essentiell. Publierte Ergebnisse implizieren, dass *P. aeruginosa* unter speziellen Bedingungen cyanogen sein kann. Ich vermute deshalb, dass diese Bedingungen bei den Kulturen für die Sekretomanalyse geherrscht haben, jedoch nicht beim Versuch der Reproduktion, da Cyanid in *P. aeruginosa*-Monokulturen und in Kulturen in SCFM2-Medium mit meinen Methoden nicht nachweisbar war. Da der Pilz Cyanid abzubauen vermag, ist anzunehmen, dass *P. aeruginosa* Cyanid in CF-Lungen in Anwesenheit von *A. fumigatus* produziert und dieses durch *A. fumigatus* detoxifiziert wird.

Letztlich zeigten Experimente mit Reinkulturen und Ko-Kulturen beider Organismen in synthetischem Sputum, dass Extrakte aus Pilzmonokulturen das Wachstum von Lungenepithelzellen stärker inhibierten als Extrakte von Ko-kulturen oder von *P. aeruginosa* Reinkulturen. Zusammengefasst implizieren meine Ergebnisse, dass *A. fumigatus* und *P. aeruginosa* in humanen CF Lungen nicht als kompetitive Antagonisten agieren sondern sich eher in einem Gleichgewicht halten, indem sie sich gegenseitig detoxifizieren.

A Introduction

1 Ecology of cystic fibrosis lung

Cystic fibrosis is a congenital, autosomal recessive defect, and a most commonly inherited genetic disorder in Caucasian populations, with an incidence of *ca* 1 in 2,400 births (O'Sullivan and Freedman, 2009). The disease is caused by a mutation in the cystic fibrosis transmembrane conductance receptor (CFTR) gene, encoding an ATP-driven chloride channel embedded in the cytoplasmic membrane (Vankeerberghen et al., 2002; Mehta, 2005). Cystic fibrosis primarily affects lungs, but is also associated with gastrointestinal, endocrine, exocrine, and reproductive issues. Approximately 70% of the cases of CF are caused by a single mutation, F508 Δ , although other substitution mutations have been recorded (de Araújo et al., 2005; Dabović et al., 1992). The mutation results in a misfolded transmembrane protein, incapable of ion transport. This dysregulation leads to defects in cation (Na⁺) and anion (Cl⁻, OSCN⁻) fluxes, resulting in disrupted intracellular Ca²⁺ homeostasis and production of thickened mucus by mucosal epithelia. The high viscosity of the mucus impairs its mucociliary clearance, resulting in build-up and clogging of small airways in the lungs (Verkman et al., 2003). The accumulation of sputum, in turn, provides an ideal environment for proliferation of aspirated pathogenic microbes, both bacterial and fungal, which cannot be readily cleared by the immune system, leading to cycles of infection and excessive inflammation, ultimately resulting in progressive lung damage and decline in function (Cohen and Prince, 2012; Stick, 2014). Current therapy for the condition relies primarily on infection and inflammation management by antibiotics, NSAIDs, and steroids (Flume et al., 2007; Rafeeq and Murad, 2017), with additional physiotherapy and diet adjustments to alleviate the syndromes. Aside from the symptomatic treatments, protein rectifiers designed to overcome the CFTR-associated deletion abnormalities appear to be promising as future therapeutic approaches (Stockman, 2013; Taylor-Cousar et al., 2016). With advanced therapeutic strategies available to patients, CF no longer equates to a death sentence within the first two decades of life; CF-afflicted people born nowadays are prospected to live up to the age of 50 (Keogh et al., 2018).

The nutrient-rich sputum produced by CF-impaired lungs is an almost indiscriminately optimal source for inhaled human pathogenic microbes. The progression of CF is therefore associated with the establishment of a polymicrobial colonisation of the lung (Valenza et al., 2008). The community of microbes in a CF lung is not at stasis; rather, it is a dynamic and interactive ecological system, heavily dependent on the health state of the host and their immune response, potential treatment measures, and communication of the colonising organisms with the host, as well as between each other (Harrison, 2007; Conrad et al., 2013). Within this system, complex levels of synergies, antagonisms, and interdependencies exist, which might complicate therapeutic efforts (Peters et al., 2012); novel approaches have been put forward,

proposed to target an entire microbiome collectively, rather than in individual components (Quinn et al., 2016). This notion is particularly valid in light of the fact that the chronic colonisation of lower respiratory tract in CF patients, and associated exacerbations, are the leading cause of morbidity and mortality in the population (Surette, 2014).

Traditionally, only a limited group of microbes were recognised as typical CF lung colonisers, with *Haemophilus influenzae* being one of the earliest, followed by *Staphylococcus aureus* and *Burkholderia cenocepacia* complex. *Pseudomonas aeruginosa* is a late coloniser, but quickly becomes the prevalent pathogen within the lung population, as well as among CF patients, affecting up to 75% of adults with the condition (LiPuma, 2010). Early antibiotic treatment was capable of suppressing the conventional pathogens, leading to the emergence of newer airway pathogens, such as MRSA, *Stenotrophomonas maltophilia*, *Mycobacterium abscessus*, or *Achromobacter xyloxidans* (Sibley et al., 2008; Dasenbrook, 2011; Hill et al., 2012). More recently, our understanding of the complexity of the microbial community in CF lung improved by the discovery of obligate anaerobic Gram-negatives (*Prevotella*, *Fusobacterium*), and Gram-positives (*Rothia*, *Gemella*, *Veilonella*, *Lactobacillus*) (Quinn et al., 2016). The analysis of Quinn et al., (2016) revealed that, ultimately, three interaction groups are established: Gram-positive anaerobes, *P. aeruginosa*, and *S. aureus*, with the latter correlating negatively with the former, suggesting antagonistic relationships. Research further suggests that, following the Climax and Attack Model (CAM), the community reaches a stable, largely antibiotic-resistant equilibrium during baseline infection stage, but the stable microbiome fragments during pulmonary exacerbation episodes (Fodor et al., 2012; Carmody et al., 2015).

While a lot of the research has been carried out with bacteria in focus, fungi have also proved to be dangerous, late-colonising emerging pathogens in CF (Blanchard and Waters, 2019). *Aspergillus fumigatus*, *Candida albicans*, *Exophiala dermatitidis*, *Scedosporium apiospermum*, *Malassezia* sp., and *Fusarium* sp. are the most commonly occurring fungal species isolated from expectorated CF sputum or BAL fluid, with *A. fumigatus* and *Malassezia* sp.'s presence correlating with exacerbation periods (Pihet et al., 2009; Soret et al., 2020). It has been established that a combined bacterial-fungal colonisation is associated with a worsened clinical progression of the disease with a poorer outcome (Amin et al., 2010; Chotirmall et al., 2010; Reece et al., 2017). At a mechanistic level, scattered data, pertaining mostly to the interaction of *C. albicans* and *A. fumigatus* with *P. aeruginosa* and *S. aureus*, have been presented over the last two decades, with almost every study claiming to have found an inhibitory mechanism (Nogueira et al., 2019). Nevertheless, complex polymicrobial communities still exist mostly at stable equilibria, pointing rather to a model where the microbial interaction and communication is more intricate than simple inhibition, and where the stability must be reached by chemical signalling in the environment. This context may provide a new viewpoint of microbial interactions and their studying.

2 *Aspergillus fumigatus*

The filamentous fungus *Aspergillus fumigatus* is a ubiquitous saprophytic ascomycete, naturally occurring in soil and compost, where it feeds on decaying organic debris. As a prolific saprophyte capable of growing on a vast variety of substrates, it plays an important part in the biosphere's role in carbon and nitrogen cycling (Rhodes, 2006). It has a robust metabolism and is capable of withstanding harsh conditions, including elevated temperatures up to 50°C (Brakhage and Langfelder, 2002). *A. fumigatus* propagates asexually by production and release of large numbers of spores into the surrounding atmosphere. These mitospores, conidia, range between 2 - 3 µm in size, aiding the organism's dispersal into a wide variety of niches. Due to their size, hydrophobicity, and ubiquity in the air, they are easily inhaled by higher animals, including humans, and penetrate deep into the respiratory system, reaching alveoli. Once within a healthy lung, a conidium is rapidly phagocytosed by alveolar macrophages and neutrophilic granulocytes, and in general poses no threat; in immunocompromised individuals, or individuals with an underlying pulmonary condition, the conidium germinates to form a hyphal network capable of penetrating adjacent host tissues, and eliciting a strong immune response in the host (Latgé, 2009; Brakhage et al., 2010). As such, *A. fumigatus* has become the most widespread and lethal airborne fungal pathogen (Brakhage, 2005; Latgé and Chamilos, 2019).

Based on the extent and invasiveness of the colonisation, and depending on the host's immune state, aspergillosis can be classified into several categories: non-invasive allergic and chronic conditions, aspergilloma, and invasive aspergillosis. The latter is a devastating , life threatening infection occurring in heavily immunocompromised patients undergoing organ or haematopoietic stem-cell transplants, suffering from haematological malignancies, chronic agranulomatous disease or HIV infection (Segal, 2009). The tissue-invasive growth of the fungus and the inability of the remaining immune system to efficiently clear the infection, combined with a lack of effective therapy, cause damage that may lead to death. Annually, ~250,000 cases of invasive aspergillosis occur on a global scale, with a mortality rate of 50 - 90%, depending on the time of diagnosis and treatment (Brown et al., 2012; Bongomin et al., 2017). Aspergilloma, a form of chronic non-invasive aspergillosis, develops as a discreet, non-invasive mass of fungal material, filling in cavities in the lungs of tuberculosis or emphysema patients (Riscili and Wood, 2009).

2.1 *A. fumigatus* infection in cystic fibrosis

In cystic fibrosis-affected lungs, microbes, including *A. fumigatus*, find almost ideal conditions for growth. The growth of the fungus on CF sputum remains non-invasive, and, as such, has not been studied to the same extent as invasive aspergillosis. Still, despite various forms of clinical manifestation, *A. fumigatus* remains the single most frequently isolated fungal pathogen in bronchoalveolar lavage fluid recovered from CF

patients (Pihet et al., 2009; Liu et al., 2013). The reported prevalence varies from 1% to 58%, presumably due to individual study sample, environmental exposure, and diagnostic capabilities, and is likely to be underdiagnosed (Armstead et al., 2014; Maturu and Agarwal, 2015). Within the context of the CF lung, the fungus can assume multiple phenotypes, resulting in a range of clinical diagnoses. *Aspergillus* colonisation is an infection with a largely symptomatic development, without obvious decline in respiratory function (Chotirmall and McElvaney, 2014). Such colonisation may, however, contribute to pulmonary inflammation and function decline in the long term (King et al., 2016). Allergic bronchopulmonary aspergillosis (ABPA) is the most well-characterised fungal condition associated with CF (Knutsen and Slavin, 2016). ABPA is mediated by Th2 hypersensitive response, seen also in asthma patients, and demonstrates as a cylindrical bronchiectasis of the central airways, which may or may not be occluded by infected mucus impaction, leading to reduced pulmonary function (Stevens et al., 2003). Distinct from ABPA is *Aspergillus* bronchitis, a recent entity described as a condition involving clinical respiratory exacerbation responsive to antifungal treatment that does not fulfil the ABPA diagnostic criteria (Shoseyov et al., 2006; Jung et al., 2017). Due to a lack of clear patient age-phenotypic demonstration of the infection, the various conditions can be perceived as a continuum of conditions, each of which can progress individually to cause lung damage (King et al., 2016). Fungal colonisation by *A. fumigatus* in CF, usually concomitant with other bacterial infections, is associated with poorer clinical outcome to the patient (Reece et al., 2017).

2.1.1 Secondary metabolism of *A. fumigatus*

Similarly to other filamentous fungi, the genome of *A. fumigatus* harbours multitude of biosynthetic genes arranged in clusters, encoding for biosynthetic enzymes producing secondary metabolites (Brakhage, 2013). Depending on the individual strain, approximately 30 - 40 biosynthetic gene clusters (BGCs) are present in *A. fumigatus* (Inglis et al., 2013; Bignell et al., 2016; Lind et al., 2018). Each cluster contains a backbone enzyme, responsible for synthesising the molecular scaffold of the secondary metabolite, and can contain a transcriptional regulatory element, a transporter, and/or a number tailoring enzymes, which chemically modify the scaffold into a single or multiple final products. Based on the type of substrate the backbone enzyme can use, and the type of reaction it catalyses, multiple categories of biosynthetic enzymes are recognised: polyketide synthases (PKSs), non-ribosomal peptide synthetases (NRPSs), and dimethylallyl tryptophan synthases (DMATs) (Brakhage, 2013).

Due to the high energy and resource requirement of secondary metabolism, the process is tightly regulated and the production of many secondary metabolites is activated upon an environmental cue or simultaneously with a particular stage of development (Brakhage, 2013; Keller, 2018). The environmental cues can have both biotic and abiotic origins, *i.e.* the secondary metabolite produced in any given situation may represent a communication signal, or an attempt of the organism to secure a

resource, underlining the physiological and ecological role of these compounds (Flak et al., 2020; Stroe et al., 2020). For example, extracellular siderophores are synthesised in response to iron starvation (discussed in detail below). Fumicyclins were discovered as pigments responsible for the yellow colouration of co-culture supernatant of *A. fumigatus* and *Streptomyces rapamycinicus* (König et al., 2013), while luteoride D and terezine D were discovered in co-culture of a different strain of *A. fumigatus* with the desert-derived *Streptomyces leeuwenhoekii* (Wakefield et al., 2017).

Due to the physiological and environmental conditioning of their production, some of the secondary metabolites of *A. fumigatus* serve as virulence determinants, aiding in the opportunistic establishment of infection process. The conidial pigment, 1,8-dihydroxynaphthalene (DHN) melanin, serves as protection from immune recognition; the deletion of the polyketide synthase producing the DHN monomer strips the fungus of a protective sheath and renders it avirulent (Langfelder et al., 1998; Heinekamp et al., 2013). Similarly, gliotoxin, an epipolythiopiperazine alkaloid produced by GliP, an NRPS, is a potent mycotoxin with pleiotropic effects. The intramolecular transannular sulphur bridge contributes to the toxicity of the compound *via* redox cycling (Scharf et al., 2012). Gliotoxin *in vivo* was shown to have antiinflammatory and immunosuppressive properties, inhibiting phagocytic activity and immunogenic ROS release, delaying apoptosis, or blocking angiogenesis, thus further delaying immune response to the infection (Scharf et al., 2012; Dolan et al., 2015). The mycotoxin is also capable of inhibiting the growth of other fungi, including *C. albicans*, *Cryptococcus neoformans*, *Fusarium graminearum*, or *Neurospora crassa* (Coleman et al., 2011; Carberry et al., 2012). Other immunosuppressive mycotoxins produced by *A. fumigatus* during infection include helvolic acid, fumitremorgins, tryptoquivaline, or fumagillin (Abad et al., 2010). Notably, fumagillin is a meroterpenoid product of a secondary metabolic supercluster located on chromosome 8, which also produces a class of hybrid polyketides/non-ribosomal peptides, pseurotins, under hypoxic conditions (Vödisch et al., 2011; Wiemann et al., 2013). The supercluster encodes a single transcription factor, which LaeA/VeA-dependently regulates the expression of both clusters within the supercluster (Wiemann et al., 2013; Dhingra et al., 2013). Fumagillin binding irreversibly inactivates type 2 methionine aminopeptidase, disabling the posttranslational processing of proteins (Sin et al., 1997). Additionally, fumagillin exhibited antifungal activity against *Malassezia furfur* (Kang et al., 2013), and pseurotin inhibited growth of phytopathogenic bacteria *Erwinia carotovora* and *Pseudomonas syringae* (Schmeda-Hirschmann et al., 2008). Thus, while many of these secondary metabolites have been studied predominantly in the context of infection and their effects on host tissues, the extent of their conservation across the fungal taxa, even among non-pathogenic strains suggests that it is conceivable that fungal secondary metabolites serve a role beyond virulence determination (Macheleidt et al., 2016; Novohradská et al., 2017; Flak et al., 2020).

2.1.2 Secondary metabolism and environmental iron acquisition by *A. fumigatus*

Almost all organisms, including *A. fumigatus*, require iron as a redox-potentiating co-factor in metalloproteins essential for fundamental cellular processes, such as DNA synthesis, carbon metabolism, or oxygen transport (Wang and Pantopoulos, 2011; Haas, 2012). Iron in the natural environment can be found in form of ferrous (Fe^{2+}) and ferric (Fe^{3+}) ions. The former, reduced form is water-soluble and potentially toxic, due to production of ROS *via* Fenton and Haber-Weiss reactions, when it rapidly oxidises upon contact with atmospheric oxygen. The oxidised form, on the other hand, is insoluble at neutral pH, forming ferric (oxo)hydroxide polymers (Caza and Kronstad, 2013). The acquisition and management of iron as a limiting resource by microbes, as well as higher organisms, is therefore an intricate process.

A. fumigatus uses reductive iron assimilation (Fe^{2+} -specific) and siderophore biosynthesis (Fe^{3+} -specific) to sequester free environmental iron (Schrettl et al., 2004; Brandon et al., 2015). The intracellular (iron-trafficking) and extracellular (iron scavenging) hydroxamate siderophores produced by the fungus are synthesised from arginine by SidC and SidD, respectively; both enzymes are NRPSs encoded within a single cluster (Schrettl et al., 2007; Blatzer et al., 2011). Fusarinine C and its *N*-acetylated derivative, triacetylfusarinine C, are produced upon low iron conditions, transported out of the cell, where they coordinate ferric ions in a stoichiometric ratio and assimilated back into the cell by MirB, a major facilitator protein transporter (Raymond-Bouchard et al., 2012). This process is particularly crucial during infection of a human host, where iron quickly becomes growth-limiting due to active iron sequestration as a defence mechanism by the host (Cassat and Skaar, 2013). Securing iron from the host environment by secondary metabolism-derived siderophores is essential for the survival and pathogenicity of *A. fumigatus* (Hissen et al., 2004; Schrettl et al., 2004). Similarly, intermicrobial competition for iron arises in microbial communities (and is discussed in greater detail below), which implies high relevance of iron acquisition strategies in microbe-host and microbe-microbe interactions, as well as clinical development of infection.

2.2.2 Isonitrile-containing secondary metabolites from *A. fumigatus* and other fungi

While a lot of attention has been dedicated to fungal PKS and NRPS products and their biosynthesis, other classes of secondary metabolites, including VOCs and isonitriles, have been less studied in terms of their underlying genetic encoding, regulation of expression, or physiological roles in native environments. Isonitrile alkaloids of various origins have, however, long been pursued for their medical and pharmacological properties (Dembitsky et al., 2015). The first discovered naturally occurring isonitrile compound was of fungal origin - xanthocillin was isolated from a fermentation broth

of *Penicillium notatum* as early as 1950s (Rothe, 1954; Beiersdorf and Ahrens, 1953). Since then, isocyanide-containing metabolites have been isolated from marine and terrestrial sources, including cyanobacteria (Rueping, 2007; Kim et al., 2012), poriferans (Avilés and Rodriguez, 2010; Emsermann et al., 2016), and nudibranchs (Jomori et al., 2015). Among fungi, xanthocillins, isonitrinic acid E, brassicicolin A, and glycosylated darlucins A and B (Fujiwara et al., 1982; Gloer et al., 1988; ZAPF et al., 1995) are only a few examples of bioactive isonitriles. Confrontation of *A. fumigatus* with the actinobacterium *Streptomyces peucetius* elicited the production of both known and new formyl xanthocillin analogues displaying high cytotoxicity (Zuck et al., 2011). One of the previously studied analogues, BU-4704, showed mild antibacterial properties in its purified form (Tsunakawa et al., 1993).

In contrast to the isonitriles from marine sources bearing a decorated isocyanoterpene backbone structure (Garson and Simpson, 2004), isonitriles from terrestrial environments are derived by modification of α -amino acids or indole alkaloids. The isonitrile moiety is responsible for their manifold biological functions, as well as the chemical capability of transition metal coordination. Indeed, naturally occurring terrestrial isonitrile compounds have been shown to form complexes with copper and serving as microbial chalkophores, involved in extracellular copper uptake (Wang et al., 2017; Lim et al., 2018). Indeed, xanthocillin and xanthocillin-like compounds in *A. fumigatus* have been shown to be produced by hybrid isocyanide synthase - NRPS enzyme gene clusters under copper starvation conditions (Lim et al., 2018).

3 *Pseudomonas aeruginosa*

Pseudomonas aeruginosa is a ubiquitous, metabolically versatile, Gram-negative gamma-proteobacterium that thrives in a variety of environments ranging from soil to aquatic habitats. Additionally, the bacterium is able to colonise surfaces of plants, fungi, and animals, including humans (Jander et al., 2000; Morales et al., 2010; Klockgether and Tümmler, 2017). Due to its metabolic versatility, *P. aeruginosa* is capable of establishing opportunistic infections in immunocompromised patients, frequently colonising environments such as open mucosal lesions and burn wounds, as well as the respiratory tract (Gellatly and Hancock, 2013). The bacterium is also largely associated with nosocomial infections, including ventilator-associated pneumonia, central line-associated circulatory infections and sepsis, or urinary catheter- and surgical/transplantation-related infections (Nathwani et al., 2014; Rosenthal et al., 2016), causing substantial mortality and morbidity, thus becoming an international public health concern. Apart from acute infections, the bacterium is able to cause persisting chronic infections in patients suffering from cystic fibrosis or chronic obstructive pulmonary lung disease, where the colonisation is also associated with a worsened clinical outcome (Gonçalves-de-Albuquerque et al., 2016; Talwalkar and Murray, 2016).

P. aeruginosa strains have large genomes (~5–7 Mbp), which account for the extensive metabolic capacity, including the ability to utilise various carbon sources and electron acceptors, and produce polymers and secondary metabolites (Moradali et al., 2017). This metabolic versatility is underpinned by a vast network of regulatory elements, which work individually or in synergies to allow for response and adaptation to various environments (Mathee et al., 2008; Frimmersdorf et al., 2010). The bacterium possesses an arsenal of inherent, tightly regulated antibiotic resistance mechanisms, often rendering antibiotic treatment attempts in patients futile, and simultaneously giving rise to multi- and pan-drug resistant strains in the recent past, posing a serious threat to healthcare systems worldwide (Hancock and Speert, 2000; Poole, 2011; CDC, 2019).

3.1 Secondary metabolism in *P. aeruginosa*

With its robust metabolic network, *P. aeruginosa*, along with other related pseudomonads, produces a vast array of secondary metabolites (Gross and Loper, 2009). Due to the demands of diverting energy and resources from primary to secondary metabolism, complex networks of regulatory functions are present in the bacterium, determining the expression patterns of secondary metabolites based on the environmental and physiological state. At the pinnacle of SM regulation is the GacS-GacA two component system, consisting of a sensory kinase (GacS) and a cognate intracellular response regulator (GacA), governing signal transduction pathways that comprise hundreds of genes (Heeb and Haas, 2001; Wei et al., 2013). Like their actinomycete counterparts, biosynthetic gene clusters in pseudomonads are considered to be rapidly evolving genetic elements (Fischbach et al., 2008), with diversity mediated by horizontal gene transfer events, followed by mutation, recombination, duplication or excision (Jenke-Kodama et al., 2006). The potential for secondary metabolic diversity is therefore highly strain-dependent; indeed, even within the *P. aeruginosa* species, a ‘core genome’ of about 5,000 genes exists, while hundreds of others can be unique to a single strain or only shared between a limited number of strains (Mavrodi et al., 2007; Mathee et al., 2008). Since the functionality and biological relevance of many *P. aeruginosa* secondary metabolites have been well studied, further detail about relevant secondary metabolites will be given in the context of their function.

3.1.1 *P. aeruginosa* secondary metabolism and iron acquisition

As introduced in section 2.1.2, iron is a limiting factor for microbial growth within both, the environmental context and the colonised host, who protects their iron reserve (Kochan, 1973). *P. aeruginosa* has developed multiple strategies to secure iron from host. Ferrous iron carried by haem moieties in haemoglobin, myoglobin, haemoglobin-haptoglobin, or haem-haemopexin complexes are readily taken up by the outer membrane-bound receptor PhuR. In the periplasm, haem is liberated by PhuT, transported through the inner membrane by PhuUVW ABC transporter complex and delivered to haem oxygenase (HemO) for liberation of iron. Additionally, free haem can be captured and imported via the Has system, using secreted HasA haemophore protein,

which translocates haem to the HasR outer membrane receptor (Ochsner et al., 2000; Caza and Kronstad, 2013). *P. aeruginosa* also possesses a low affinity Fe²⁺ uptake system, whose main component, an iron permease FeoB, transports iron into cytoplasm, hydrolysing GTP (Cartron et al., 2006; Sestok et al., 2018).

The oxidised, Fe³⁺ form of iron, needs to be scavenged from the environment by siderophores. *P. aeruginosa* produces two structurally very different molecules, pyoverdine and pyochelin, both capable of binding ferric ions (Bullen et al., 1974; Minandri et al., 2016). Pyoverdines, a class of cyclic peptide hydroxamate siderophores containing a dihydroxyquinoline chromophore, are NRPS-synthesised, yellow-green compounds responsible for the characteristic fluorescent properties of certain pseudomonads (Gross and Loper, 2009). Their two hydroxamate residues and the chromophore core create a strong iron coordination centre, making pyoverdines the high affinity siderophores, essential for infection establishment (Briskot et al., 1986; Visca et al., 2007). Pyoverdines have also been implicated in interkingdom microbial interaction relevant to cystic fibrosis (discussed in greater detail below). Pyochelin, in contrast, is a salicylate siderophore, forming 2:1 complexes with iron with a lower affinity than pyoverdines, using the salicylate moiety and two cysteine residues for coordination (Tseng et al., 2006). Pyochelin is produced by an NRPS cluster, whose peptidyl carrier starter unit is primed with a chorismate-derived salicylic acid residue (Youard et al., 2011). Both pyoverdine and pyochelin are actively transported into *Pseudomonas* cells by dedicated transport systems: FptA and FpvA for transport of pyochelin and pyoverdine across FpvA for transport of pyochelin and pyoverdine, respectively, across the outer membrane (Schalk and Guillon, 2013). The native siderophores are then transported into cytoplasm mainly by TonB1, one of the TonB triad (Takase et al., 2000). The genome of *P. aeruginosa* encodes over 30 more TonB-dependent outer membrane receptors, which are mostly dedicated to the transport of xenosiderophores and acquisition of iron by metabolic piracy (Cornelis and Matthijs, 2002).

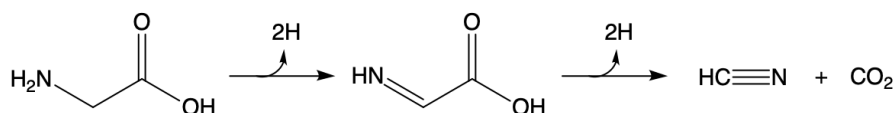


Figure 1. Synthesis of cyanide in *P. aeruginosa* from glycine by oxidative decarboxylation, via the HcnABC operon (Castric, 1977).

Additionally, phenazines, anthranilic acid-derived pigments with a wide spectrum of functions (Mavrodi et al., 2006), are used by *P. aeruginosa* for extracellular iron processing. Phenazines is an umbrella term for four tricyclic alkaloids secreted by *P. aeruginosa*: pyocyanin (blue), phenazine-1-carboxylic acid (yellow), phenazine-1-carboxamide (yellow), and 1-hydroxyphenazine (orange). All these compounds are redox-active, and phenazine-1-carboxylic acid has been shown to reduce extracellular

ferric iron into its ferrous form, improving biofilm development (Wang et al., 2011). Due to their redox properties, phenazines have also been found to be instrumental in microbe-host, as well as microbe-microbe interaction (Lau et al., 2004; Briard et al., 2015).

3.1.2 Cyanide production in *P. aeruginosa*

Pseudomonas belongs to a small number of microorganisms capable of producing cyanide (Goldfarb et al., 1967). Although elements of the precise mechanism of the reaction remain unknown, cyanide is produced in *P. aeruginosa* by decarboxylative oxidation of glycine, synthesising HCN and CO₂ stoichiometrically (Figure 1) (Castric, 1977; Wissing, 1975). Cyanogenic *Pseudomonas* strains can metabolise threonine into glycine, making it serve as an additional precursor to cyanogenesis (Castric, 1977). Cyanogenic pseudomonads (e.g. *P. aeruginosa*, *P. fluorescens*, *P. entomophila*, *Burkholderia cenocepacia* complex) encode an operon of three HCN biosynthetic genes, *hcnABC* (Laville et al., 1998), the latter two of which resemble amino acid oxidases of other bacterial species (Blumer and Haas, 2000). The expression and synthesis of cyanide in *Pseudomonas* is tightly regulated at several levels, and dependent on specific environmental conditions for function. The production of HCN is optimal at elevated temperature (34 - 37°C) under microaerobic, but not anaerobic, conditions ([O₂] < 5%), at high population densities (Castric, 1975; Blumer and Haas, 2000; Worlitzsch et al., 2002; Neerincx et al., 2015). At the transcriptional level, cyanogenesis in *P. aeruginosa* is controlled by multiple systems, targeting two different transcriptional start sites (T1, T2). While T1 is regulated by the *las* and *rhl* quorum sensing systems, T2 depends on a synergistic regulatory effect of RhlR and LasR (quorum sensing), and ANR (anaerobic regulator) (Pessi and Haas, 2000). Additionally, the transcriptional start of the *hcnA* promoter is directly regulated by AlgZR, a two-component sensory system. The histidine kinase AlgZ embedded in the cytoplasmic membrane was suggested to sense and react to microaerobic conditions and activate AlgR (Cody et al., 2009). AlgR is responsible for the control of a variety of virulence factors, including alginate production, biofilm formation, quorum sensing, or twitching mobility (Lizewski et al., 2002; Lizewski et al., 2004; Okkotsu et al., 2014). Upon a phenotypic switch to alginate production and mucoidy, AlgR becomes an activator, binding directly to the *hcnA* promoter (Carterson et al., 2004). The mechanism of synergy between AlgR and ANR remains poorly understood.

Bacteriogenic cyanide exists as volatile HCN gas under physiological conditions at pH 7, making it readily diffusible in the surrounding fluids (Blumer and Haas, 2000), rendering the CF lung replete with thick sputum ideal for pseudomonadal cyanogenesis. While no acute or chronic cyanide toxicity has been reported from *P. aeruginosa*-colonised CF patients, elevated cyanide levels can be reliably detected in their breath and sputum (Ryall et al., 2008; Sanderson et al., 2008; Gilchrist et al., 2015), that may well influence the function of adjacent tissues and contribute to long-term damage. It has

been postulated that cyanogenesis may be a factor contributing to the colonisation success of *P. aeruginosa* and exclusion of other pathogens.

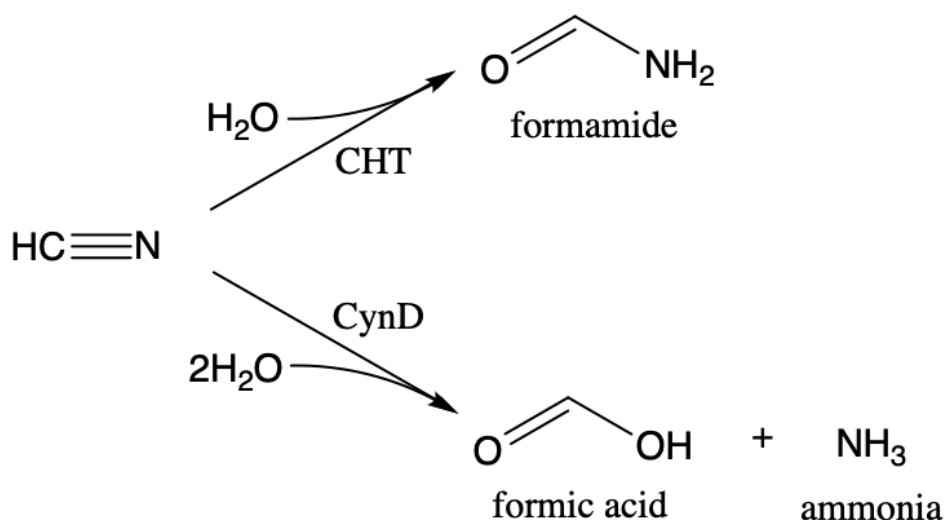


Figure 2. Enzymatic degradation of cyanide: simple hydrolysis into formamide by cyanide hydratase (CHT; upper), and hydrolysis yielding formate and ammonia by bacterial cyanide dihydratase/cyanidase (CynD; lower).

3.1.2.1 Cyanide detoxication

Enzymatic cyanide detoxication mechanisms are common among fungi and have been studied primarily in pathogenic species associated with plants, *e.g.* *Fusarium solani* (Barclay et al., 1998), *Leptosphaeria maculans* (Sexton and Howlett, 2000), *Gloeocercospora sorghi* (Wang and VanEtten, 1992), or *Giberella zeae* (Basile et al., 2008). In fungal pathogens, cyanide-degrading enzymes are produced as a counter-measure to the plant's deployment of protective cyanogenic glycosides and cyanolipids (Poulton, 1990). More recently, genome mining revealed the presence of cyanide-degrading enzymes also in the genomes of non-plant-pathogenic species *Neurospora crassa* and *A. nidulans* (Basile et al., 2008). These fungal cyanide hydratases (CHTs), belonging to the nitrilase superfamily, convert cyanide into less toxic formamide via a simple hydrolysis (Figure 2) (Kobayashi and Shimizu, 1994). Cyanide dihydratases or cyanidases, a similar class of enzymes found predominantly in bacteria, perform an analogous function, catalysing the biotransformation of cyanide into formate and ammonia (Watanabe et al., 1998). The functional dichotomy in the catalysis mechanism is caused by slight differences in the enzyme active site, underpinning the various leaving groups (Wang and VanEtten, 1992; Jandhyala et al., 2005). Due to their structural and functional stability in a wide range of conditions, no requirement for co-factors, high expression levels and retention of function in their purified form, both classes of cyanide-degrading nitrilases have been suggested as a possible approach to bioremediation of cyanide waste (Jandhyala et al., 2005; Basile et al., 2008).

4 *Aspergillus* - *Pseudomonas* interaction

Due to their co-occurrence in cystic fibrosis lung, and the worsened immunological consequences of co-colonisation for the patient, the interplay between *A. fumigatus* and *P. aeruginosa* has garnered attention and been under scrutiny for several years (Kolwijck & van, 2014). Studies co-culturing *A. fumigatus* and *P. aeruginosa* *in vivo*, *ex vivo*, and *in vitro* have determined a number of mechanisms through which the

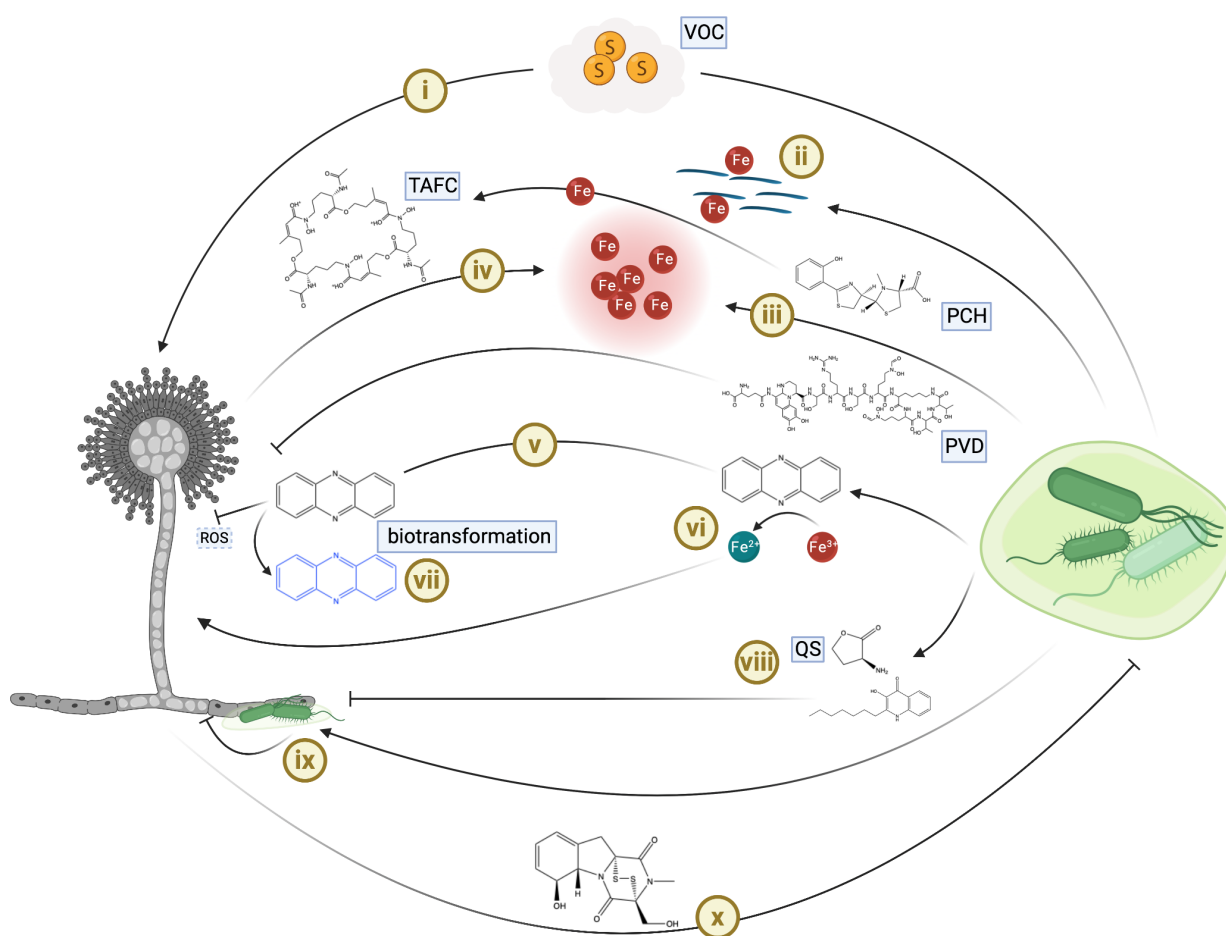


Figure 3. Currently documented interactions of *A. fumigatus* and *P. aeruginosa*. i) enhancement of fungal growth by VOCs; ii) Pf4 phage-mediated scavenging of iron results in arrest of fungal growth; iii) pseudomonadal siderophores, pyoverdine (PCH) and pyochelin (PCH), scavenge iron, effectively starving the fungus. Exchange of iron from PCH to TAFc was documented; iv) TAFc, secreted siderophore of *A. fumigatus* can restore fungal growth by iron sequestration; v) phenazines penetrate fungal cells, causing ROS and RNS generation; vi) *A. fumigatus* can capitalise upon reduction of environmental Fe by phenazines; vii) the fungus biotransforms phenazines into less toxic compounds; viii) quorum signaling molecules of *P. aeruginosa* inhibit *A. fumigatus*; ix) attachment of *P. aeruginosa* to fungal hyphae causes release of mildly inhibitory bacterial dirhamnolipids and incites fungal cell wall restructuring; x) gliotoxin of *A. fumigatus* inhibits *P. aeruginosa* growth and diminishes its inhibitory effects on the fungus.

microbes communicate, antagonise, or synergise. An overview of the molecular mechanisms is provided in Figure 3.

In vitro models have established that *P. aeruginosa* physically adheres to the galactosaminogalactan (GAG) of hyphal cell wall of *A. fumigatus* in co-culture, eliciting increased synthesis of GAG and cell wall thickening, hyphal melanisation by DHN- and pyo-melanin, as well as hyphal hyperbranching in the fungus (Briard et al., 2017). The attached bacterium prolifically produced dirhamnolipids, non-diffusible surfactant molecules produced under stress conditions (Van et al., 2009), postulated to cause the changes in fungal cell wall architecture.

Small soluble molecules secreted by the interaction partners form a basis for communication. Quorum signalling molecules of *P. aeruginosa*, namely quinolones (PQS), homoserine lactones (HSLs), and phenazines, can be found in CF sputum and are known to modulate pathogenicity of *P. aeruginosa* (Wilson et al., 1988; Chambers et al., 2005; Mowat et al., 2010). *N*-3-oxododecanoyl-L-homoserine lactone (13-oxo-C12-HSL), an inducer of IFN γ and inflammatory processes in the host, inhibits *A. fumigatus* (and *C. albicans*) hyphal growth and biofilm formation, potentially by affecting fungal transcription regulation (Hogan et al., 2004; Mowat et al., 2010). Conidial germination and fungal biofilm growth and structure are also modulated by *Pseudomonas* quinolone signal (PQS) (Reen et al., 2016). The antifungal effect was, however, later found to be paradoxically dependent on environmental iron concentration: under low iron, PQS was inhibitory; upon iron supplementation, and with fungal siderophores present, PQS supported fungal growth even more than iron alone (Sass et al., 2019).

Owing to the nature of iron as a coveted limiting nutrient, extracellular siderophores represent a battle mechanism for each organism to secure sufficient iron for survival and propagation. A single study with singly and multiply gene-depleted *P. aeruginosa* demonstrated that pyoverdine, the high affinity pseudomonadal siderophore, is the single most important antifungal factor in the interaction (Sass et al., 2018). Iron chelation by pyoverdine effectively starves the fungus of the nutrient, causing the activation of hapX pathway and production of TAFC, a competing iron-binding molecule with a similar iron dissociation constant. This effect is abated by excessive iron supplementation (Briard et al., 2019). These results were corroborated by the finding that sequestration of iron by TAFC can protect the fungus from bacterial competition (Sass et al., 2019).

Pyochelin's affinity to iron, as well as other divalent cations, results in the molecule's ability to inhibit *A. fumigatus in vitro* (Briard et al., 2019). This effect is dependent on the concentration of pyochelin being above 125 μ M, since lower concentrations resulted in a boost in growth of *A. fumigatus* producing TAFC (but not a non-producing mutant). Thus, pyochelin is presumably used by *A. fumigatus* as an external ferrochelator, from which ferric iron can be dislodged by the high-affinity siderophore TAFC. Surprisingly, the inhibition of *A. fumigatus* sufficient amounts of pyochelin cannot be abolished by iron supplementation, which led to the finding that, like in bacteria and host cells (DeWitte et

al., 2001; Adler et al., 2012), pyochelin penetrates the fungal cell and causes ROS and RNS production (Briard et al., 2019). These findings underline the intricacy of the conditions required for a particular mode of interaction between the microbes and should serve as a cautionary tale against blanket statements.

Phenazines, molecules used for both quorum sensing and iron acquisition (Jimenez et al., 2012), show potent antagonistic effects against target organisms, attributed to their redox potential (see above). These molecules penetrate the fungal cell, are oxidised in a NapA-dependent reaction, triggering ROS and RNS generation by mitochondria (Briard et al., 2015; Zheng et al., 2015). *A. fumigatus* responds by engaging Sod2, the mitochondrial superoxide dismutase instrumental in oxidative stress response and self-protection against phenazines (Briard et al., 2015). In an attempt to detoxify and mineralise phenazines, the fungus biotransforms pyocyanin into dimers, and phenazine-1-carboxylic acid into 1-methoxyphenazine (1-MP) and phenazine-1-sulphate. Of the latter two, 1-MP is highly antifungal, while the sulphated congener is not, suggesting that 1-MP is an intermediate in the detoxication process (Moree et al., 2012). 1-hydroxyphenazine (1-HP) is an iron chelator, capable of causing iron starvation and induction of adaptation to low iron conditions in *A. fumigatus* (Briard et al., 2015). Paradoxically, the other three phenazines at low concentration enhance fungal activity, presumably by reducing extracellular ferric iron to its ferrous form, which can then be taken up by the fungal low affinity ferrous iron uptake.

Pf4, an inovirus phage abundantly produced by *P. aeruginosa*, including CF isolates (Manos et al., 2008), binds to *A. fumigatus* hyphae and biofilm extracellular matrix, inhibiting fungal metabolic activity primarily by passive iron sequestration (Penner et al., 2016).

Surprisingly, the indirect contact between the fungus and the bacterium via volatile organic compounds (VOCs) results in fungal growth promotion. In sulphur-starved environment, such as the CF lung, *A. fumigatus* utilises VOCs in the gas phase as an exogenous source of sulphur (Briard et al., 2016). This involuntary, gas signal-mediated synergy is only effective while no direct physical contact between colonies is present.

Conversely, *A. fumigatus* has the ability not only to resist the various antagonistic effects by *P. aeruginosa* by activation of stress response pathways, xenobiotic biotransformation, and iron sequestration, but also to actively inhibit the bacterium using its own metabolic potential. Secretion of gliotoxin by the fungus demonstrably suppressed the inhibitory activity and growth of *P. aeruginosa* (Manavathu et al., 2014). Further studies will reveal whether more synergies between the microbes or antagonisms directed against the bacterium exist.

5 Aim of this study: Studying interactions relevant to cystic fibrosis

Understanding infection and pathophysiology was long focused solely on a single microbe at a time. However, the appreciation that microbes are seldom isolated, and usually occur in complex consortia in any given environment, is becoming more prominent (Netzker et al., 2018), and studies focusing on landscaping entire interactomes are multiplying (Reen et al., 2018; Dohlman & Shen, 2019). While studying microbial interactions and drawing conclusions and implications relevant to pathogenicity, it is of paramount importance to select culture setup that correlates best with the native infection conditions.

Selecting conditions that allow for a balanced growth of *A. fumigatus* and *P. aeruginosa*, as well as other bacteria (*i.e.* one partner does not overgrow the other) has led to establishment of multiple *in vitro* combined biofilm models, where biofilms were grown on Sabouraud dextrose broth (Manavathu et al., 2014), RPMI-MOPS agar (Briard et al., 2017), RPMI-MOPS with 10% (v/v) bovine foetal serum (Melloul et al., 2016), or RPMI with 2% (w/v) glucose (Ramírez et al., 2015). However, the fact that the physiology of individual microbes, as well as co-cultures, is highly dependent on the inoculum, medium composition and phase, pH, or incubation conditions, has been acknowledged for a long time (Goers et al., 2014; Cornforth et al., 2018; Keller, 2018). *P. aeruginosa* interaction with *A. fumigatus* shows different inhibitory outcomes depending on growth conditions, phenotype and age of the bacterial culture (Ferreira et al., 2015). Fungal gliotoxin production is also subjected to favourable culture conditions (Belkacemi et al., 1999; Scharf et al., 2012). Studies about inhibitory activity of various secreted small molecules described in previous sections draw conclusions from experiments often performed on artificial media, which often do not reflect the metabolic richness of sputum of cystic fibrosis patients, and the consequences this may have on the microbial physiology and interaction (Palmer et al., 2005; Palmer et al., 2007). While no standardised model to study interaction of microbes in CF context has been established to date, the present work attempts to adjust and correct for the discrepancies arising from medium variation by studying the interaction of *A. fumigatus* and *P. aeruginosa* in a synthetic cystic fibrosis sputum medium (SCFM2) (Turner et al., 2015), coming as close as possible to the chemistry of genuine sputum as possible in a laboratory setup. Further, it attempts to identify particular physiological processes within the partners that contribute to the process of interaction.

B Materials and Methods

1 Strains and Materials

1.1 Bacterial strains

Table 1. Bacterial strains used in this study

Strain	Genotype	Reference
<i>Escherichia coli</i>		
NEB Turbo	F' <i>proA</i> ⁺ <i>B</i> ⁺ <i>lacI</i> ^q Δ <i>lacZ</i> M15 / <i>fhuA2</i> Δ (<i>lac-proAB</i>) <i>glnV galK16 galE15</i> <i>R(zgb-210::Tn10)</i> Tet ^S <i>endA1 thi-1</i> Δ (<i>hds-mcrB</i>)5	New England Biolabs
<i>Pseudomonas aeruginosa</i>		
PAO1	wild-type strain	DSM 22644
Δ <i>hcnB</i>	derived from PAO1, markerless deletion	this study
Δ <i>pvdD</i> Δ <i>pchEF</i>	derived from PAO1, markerless deletion	University of Münster
<i>Agrobacterium tumefaciens</i>		
NTL4(pCF218)(pCF372)	Ti-, <i>traR-lacZ</i> , <i>tral-lacZ</i>	Kawaguchi et al., 2008
<i>Chromobacterium violaceum</i>		
CV026	double transposon mutant of ATCC31532, violacein and AHL negative	McClellan et al., 1997

1.2 Fungal strains

Table 2. Fungal strains used in this study

Strain	Genotype	Reference
<i>Aspergillus fumigatus</i>		
CEA17 Δ <i>akuB</i>	<i>akuB</i> ^{KU80} :: <i>pyrG</i> ; <i>PyrG</i> ⁺ , Δ <i>akuB</i>	da Silva Ferreira et al 2006
Δ AFUB_045460	derived from CEA17 Δ <i>akuB</i> ; AFUB_045490:: <i>ptrA</i> ; Pt ^R	this study
Δ <i>chtA</i>	derived from CEA17 Δ <i>akuB</i> ; <i>chtA</i> (AFUB_033190):: <i>ptrA</i> ; Pt ^R	this study
CF10	wild-type strain, cystic fibrosis isolate	University of Münster
Δ CF10_04996	derived from CF10; CF10_04996:: <i>ptrA</i> ; Pt ^R	this study
Δ CF10_01681	derived from CF10; CF10_01681:: <i>ptrA</i> ; Pt ^R	this study

1.3 Plasmids

Table 3. Plasmids used in this study

Name	Features	Reference
pUC18	Amp ^R	Norrande et al., 1983
pUC18_CF10_04996KO:: <i>ptrA</i>	Amp ^R ; CF10_04996 5' flank- <i>ptrA</i> -CF10_04996 3' flank; Pt ^R	this study
pUC18_CF10_01681KO:: <i>ptrA</i>	Amp ^R ; CF10_01681 5' flank- <i>ptrA</i> -CF10_01681 3' flank; Pt ^R	this study
pUC18_Afu2g17500* <i>chtA</i> KO:: <i>ptrA</i>	Amp ^R ; <i>chtA</i> 5' flank- <i>ptrA</i> - <i>chtA</i> 3' flank; Pt ^R	this study
pEXG2	Gm ^R	Rietsch et al., 2005
pEXG2_Δ <i>hcnB</i>	Gm ^R ; <i>hcnB</i> 5'flank- <i>hcnB</i> 3' flank	this study

1.4 Oligonucleotides

1.4.1 PCR primers

Table 4. PCR primers used in this study

Name	Target	5'-3' sequence
oMIF65	<i>ptrA</i> cassette forward	ATGGCCTAGATGGCCTCTTG
oMIF129	<i>ptrA</i> cassette reverse	CCGTAATCAATTGGCCTGA
oMIF141	CF10_01681 5' flank forward	CGACGTTGTAACGACGGCCAGTGCC AGGCCACATCCATGTCGCTTTTG
oMIF142	CF10_01681 5' flank reverse	CAAACAAAGATGCAAGAGGCCATCTAG GCCATGCATACCAAGTTTCTTG
oMIF143	CF10_01681 3' flank forward	CCAATGGGATCCCGTAATCAATTGGCCT GAAAGTCTATTGCAACAATCTC
oMIF144	CF10_01681 3' flank reverse	CCTCTAGAGTCGACCTGCAGGCATGCAA GCTCATCAGGAGATAGAGCAAG
oMIF145	CF10_01681 Southern blot probe forward	TATCTTTCTGAAGGAGGTCG
oMIF146	CF10_01681 Southern blot probe reverse	TGGCTGTGTCCCGTATG
oMIF156	CF10_04960 5' flank forward	CACGACGTTGTAACGACGGCCAGTG CCTACTGAAACCAAGCGCCATAG
oMIF157	CF10_04960 5' flank reverse	AACAAAGATGCAAGAGGCCATCTAGGC CATGATGCATGGTACTGACTG
oMIF158	CF10_04960 3' flank forward	CCAATGGGATCCCGTAATCAATTGGCCT GAAGCCACGAGTATTCCTGGG
oMIF159	CF10_04960 3' flank reverse	CTCTAGAGTCGACCTGCAGGCATGCAA CTGCGGATTGGAGGCCGAACC
oMIF312	<i>chtA</i> 5' flank forward	CGACGTTGTAACGACGGCCAGTGCC AGAGCCCTGCTGACATACATC

oMIF313	<i>chtA</i> 5' flank reverse	ACAAAGATGCAAGAGGCCATCTAGGCC ATGGTGCGAAGTATATGAGTTGG
oMIF314	<i>chtA</i> 3' flank forward	ATGGGATCCCGTAATCAATTGGCCTGAA CATTGCTGTCTGTTGAGACTC
oMIF315	<i>chtA</i> 3' flank reverse	TAGAGTCGACCTGCAGGCATGCAAGCTC TCAACGATCTCATGCAGCG
oMIF317	<i>chtA</i> Southern blot probe forward	GAGAGTCACTATGACTACTCC
oMIF336	<i>hcnB</i> 5' flank forward	GAGCCGGAAGCATAAATGTAAAGCAGT CGGACATGACGGAACGAC
oMIF337	<i>hcnB</i> 5' flank reverse	GTTTCCACCCGCATGCCC
oMIF338	<i>hcnB</i> 3' flank forward	TCCGGCCGGGCATGCGGGTGGAAACTA CCCTGATCGCCGGCAG
oMIF339	<i>hcnB</i> 3' flank reverse	ATCATGCGCACCCGTGGAATAATT AATCGAGCGCGCTCGATG
oMIF340	intact sequence upstream from <i>hcnB</i>	CACCGACAAGCTCAGCGC
oMIF341	intact sequence downstream from <i>hcnB</i>	GCGGGTGCGCATCTTCAG
pEXG2_forward	pEXG2, upstream from insertion site	CACTAAATAATAGTGAACGGCAGGT
pEXG2_reverse	pEXG2, downstream from insertion site	AACGACAGGAGCACGATCAT

1.4.2 qRT-PCR primers

Table 5. qRT-PCR primers used in this study

Name	Target	5'-3' sequence
q_cox5_forward	<i>cox5</i>	ATCTGTTCCGAAGCCCAAG
q_cox5_reverse	<i>cox5</i>	TCACTGCTGACACCGTAGAG
q_chtA_forward	<i>chtA</i>	TGGTCGGATCTTTGGTCCAGAC
q_chtA_reverse	<i>chtA</i>	TGGCCTCCAAAATCAGCCAGTG
q_yap1_forward	<i>yap1</i>	TTTAGCGAGGCGACCAAGCAAC
q_yap1_reverse	<i>yap1</i>	AGGTGAGCATTGCGACTTGCC
q_ccp1_forward	<i>ccp1</i>	ACTGACAAGACCACCAAGACCC
q_ccp1_reverse	<i>ccp1</i>	TGACGAAAGCGTCCGAAAAATCC
q_sod2_forward	<i>sod2</i>	TCCAGCCTCTTCTGGCATTGAC
q_sod2_reverse	<i>sod2</i>	TGGACAATCTATGCGGAGAAGCG
q_aspB_forward	<i>aspB</i>	AGATTTCTCGCGCCGTGTTGTG
q_aspB_reverse	<i>aspB</i>	TTTGGTTATCGCCGCCGTTAAG
q_cat1_forward	<i>cat1</i>	AACTCAGCTAGTGGTGCAAGCTC
q_cat1_reverse	<i>cat1</i>	ACAGTCTTGCCGAACCGGAATC
q_encC_forward	<i>encC</i>	ACACAGACATAGCCCGCAGATTG
q_encC_reverse	<i>encC</i>	AATCCCCATGACTGAACACGCAG
q_fqzB_forward	<i>fqzB</i>	AACAACGTGCTAATGGAGGCGG

q_fqzB_reverse	fqzB	CGGATTGGGAAACGCAAAGACAC
q_AFUB_016570_forward	AFUB_016570	ATCGACTGTCGCCAATGCCAAC
q_AFUB_016570_reverse	AFUB_016570	TGCACTCGGCCAACATCAACTG
q_AFUB_079820_forward	AFUB_079820	GTGCTACAATTCCAGTTGCGAGC
q_AFUB_079820_reverse	AFUB_079820	TTGAACGAAGTGGGAAGCGAGG
q_gliP_forward	<i>gliP</i>	AAATGGCGTTTGAAGGCCGCTC
q_gliP_reverse	<i>gliP</i>	TGGTGCTGACTCAACCCATGTTC
q_fma-PKS_forward	<i>fma-PKS</i>	AGCCTCTTGTCTTGCCCAATC
q_fma-PKS_reverse	<i>fma-PKS</i>	TCGACTGCATCCGTAA GCGAAG
q_psoA_forward	<i>psoA</i>	TGGCGGCCTGATCTACcTCAC
q_psoA_reverse	<i>psoA</i>	GCGGATCGACAAATCCA cCCAC
q_gyrA_forward	<i>gyrA</i>	TGTGCTTTATGCCATGAGCGA
q_gyrA_reverse	<i>gyrA</i>	TCCACCGAACCGAAGTTGC
q_hcnA_forward	<i>hcnA</i>	AGACCGTGCTCAACGTGCTC
q_hcnA_reverse	<i>hcnA</i>	ATACGCCCATGCCGCAGAAG

1.5 Standard media and supplements

Table 6. Media used for cultivation of microorganisms

Medium	Ingredient	Concentration
Bacterial media		
<i>Lysoygeny broth (LB) medium</i> (Miller 1972)	Tryptone	10 g/L
	Yeast extract	5 g/L
	NaCl*	10 g/L
	Agar, where indicated	15 g/L
	*for NSLB, salt was omitted	
<i>M9 medium</i>	Na ₂ HPO ₄ x 7 H ₂ O	12.8 g/L
	KH ₂ PO ₄	3 g/L
	NaCl	0.5 g/L
	NH ₄ Cl	1 g/L
	Supplemented with sterile:	
	Glucose	4 g/L
	MgSO ₄	1 mM
	CaCl ₂	0.2 mM

<i>SOC outgrowth medium</i>	Tryptone	20 g/L
	Yeast extract	5 g/L
	NaCl	10 mM
	KCl	2.5 mM
	MgCl ₂	10 mM
	MgSO ₄	10 mM
	Glucose	20 mM
<i>Vogel-Bonner minimal medium (VBMM)</i>		
	MgSO ₄ x 7 H ₂ O	0.2 g/L
	Citric acid	2 g/L
	K ₂ HPO ₄	10 g/L
	NaNH ₄ HPO ₄ x 4 H ₂ O	3.5 g/L
	Agar, where indicated	15 g/L
Fungal media		
<i>Aspergillus minimal medium</i> (Pontecorvo et al., 1953)	NaNO ₃	6 g/L
	KH ₂ PO ₄	1.52 g/L
	KCl	0.52 g/L
	MgSO ₄ x 7 H ₂ O	0.52 g/L
	Hutner's trace elements	1X
	Agar, where indicated	15 g/L
	MgSO ₄ und Hutner's trace elements were added after autoclaving	
Hutner's trace elements, 1,000X	ZnSO ₄ x 7 H ₂ O	22 g/L
	FeSO ₄ x 7 H ₂ O	5 g/L
	CuSO ₄ x 5 H ₂ O	1.6 g/L
	MnCl ₂ x 4 H ₂ O	5 g/L
	H ₃ BO ₃	11 g/L
	(NH ₄) ₆ Mo ₇ O ₂₄ x 4 H ₂ O	1.1 g/L
	CoCl ₂ x 6 H ₂ O	1.6 g/L
	Na ₂ EDTA	50 g/L
	Trace elements solution autoclaved, cooled to 60 °C and brought to pH 6.5 - 6.8 with KOH	
<i>Malt medium</i>	Malt extract	20 g/L

Yeast extract	2 g/L
Glucose	10 g/L
NH ₄ Cl	0.25 g/L
K ₂ HPO ₄	0.25 g/L

Synthetic cystic fibrosis sputum medium (SCFM2)

(Turner et al., 2015)	NaH ₂ PO ₄	1.3 mM
	Na ₂ HPO ₄	1.25 mM
	KNO ₃	0.348 mM
	K ₂ SO ₄	0.271 mM
	NH ₄ Cl	2.281 mM
	KCl	14.943 mM
	NaCl	51.848 mM
	MOPS	10 mM
	Serine	1.446 mM
	Glutamic acid hydrochloride	1.549 mM
	Proline	1.661 mM
	Glycine	1.203 mM
	Alanine	1.780 mM
	Valine	1.117 mM
	Methionine	0.633 mM
	Isoleucine	1.121 mM
	Leucine	1.609 mM
	Ornithine hydrochloride	0.676 mM
	Lysine hydrochloride	2.128 mM
	Arginine hydrochloride	0.306 mM
	Tryptophan (in 0.2 M NaOH)	0.013 mM
	Aspartic acid (in 0.5 M NaOH)	0.827 mM
	Tyrosine (in 1 M NaOH)	0.802 mM
	Threonine	1.072 mM
	Cysteine hydrochloride	0.160 mM
	Phenylalanine	0.530 mM
	Histidine hydrochloride x H ₂ O	0.519 mM
	D-glucose	3.2 mM
	CaCl ₂ x 2 H ₂ O	1.754 mM

MgCl ₂ x 6 H ₂ O	0.606 mM
FeSO ₄ x 7 H ₂ O	3.6 µM
N-acetylglucosamine	0.3 mM
1,2-dioleoyl-sn-glycero-3-phosphocholine (DOPC; dissolved in chloroform)	100 µg/mL
Salmon sperm DNA	0.6 mg/mL
Porcine gastric mucin	5 mg/mL
Agar, where indicated	15 g/L
pH adjusted to 6.8 with HCl	

Where appropriate, the following supplements were added to the medium:

Table 7. Medium supplements used for cultivation of bacteria and fungi

Function	Chemical	Concentration
<i>Antibiotic</i>	Carbenicillin	60 µg/mL
	Gentamicin (for <i>E. coli</i>)	10 µg/mL
	Gentamicin (for <i>P. aeruginosa</i>)	60 µg/mL
	Pyriithiamine	0.1 µg/mL
<i>Carbon source</i>	D-glucose (for AMM)	50 mM
<i>Osmotic stabiliser</i>	Sorbitol	1 M

2 Cultivation methods

2.1 Axenic culture conditions

2.1.1 Cultivation of *Escherichia coli*

E. coli cells were plated on LB agar and, following excessive liquid evaporation, were incubated at 37°C for 16 h. For plasmid isolation (*E. coli*) or overnight pre-cultivation followed by medium exchange (*E. coli*, *P. aeruginosa*), liquid cultures were established by inoculating LB medium with single colonies and incubation at 37°C for 16 h, with agitation at 200 rpm. Antibiotic supplements were added where appropriate (Table 7).

2.1.2 Cultivation of *Pseudomonas aeruginosa*

For plate and liquid cultivation, *P. aeruginosa* cells were treated in the same manner as *E. coli*.

For transformation purposes, a single colony of *P. aeruginosa* was inoculated in 20 mL liquid LB and grown as a standing culture overnight to stationary phase at 42°C.

2.1.3 Cultivation of *Aspergillus fumigatus*

A. fumigatus strains were propagated on AMM agar plates to allow for conidiation (Brakhage and Van den Brulle, 1995). Spore suspension of each respective strain was streaked on AMM agar using an inoculation loop; plates were incubated at 37°C for 5 days prior to harvesting. Conidia were collected in 10 mL sterile water, filtered through a 0.4 µm pore size cell strainer (BD Biosciences, Heidelberg) to remove hyphal and medium debris.

For cultivation of *A. fumigatus* in liquid media, 10⁶ conidia/mL were inoculated in 50 mL AMM and shaken at 37°C, 200 rpm for 16 h. For co-cultivation experiments, a pre-cultivation of 16 h was followed by straining of mycelial biomass and medium exchange.

2.2 Co-cultivation conditions

To emulate the environment of a CF-impaired lung overproducing sputum, synthetic cystic fibrosis sputum medium (SCFM2) was used for co-cultivation experiments, unless otherwise indicated (Turner et al., 2015). Where indicated, mucin was omitted from the medium. For most experiments, pre-grown bacteria and fungal mycelia were combined to observe effects of the interaction of mature organisms, rather than suppression of growth. After a 16 h pre-culture of *A. fumigatus* in AMM as described above, fungal mycelium was strained from the medium using Miracloth gauze (Merck Millipore, Darmstadt), washed with sterile PBS, and a small amount of biomass scooped into 50 mL of freshly prepared SCFM2 using a scapula. Similarly, the *P. aeruginosa* bacterial pre-culture cultivated to early stationary phase overnight in LB was centrifuged at 3200x *g* for 15 min to sediment the biomass. The culture supernatant and the thick, mucoid, alginate suspension were removed, the pellet washed twice with PBS, resuspended in a small amount of SCFM2 and added to the co-culture. Each 50 mL *P. aeruginosa* pre-culture was split three-way to simulate high density of the bacterial symbiont population in the lung, but to prevent a bacterial overload in the co-culture. The co-cultivation was carried out at 37 °C, shaken at 200 rpm for 24 h.

To investigate the interaction of the partners on solid media, 20 mL of each respective medium were poured in a standard-sized Petri dish (Ø 8 cm), and the microbes were added in 2 µL droplets containing spores or bacteria. The drops were set 1 cm apart, each droplet containing a total of 10³ colony-forming units (CFU). The plates were sealed with Parafilm (Bemis, Neenah, WI) and incubated at 37 °C for 24 - 72 h.

2.3 Cell count determination

Conidia (*A. fumigatus*) and cell (*P. aeruginosa*) counts in suspension were determined using a CASY Cell Counter + Analyser System Modell TT (Roche Innovatis, Reutlingen). For each sample, a 1:100 suspension dilution was prepared, of which 100 µL were mixed with 10 mL CASYton solution (Roche Innovatis, Reutlingen) before counting. Only viable cell counts were considered.

2.4 Biomass measurement

For biomass dry weight determination, 10⁶ conidia were inoculated in 100 mL liquid AMM supplemented with appropriate concentrations of KCN where appropriate and cultivated at 37°C, 200 rpm for 72 h. Mycelia were collected by straining through

Miracloth gauze (Merck Millipore, Darmstadt), washed with water, flash-frozen in liquid nitrogen and lyophilised for 24 h before weighing.

3 Molecular biology methods

3.1 Nucleic acid isolation

3.1.1 Isolation of genomic DNA

Total genomic DNA from *A. fumigatus* strains was isolated essentially as previously described (Schroeckh et al., 2009). In brief, mycelia from overnight pre-cultures were collected by straining through Miracloth gauze (Merck Millipore, Darmstadt), washed, excess liquid squeezed out, and homogenised by grinding under liquid nitrogen with a pestle and mortar. Approximately 100 µg of powdered mycelia were placed in a 2 mL Eppendorf tube and suspended in 500 µL lysis buffer (aqueous 50 mM Tris-HCl pH 8.0, 3% (w/v) SDS, 50 mM EDTA), followed by incubation at 65°C for 30 min with gentle agitation. After the incubation step, each sample was vigorously vortexed and placed on ice before addition of 250 µL MPC Protein Precipitation Reagent (Epicentre Biotechnologies, Madison, WI). Samples were centrifuged at 11,000x *g* for 10 min to allow for sedimentation of the lysed biomass and precipitated protein. Supernatant was transferred to a fresh Eppendorf tube, treated with 500 µL isopropanol and incubated at -20°C for 20 min to precipitate DNA. The DNA pellet was collected by centrifugation at 11,000x *g* for 10 min, supernatant removed, and the pellet washed twice with 500 µL 70% (v/v) aqueous ethanol to remove impurities, with intermediate centrifugation steps (13,000x *g*, 3 min). Finally, the supernatant was removed and the obtained pellet was allowed to air-dry at room temperature for *ca.* 5 min, followed by resuspension in 100 µL water and incubation at 37°C to facilitate dissolving.

Total genomic DNA of *P. aeruginosa* was obtained using the same process, modified in the initial steps: bacterial biomass was collected by centrifugation at 13,000x *g* for 5 min, supernatant removed, and the pellet resuspended in lysis buffer.

Genomic DNA concentration was approximated with a NanoDrop ND-1000 spectrophotometer (Thermo Fisher Scientific, Dreieich). All genomic DNA was stored at 4°C.

3.1.2 Isolation of RNA from *A. fumigatus*

For RNA isolation, mycelia from the main cultures were strained through Miracloth gauze (Merck Millipore, Darmstadt), washed, and flash-frozen in liquid nitrogen. A small part of the pellet (approximately 100 mg) was transferred to an RNase-free tube pre-filled with zirconium beads (∅ 1 mm) and lysis buffer, and homogenised with a FastPrep-24 tissue homogeniser (MP Biomedicals, Eschwege). Total RNA was isolated from the sampled using the Universal RNA Purification Kit (EurX, Gdańsk) according to the manufacturer's instructions, including on-column DNase treatment. RNA was eluted in 20 µL nuclease-free water and the concentration of RNA measured using NanoDrop ND-1000 spectrophotometer (Thermo Fisher Scientific, Dreieich). Only RNA with high purity $A_{260/280} \sim 2$ was used for further experiments.

For transcriptome analysis, RNA quality and integrity were further ascertained by capillary electrophoresis using the QX RNA QC Kit v2.0 (Qiagen, Hilden). Only RNA

samples with RNA integrity number (RIN) higher than 7 were selected for further analysis. RNA isolated from three biological samples was pooled and 9 µg of nucleic acid were processed for the library preparation. Library construction, Illumina next-generation sequencing, mapping, and normalisation of the transcript reads were carried out by StarSEQ GmbH (Mainz, Germany). Transcript levels were normalised for sequencing depth and gene length by counting the number of transcripts per million (TPM) (Wagner et al., 2012).

3.1.3 Isolation of plasmids from *E. coli*

GeneJET Plasmid Miniprep Kit (Thermo Fisher Scientific, Dreieich) was used to isolate plasmid DNA from 3 mL cultures of *E. coli* cultivated for 6 - 16 h. The kit was employed according to the manufacturer's instructions; the final elution was performed using water heated up to 60°C. Plasmid concentration was measured by NanoDrop ND-1000 spectrophotometer (Thermo Fisher Scientific Dreieich).

3.1.4 Isolation of DNA fragments from agarose gel

DNA fragments separated on agarose gel by electrophoresis were extracted using GeneJET Gel Extraction Kit (Thermo Fisher Scientific, Dreieich) according to the manufacturer's instructions. DNA was eluted with water at 60°C and the concentration measured by NanoDrop ND-1000 spectrophotometer (Thermo Fisher Scientific Dreieich).

3.2 Manipulation of nucleic acids

3.2.1 DNA restriction digestion

Genomic and plasmid DNA were digested in required amounts with restriction endonucleases (New England Biolabs, Frankfurt a.M.) in a total volume of 20 - 100 µL per reaction, using the appropriate buffer (NEBuffer 1.1, 2.1, 3.1, CutSmart) and temperature conditions. Each reaction was incubated for a minimum of 1 h.

3.2.2 Cloning and DNA assembly

Plasmids created in this study were assembled by ligating respective DNA fragments into a single construct using the Gibson assembly method homologous region overlaps (Gibson et al., 2009; Gibson, 2011). Briefly, the desired cloning DNA fragments were amplified by PCR using primers with a 20-bp annealing region to the amplified sequence, and a 25 - 30-bp tail region homologous to the terminal sequence of the adjacent DNA fragment in the final cloning construct. Such tailed, or partially tailed, DNA fragments were either separated on agarose gel and extracted, or treated with *DpnI* restriction enzyme to remove residual template, which could interfere with the cloning process and/or reduce the efficiency of the subsequent transformation. Purified DNA fragments in appropriate molar amounts were mixed with NEBuilder HiFi Master Mix (New England Biolabs, Frankfurt a.M.) according to the manufacturer's guidelines and incubated at 50°C for 1 h. Following the reaction, 3 µL of the resulting mixture were used to transform NEB Turbo Competent *E. coli* (New England Biolabs, Frankfurt a.M.) (please refer to section Section 3.4.1 of Materials and Methods for procedure).

3.2.3 Polymerase chain reaction (PCR)

For cloning and sequencing fragment amplification, Phusion Flash High-Fidelity PCR Master Mix (Thermo Fisher Scientific, Dreieich) was used. MyTaq Red Mix DNA polymerase (Bioline, Luckenwalde) was employed for routine screening of transformant colonies and for digoxigenin-11-dUTP-labelled Southern and Northern blot probe synthesis. Generally, 10 ng of template DNA were used to be amplified by 10 pmol/ μ L of each primer in a 20 μ L reaction. All DNA fragments were amplified in a Biometra TAdvanced thermal cycler (Analytik Jena, Jena).

3.2.4 Agarose gel electrophoresis

The separation of DNA fragments was performed using 1% (w/v) agarose gels stained with 1 μ g/mL ethidium bromide. Samples of 10 - 20 μ L containing 1X Gel Loading Dye Purple (New England Biolabs, Frankfurt a.M.) were loaded in individual wells with GeneRuler 1 kb DNA Ladder used as a size standard marker. The gels were submerged in 1X TAE running buffer (40 mM Tris-HCl pH 8.5, 20 mM acetic acid, 1 mM EDTA) under electric field (130 V, 400 mA) to allow for electrophoretic separation of loaded DNA. For Northern blot analysis, RNA was separated on a 1.2% (w/v) agarose gel containing 2% (v/v) formaldehyde dissolved in 1X running buffer (40 mM MOPS, 10 mM sodium acetate, 2 mM EDTA, pH 7.0). 10 μ g RNA were suspended in the same volume of loading buffer (50% (v/v) formamide, 5% (v/v) formaldehyde, 1X running buffer, 8% (v/v) glycerol, 20 μ g/mL ethidium bromide, bromophenol blue). RNA was denatured at 70°C for 20 min prior to loading on the gel.

3.2.5 First-strand complementary DNA (cDNA) synthesis

Reverse transcription of 1.5 μ g in 17 μ L purified total RNA was carried out using Maxima H Minus Reverse Transcriptase (Thermo Fisher Scientific, Germany) according to modified manufacturer's protocol. Briefly, RNA was primed with oligo(dT)₁₈ primer at 70°C for 10 min, the mix incubated on ice, and following ingredients added: 2.5 μ L nuclease-free water, 1.5 μ L dNTPs 25 mM (Bioline, Luckenwalde), 6 μ L 5X RT Buffer (Thermo Fisher Scientific, Dreieich), 1 μ L Maxima H Minus Reverse Transcriptase (Thermo Fisher Scientific, Germany), 1 μ L RNaseOUT Recombinant Ribonuclease Inhibitor (Invitrogen, Schwerte). The incubation time was extended to 2.5 h at 46°C. The remaining RNA in the mixture was removed by alkaline hydrolysis: 15 μ L 1M NaOH_(aq) were added to the mixture after the reaction and incubated at 70°C for further 10 min. The reaction was stopped by neutralisation with 15 μ L 1M HCl_(aq), and cDNA was precipitated by addition of 6 μ L 3M sodium acetate at pH 5.2, 150 μ L pure ethanol, and 4 μ L linear acrylamide (5 mg/mL) at -20°C for 15 min. cDNA pellet was sedimented by centrifugation at 13,000x *g* for 10 min and washed twice with 70% (v/v) ethanol. The pellet was allowed to air-dry and was subsequently reconstituted in 20 μ L nuclease-free water. The concentration of nascent cDNA was determined with NanoDrop ND-1000 spectrophotometer (Thermo Fisher Scientific, Dreieich).

3.2.6 qRT-PCR analysis

Complementary DNA containing sequences of interest was amplified on an Applied Biosystems QuantStudio 3 Real-Time PCR System (Thermo Fisher Scientific, Dreieich), using FrameStar 96-well qPCR plates (4titude, Berlin), and Applied Biosystems MicroAmp Optical Adhesive Film (Thermo Fisher Scientific, Dreieich). A total amount of

20 ng of cDNA per reaction was amplified using MyTaq HS Mix 2X (Bioline, Luckenwalde) polymerase, target-specific primers listed in Table 5 and EvaGreen (Biotium, Fremont) fluorescent reporter. The constituents of each reaction and their respective amounts are listed in Table 8. Primer efficiency was determined by constructing a standard curve, calculated using the amplification values in a 7-fold serial dilution of gDNA (4 technical replicates per dilution). Only primer pairs with amplification efficiency within the range of 90 - 100% were used. The two-step qRT-PCR parameters were the following: 2 min initial denaturation step at 95°C, followed by 5 s denaturation at 95°C and 20 s combined primer annealing and extension at 60°C, repeating for 40 cycles. *A. fumigatus* cytochrome c oxidase subunit V (Afu5g10560) used as an internal control for calculation of expression levels. Each target gene was analysed from combined three biological replicates in technical quadruplicates. The relative fold change values of each gene were calculated as $2^{-\Delta\Delta C_t}$.

Table 8. qRT-PCR reaction mixture

Reagent	Amount
cDNA	20 ng in 2 μ L
Primer (forward)	0.4 μ L
Primer (reverse)	0.4 μ L
EvaGreen	1 μ L
MyTaq HS Mix 2X	10 μ L
Water	6.2 μ L
Total volume	20 μL

3.3 Transfer of nucleic acids on membranes

3.3.1 Southern blot analysis

Southern blot analysis was employed for verification of putative transformant strains, following the method described previously (Liebmann et al., 2004). Briefly, *ca.* 10 μ g genomic DNA were digested with appropriate restriction endonucleases overnight, loaded onto an 1% (w/v) agarose gel and separated at low voltage throughout the length of the gel. The gel was washed with 0.25 M HCl twice for 10 min to depurinate, DNA denatured by washing with 1.5 M NaCl/0.5 M NaOH twice for 20 min, and neutralised with 1.5 M NaCl/0.5 M Tris pH 7.5 twice for 15 min. The DNA was allowed transfer overnight onto an Amersham Hybond ECL nitrocellulose membrane (GE Healthcare, Freiburg) by capillary blotting. The DNA was cross-linked on to the membrane matrix using a UVC500 UV Crosslinker (Hofer, Holliston) at 120 mJ/cm² for 2 min. The membrane was then pre-hybridised by submerging in 20 mL hybridisation solution (5X SSC, 0.1% (w/v) SDS, 50 g/L dextran sulphate, 0.5X Western Blocking Reagent (Roche Diagnostics, Mannheim)) at 65°C. The membrane-bound DNA was allowed to hybridise overnight at 65°C with a denatured probe added after the pre-hybridisation step. Prior to visualisation, the hybridisation solution was discarded and the membrane washed with 2X SSC/0.1% (w/v) SDS twice for 15 min at 65°C, 1X SSC/0.1% (w/v) SDS twice for 15 min at 65°C, and twice again for 10 min with 0.1X SSC at 65°C. The final washing step with a maleic acid buffer (0.1 M maleic acid, 0.15 M NaCl, 0.3% (v/v) Tween 20, pH 7.5) was performed at RT for 5 min. Subsequently, the membrane was incubated in blocking solution (0.1 M maleic acid, 0.15 M NaCl, 1X Western Blocking Reagent (Roche

Diagnosics, Mannheim)) for 30 min at RT to prevent unspecific binding of antibody fragments. The membrane was then incubated for 1 h in blocking solution supplemented with 37.5 mU/mL Anti-Digoxigenin-AP, Fab fragments from sheep (Merck, Darmstadt). After incubation, the unbound probe was removed by washing twice for 15 min with the washing buffer. Following the washing step, the membrane was equilibrated in detection buffer (0.1 M Tris-HCl pH 9.5, 0.1 M NaCl), transferred between two sheets of plastic foil, treated with CDP Star “ready-to-use” chemiluminescent substrate (Roche Diagnostics, Mannheim).

3.3.2 Southern blot probe generation

Non-radioactive, digoxigenin-labelled probes were generated for hybridisation onto the membranes in the Southern blot analyses. The probes were obtained by PCR-amplifying regions of interest out of genomic DNA using MyTaq Red Mix DNA polymerase (Bioline, Luckenwalde) and primers listed in Table 4. The reaction was supplemented with 50 µM digoxigenin-11-dUTP.

3.4 Transformation of cells with nucleic acids

3.4.1 Transformation of *E. coli*

Chemically competent *E. coli* cells were transformed by the CaCl₂ method described previously (Sambrook et al., 1989). In short, 50 µL of bacterial cell suspension mixed with 2 - 10 µL of the selected DNA fragment or plasmid were incubated on ice. After incubation, the cells were submerged in a water bath at 42°C for 1 min to heat shock, cooled down on ice, and suspended in 500 µL SOC outgrowth medium. The suspension was then incubated at 37°C for 30 - 60 min and plated on LB agar. Based on the presence of a selection marker in the transformed strain, the medium was supplemented with 60 µg/mL carbenicillin (Carl Roth, Karlsruhe) where appropriate.

3.4.2 Transformation of *P. aeruginosa*

Transformation of *P. aeruginosa* was based on a modified method of (Hmelo et al., 2015) and (Huang & Wilks, 2017). Briefly, a deletion plasmid was constructed using a pEXG2 backbone with a gentamicin resistance cassette (*aacC1*, Gm^R) and a sucrose counter-selection cassette (*sacB*) (Rietsch et al., 2005). Two regions flanking the region of interest in *P. aeruginosa* genome were amplified and inserted adjacent to one another into the backbone between *Hind*III and *Eco*RI restriction sites. An overnight pre-culture was prepared by inoculating a single fresh colony of *P. aeruginosa* in 20 mL LB medium, incubated as a standing culture overnight at 42°C, until a stationary phase of growth was achieved. An aliquot of 4 mL for each intended transformation event was removed from the culture, and the cells sedimented by centrifugation at 13,000x *g* for 1 min at room temperature. The pellet was resuspended in 1 mL 1 mM MgSO₄ solution, centrifuged, and the wash step repeated. Subsequently, the supernatant was discarded and the pellet resuspended in 50 µL 1 mM MgSO₄. The suspension was carefully transferred into a 2 mm gap electroporation cuvette at room temperature, placed in Eppendorf Eporator (Eppendorf, Wesseling-Berzdorf), and electroporated by pulsing with 2.2 kV for 5 ms. After pulsing, 1 mL SOC outgrowth medium at RT was added and the cells transferred to a 5 mL tube for a 2 h outgrowth incubation with shaking at 37°C. Transformed cells were pelleted by centrifugation (13,000x *g*, 1 min), 700 µL of the supernatant removed and the pellet resuspended in the remaining volume. The cells were spread out on VBMM agar

plates containing 60 µg/mL gentamicin and incubated at 37°C until colonies appeared (approximately 60 hours). These colonies were further streaked out on VBMM agar + Gm for purification and selection of merodiploids with gentamicin resistance, *i.e.* with the plasmid integrated in the genome. The merodiploids were subsequently streaked on no-salt LB (NSLB) agar plates with 15% (w/v) sucrose, to allow for counter-selection of double cross-over mutants with a markerless deletion of the DNA region of interest.

3.4.3 Transformation of *A. fumigatus*

The transformation method for *A. fumigatus* was adapted from that of Balance and Turner (Ballance & Turner, 1985). Mycelia from an overnight culture (liquid AMM, 37°C, 200 rpm) were strained over Miracloth gauze (Merck Millipore, Darmstadt) were washed with 0.6 M KCl. A small amount was then scooped out and suspended in a solution of Vinotaste Pro enzymes (Novozymes, Copenhagen; 2 g mixture in 20 mL 0.6 M KCl). This suspension was incubated at 30°C with gentle agitation of 80 rpm for 2-3 h. Protoplast generation was monitored by light microscopy in 30 min intervals; upon sufficient degradation of the cell wall material, protoplasts were filtered through a cell strainer (pore size 40 µm), topped up to 50 mL with 0.6 M KCl and centrifuged for 10 min at 4°C, 3,200x *g* to pellet the biomass. The pellet was washed with a 0.6 M KCl/0.1 M Tris-HCl pH 7.0 solution, broken up by gentle pipetting, undigested remnants of hyphal material removed, and protoplasts centrifuged as previously. The new pellet was disturbed by pipetting in flow-back supernatant and washed with a 0.6 M KCl/10 mM CaCl₂/0.1 M Tris-HCl pH 7.5 solution. After another centrifugation step, the pellet protoplasts were resuspended in 100-500 µL 0.6 M KCl/10 mM CaCl₂/0.1 M Tris-HCl pH 7.5 solution. 50 µL of the suspension (equivalent to approximately 5 x 10⁷ protoplasts) were used for each individual transformation event, including controls. Plasmid suspension (5-10 µg, up to 15 µL) was added into the protoplast suspension, followed by 15 µL PEG solution (25% (w/v) PEG 8,000, 50 mM CaCl₂, 10 mM Tris-HCl). Controls incorporated the same volume of sterile water instead of plasmid suspension. The mixture was combined by gentle tapping on the tube and incubated on ice for 20 min. Afterwards, additional 500 µL PEG solution were added and the mixture incubated on ice for additional 5 min. The reaction was then stopped by the addition of 1 mL of the 0.6 M KCl/10 mM CaCl₂/0.1 M Tris-HCl pH 7.5 solution. The transformed protoplasts were split four-way: 400 µL of the mixture was suspended in 10 mL liquefied transformation agar (AMM, 1 M sorbitol) at 55°C, mixed by inversion and poured over previously prepared transformation agar plates. The top agar was allowed to solidify and the plates were incubated at 37°C for 3-4 days, until sporulating colonies appeared. Each colony was transferred from the transformation plate and streaked out on selection-containing AMM agar plates multiple times to purify the transformant from wild-type contamination. Selection for pyrithiamine resistance was applied when obtaining fungal mutant; AMM agar was supplemented with 0.1 µg/mL pyrithiamine (Sigma-Aldrich, Hamburg).

4 Biochemical and analytical methods

4.1 Protein isolation from co-cultivation supernatant

The total secreted proteins were extracted from the culture supernatant of *A. fumigatus* axenic cultures and *A. fumigatus* challenged with *P. aeruginosa* for 24 h in SCFM2 medium excluding mucin, in triplicates, under conditions described in Section 2.2 of Materials and Methods. Whole supernatants were initially sterilised by centrifugation

(3,200x *g* for 15 min) and subsequently sterile-filtered using pore size 0.22 μm syringe filters to remove fungal and bacterial biomass. Each 50 mL filtrate was treated with 1 tablet of cOmplete Mini EDTA-free Protease Inhibitor Cocktail (Roche, Grenzach) and acidified with trifluoroacetic acid (TFA) to a final concentration of 0.1% (v/v) TFA, pH 2-3. Subsequently, the supernatants were aspirated onto pre-conditioned Chromabond SPE-C4 cartridges (Macherey-Nagel, Düren), washed with 5% aqueous methanol / 0.1% trifluoroacetic acid (TFA) (v/v), and eluted with 0.1% TFA in 80:20 acetonitrile:water (v/v). The eluents were aliquoted into three tubes each and evaporated to dryness using SpeedVac (Eppendorf, Wesseling-Berzdorf), combining the three aliquots in a single tube when the volume was sufficiently low. The dry pellets resolubilised and denatured with 50 mM triethylammonium bicarbonate (TEAB) in 50% (v/v) aqueous trifluoroethanol (TFE), using ultrasonic bath and pipetting to aid dissolving. Proteins were reduced by adding 2 μL of reduction buffer (500 mM tris(2-carboxyethyl)phosphine (TCEP) in 100 mM TEAB) in 55°C for 1 hour and alkylated with 12.5 mM iodoacetamide (IAA) in the dark at room temperature for 30 min. Proteins were precipitated, concurrently with sample delipidation, by washing with ice-cold methanol and chloroform (Wessel & Flügge, 1984). After precipitation, the methanolic supernatant was discarded and the protein pellet dried in SpeedVac (Eppendorf, Wesseling-Berzdorf), resolubilised in 100 mM TEAB by sonication. The protein solution was treated with a combination of rLysC and Trypsin Gold proteases (Promega, Walldorf), mixed gently and incubated at 37°C for 16 h to allow for a complete protein digestion. The reaction was stopped by addition of 10 μL 10% (v/v) formic acid and the liquid was evaporated to dryness in SpeedVac. The pellet was resolubilised in 25 μL 0.05% (v/v) TFA and 2% (v/v) MeCN in water by pipetting and sonication, and filtered through a 0.2 μm pore size spin column (Merck-Millipore, Darmstadt).

4.2 Measurement of cyanide concentrations in cultures

Orion solid-state combination cyanide ion-selective electrode (ISE) (Thermo Fisher Scientific, Germany), set up according to the manufacturer's instructions and connected to a benchtop pH/mV meter (Mettler Toledo, USA), was used to measure cyanide content in liquid cultures. Supernatants from cultures of *A. fumigatus* treated with various concentrations of KCN were isolated by pelleting the biomass by centrifugation at 3,200x *g* for 25 min at room temperature. Aqueous 10 M NaOH solution was used with 1:100 dilution factor to adjust ionic strength of the samples and stabilise CN⁻ ions in solution at pH > 10. Cyanide-selective ISEs suffer from a hysteresis (carryover) effect between measurements. To adjust for this, the electrode was submerged in each sample for 2 min prior to taking a measurement. The samples were gently stirred with magnetic beads both during the adjustment and the measurement period. The electric potential readings were converted into concentration values through calculating inverse log of the apparent measured values, based on the trendline equation of a fresh calibration curve for each experiment. The calibration curve was prepared by repeated measurements of the electric potential 1 mM, 500 μM , 250 μM , 100 μM , and 50 μM solutions of KCN prepared in the same medium as the queried samples, with ionic strength adjusted. Empirically, values measured for concentrations of cyanide below *ca.* 50 mM were outside of the linear quantitative range of the instrument.

4.3 Extraction of secondary metabolites

For secondary metabolic profiling of combined cultures, pre-cultures were prepared for *A. fumigatus* and *P. aeruginosa* as described above. A small amount of mycelium was

suspended in 50 mL SCFM2 and where appropriate, an aliquot of washed *P. aeruginosa* overnight culture was added. After 24 hours of main cultivation, the cultures were homogenised using T 25 ULTR-TURRAX (IKA-Werke, Staufen) and washed excessively with ethyl acetate. The organic phase of each sample was separated, dehydrated with anhydrous Na₂SO₄, solids removed by filtration over paper filter and the organic sample reduced to complete dryness *in vacuo*. Each extract was reconstituted in 1 mL methanol, filtered through 0.2 µm-pore-size polytetrafluoroethylene filter (Carl Roth, Karlsruhe) and stored at -20°C until further analysis.

4.3.1 Extraction and purification of triacetylfusarinine C

A culture of *A. fumigatus* wild-type strain was prepared in AMM (total volume of 1 L) as described above and incubated at 37°C, shaken at 200 rpm for 48 h to allow for iron depletion of the medium and the induction of iron starvation pathways in the fungus. Given that triacetylfusarinine C is a secreted siderophore metabolite, mycelia were separated by filtration over Miracloth gauze (Merck-Millipore, Darmstadt), and the extraction proceeded exclusively with the culture supernatant. The liquid was washed three times with chloroform in a 10:1 volumetric ratio, removing the organic phase after each washing step with a separation funnel. The chloroform extract was subsequently evaporated to almost complete dryness under vacuum and resuspended in a small amount of ultrapure water. The crude extract was split into halves, one half left untreated, and the other treated with 10 mM FeCl₃ solution in 10% (v/v) HCl to saturate TAFC with iron. Each extract was further purified from contaminating metabolites and free iron by loading onto an amphipathic Chromabond HLB SPE column (Macherey-Nagel, Düren). Each column was pre-conditioned and equilibrated by washing with 5 mL methanol and 5 mL water, the sample slowly aspirated and dried for 10 min on the resin using vacuum manifolds. The analyte-bound resin was washed with 10 mL 10 - 30% (v/v) aqueous MeOH in 10% increments and TAFC eluted with 40% (v/v) MeOH_(aq). Organic solvent was evaporated under reduced pressure and the concentration of TAFC in the water phase spectrophotometrically estimated by measuring absorbance of the solution at 440 nm on NanoDrop ND-1000 (Thermo Fisher Scientific, Dreieich) and feeding into the Beer-Lambert equation; molar attenuation coefficient of TAFC is $\epsilon = 2996 \text{ M}^{-1} \text{ cm}^{-1}$ (Misslinger et al., 2018).

4.4 LC-MS analysis of extracted microbial secondary metabolites

Sample analysis was performed on an ultrahigh performance liquid chromatography-mass spectrometry (LC-MS) system consisting of an UltiMate 3000 binary rapid separation liquid chromatograph equipped with a photodiode array detector and an LTQ XL mass spectrometer with an electrospray ion source and linear ion trap (Thermo Fisher Scientific, Dreieich). The samples (10 µL injection volume) were loaded onto a 150 by 4.6 mm Accucore reversed-phase (RP) column with particle size 2.6 µm (Thermo Fisher Scientific, Dreieich) and eluted for 21 min with the following mobile phase gradient: 0:100 MeCN + 0.1% (v/v) formic acid:water + 0.1% (v/v) formic acid increased to 80:20 in 15 min, then to 100:0 in 2 min, held at 100:0 for additional two minutes and reversed to 0:100 in 2 min, with a flow rate of 1 mL/min. The results were visualised and interpreted using the Xcalibur Software (Thermo Fisher Scientific, Dreieich).

4.4.1 HPLC-HRESI-MS analysis

High resolution mass spectrometry of the samples was performed on a Thermo Fischer Q Exactive Hybrid Quadrupole-Orbitrap mass spectrometer with an electrospray ion source and an Accela HPLC system (Thermo Fisher Scientific) equipped with an Accucore (150 x 2.1 mm, 2.6 μm particle size) C18 column with mobile phase flow rate of 0.2 $\text{mL}\cdot\text{min}^{-1}$ with the following gradient: 95% water + 0.1 % (v/v) formic acid (solvent A) with 5 % acetonitrile + 0.1 % (v/v) formic acid (solvent B) for 0.1 minute, to 98% solvent B in 10 minutes, held constant for 12 minutes (Dr. Kirstin Scherlach Biomolecular Chemistry, Leibniz-HKI).

4.5 MALDI-TOF-IMS analysis

Samples for MALDI-TOF imaging MS were prepared directly on sterilised indium tin oxide (ITO)-coated glass slides with 3 mL of SCFM2 + 1% (w/v) agar carefully deposited on the reflective surface. For axenic cultures, 10^3 CFU in 2 μL droplets of either *A. fumigatus* conidia or PBS-washed *P. aeruginosa* from pre-culture were placed centrally onto the agar surface. For co-cultivation, droplets of both microbes were placed on the midline of the slide latitudinally, 1 cm apart. Inoculated slides were placed in Petri dishes, sealed, and incubated at 37°C for 48 h. After cultivation, the slides were placed in a hybridisation oven at 37°C uncovered and dried overnight. Dried slides were sprayed uniformly with a mixture of 1:1 mixture of 2,5-dihydroxybenzoic acid and α -cyano-4-hydroxycinnamic acid dissolved in 70:25:5 MeCN:MeOH:water (v/v/v) using an automatic ImagePrep 2.0 system (Bruker Dalonics, Bremen) in 60 consecutive cycles of 41 s (1 s spray, 10 s incubation, 30 s active drying) (Hoffmann & Dorrestein, 2015). The sample slides were rotated 180° after 30 cycles. The samples were analysed with an UltrafleXtreme MALDI TOF-TOF device (Bruker Daltonics, Bremen), operated with a positive reflector mode using flexControl 3.0 software. The analysis was carried out within a 100 - 3,000 Da range, using a type 4 laser set at 30% intensity, accumulating 1,000 shots by tanking 50 random shots at each raster position, with raster width set at 200 μm . The acquisition method was calibrated externally using Peptide Calibration Standard II (Bruker Daltonics, Bremen), containing bradykinin 1 - 7, angiotensins I and II, substance P, bombesin, ACTH [1-17], ACTH [18-39], and somatostatin 28. The acquired data were processed with flexAnalysis 3.3, subtracting baseline and aligning endogenous peaks originating from the complex medium. Processed spectra were visualised and interpreted with flexImaging 3.0 and SCILS Lab 2015b, respectively. Chemical images representing heat maps of compound abundance were obtained from data normalised to total ion count with weak denoising (Dr. Maria García-Altares Pérez, Biomolecular Chemistry, Leibniz-HKI).

4.6 Radioactive labelling and siderophore internalisation measurement

Aliquots of washed overnight culture of *P. aeruginosa* and *E. coli* strains were prepared in triplicates, each containing 5×10^8 cells and suspended in 1 mL PBS before a siderophore solution was added. Radioactive gallium-68 was eluted from a 40 mCi $^{68}\text{Ge}/^{68}\text{Ga}$ generator with the mother nuclide bound as an oxide on dodecyl-3,4,5-trihydroxybenzoate silica. The generator was eluted automatically, using a peristaltic pump and a dispenser unit, as described before (Greiser et al., 2016; Petrik et al., 2010). Briefly, a positively charged polystyrene (PS-H⁺) SPE cartridge (Macherey-Nagel, Düren) was pre-conditioned with 1 mL of 1 M HCl and washed with 5 mL of water. The silica column of the ^{68}Ga generator was eluted with 4 mL 50 mM HCl and the eluate loaded

onto the PS-H⁺ column. The column was washed with 5 mL water, dried with 5 mL air and ⁶⁸Ga eluted with 1 mL 5M acidified NaCl solution (pH 4.6). Radioactively labelled TAFC was prepared by combining 50 mg TAFC dissolved in 70 µL water, acidified with 30 µL 1.1 M aqueous sodium acetate solution, with 300 µL of the ⁶⁸Ga eluate (~30 - 35 MBq of ⁶⁸GaCl₃). The mixture was rested for 10 min at room temperature, after which additional 100 µL sodium acetate solution were added. Radiochemical purity of the radioactively labelled siderophore was determined by thin layer chromatography (TLC) analysis on 80 mm silica gel coated aluminium plates using 0.1 M aqueous sodium citrate as eluent and analyse the plates with a TLC radioactivity scanner. Gamma activity of the labelled siderophore was measured using a gamma well counter; the value served as a reference point to correct for decay in subsequent measurements. Aliquots of *P. aeruginosa* were supplemented with ⁶⁸Ga-TAFC at a final concentration of 10 µM in each sample. The mixtures were incubated at RT for 60 min to allow for internalisation of bacteria. Subsequently, the bacteria were centrifuged and washed three time with PBS to remove remaining free radioactive isotopes in solution. The radioactivity of the bacterial biomass was measured in a gamma well counter. The results were corrected for decay and are represented as radioactivity at reference time (Bq/sample).

5 Microscopy

A co-cultivation of *A. fumigatus* and *P. aeruginosa* was prepared by suspending a small amount of pre-grown fungal mycelia and 10⁶ bacteria in 5 mL SCFM2 in a microscopy chamber. A confocal laser scanning microscopy (CLSM) system (Zeiss LSM 780, Carl Zeiss Jena) was employed for acquisition of video footage of the co-cultivation of the microorganisms. The system was equipped with a 20x (numerical aperture, NA; 0.4) objective lens in an inverted configuration. Prior to imaging, the objective lens and the stage were preheated to 37°C for 3 hours and the temperature was held constant during the experiment. The footage was acquired for the duration of 2 hours from the beginning of the co-cultivation.

C Results

1 Establishment of a cystic fibrosis sputum-mimicking *in vitro* model of co-cultivation

1.1 Microbiological analysis of *A. fumigatus* under cystic fibrosis sputum-mimicking conditions

The microbiological profile of cystic fibrosis has long been associated primarily with bacterial pathogens. However, the involvement of fungi in pathogenesis and clinical manifestation of CF is becoming ever more apparent, with *A. fumigatus* staling the spotlight as an established pulmonary opportunist. With the phenotypic dependency of microbes on the experimentally used cultivation media in mind, it is assumed that CF represents a specific setting, different from that encountered by the nature-derived opportunistic pathogens in their native habitats. It is therefore crucial to elucidate both, the behaviour of fungi themselves and their interactions with other species present in the CF lung, using the closest possible approximation of native cystic fibrosis sputum conditions that can be achieved.

The efforts to emulate the CF milieu in published literature vary drastically, with some authors relying on media that best support the particular phenotype the authors set out to study (Manavathu et al., 2014), or artificially modified media better suited to support optimum cell line growth (Ramírez et al., 2015; Ferreira et al., 2015). In an attempt to account for all the essential functionalities of CF sputum, the first medium artificial sputum medium (ASM) was formulated (Sriramulu et al., 2005). This medium incorporates components such as mucin, DNA, intrinsic iron chelator, salts, and amino acids. A better formulation was proposed by the work of (Palmer et al., 2005), further enhanced as described by (Turner et al., 2015). The authors measured the salt, amino acid, DNA, and mucin composition of sputum samples from 14 patients, and defined a medium recipe by determining median values of the measured concentrations. In the present work, the medium was adapted by substituting bovine submaxillary gland mucin for non-mucus-forming porcine gastric mucin, previously used in a yet different artificial sputum medium (Kirchner et al., 2012).

1.1.1 SCFM2 is suitable for cultivation of *A. fumigatus* and *P. aeruginosa* monocultures

To determine the suitability of the SCFM2-based model for subsequent experiments, a phenotypic analysis of *A. fumigatus* in SCFM2 was performed. Due to the availability of previously published material determining *P. aeruginosa* growth on the medium (Palmer et al., 2007), the bacterium was not included in the detailed analysis.

The initial comparison of each respective interaction partner grown as monocultures on SCFM2 agar plates revealed striking similarities to growth rates on optimal media, *i.e.* LB for *P. aeruginosa* and AMM for *A. fumigatus* (Figure 4). Within 24 hours after inoculation, the radial growth of both the bacterium and the fungus were comparable between the established and newly tested media, supporting the use of SCFM2 as a suitable

background for *in vitro* ecological studies of the microbial interactions in cystic fibrosis-mimicking conditions.

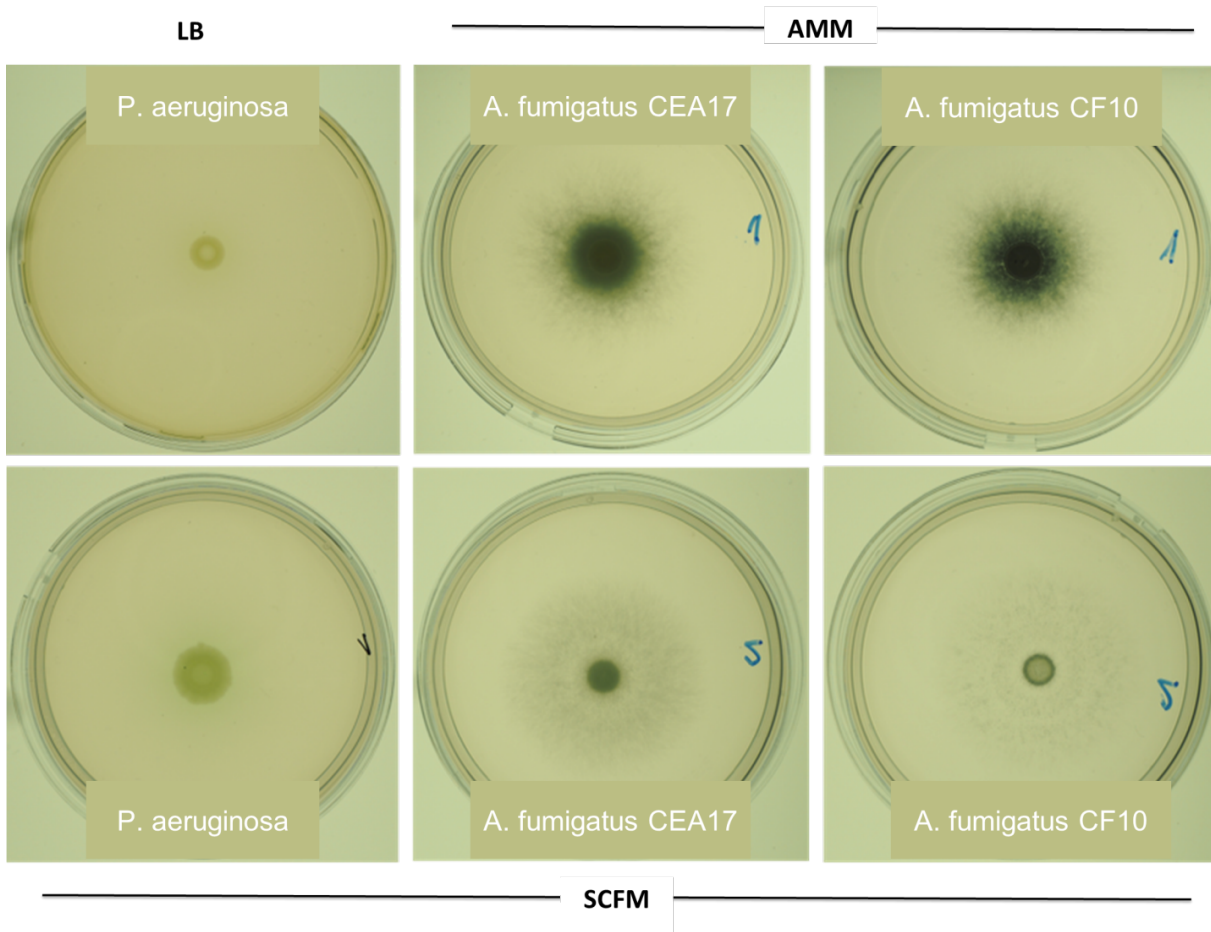


Figure 4. Growth of *P. aeruginosa* and *A. fumigatus* CEA17 Δ *akuB* and CF10 on SCFM2 solid medium. SCFM2 agar is capable of supporting the growth of the fungus and the bacterium alike. The colony diameter observed for *P. aeruginosa* is similar between LB and SCFM2 agar. Comparably, SCFM2 supports radial growth of both tested strains of *A. fumigatus* to a similar extent as AMM. A prominent reduction in conidiation is evident in *A. fumigatus* grown on SCFM2 agar.

To further evaluate the phenotypic characteristics of *A. fumigatus* grown in SCFM2 in comparison to AMM, further microbiological assays were carried out. The summary results of these assays are shown in Figure 5. In contrast to liquid AMM, both strains of *A. fumigatus* grown from conidia in liquid SCFM2 for 24 h developed biomass more slowly, growing to less than half of the amount of biomass measured in AMM (Figure 5A); this is surprising, given the nutrient-richness of the sputum-mimicking medium. The apparent lag in biomass formation is, however, supposedly a function of the phase of the medium. When inocula of the same concentration (10^3 conidia in 2 μ L) were deposited on SCFM2 agar and allowed to grow at 37°C for 72 h, the radial growth of the colonies was comparable between the strains and media (Figure 5B). Interestingly, *A. fumigatus* grown on SCFM2 agar prolifically produced aerial hyphae, but failed to sporulate to the extent it does even on minimal medium. Indeed, the numbers of conidia retrieved from plates after 5 days of growth showed a decrease of approximately two orders of magnitude from AMM to SCFM2 agar (Figure 5C).

1.1.2 SCFM2 supports a balanced growth of *A. fumigatus* and *P. aeruginosa* in co-cultivation

While the results of microbiological analyses of monocultures supported the use of SCFM2 as a fitting medium for studying *A. fumigatus* as a pathogen in cystic fibrosis, the qualifying criterion introduced above remains a balanced growth of both microbes in co-culture, where neither of the partners significantly overgrows the other. To test this, droplets of each microbe suspension containing 10^3 CFU were inoculated on SCFM2 agar plates in 1 cm distance and allowed to grow for 48 hours at 37°C. Independent of the strain, the microbes overcame the initial supposed inhibition in the interaction zone and formed a zone of a combined mucoid growth within the first day (Figure 6).

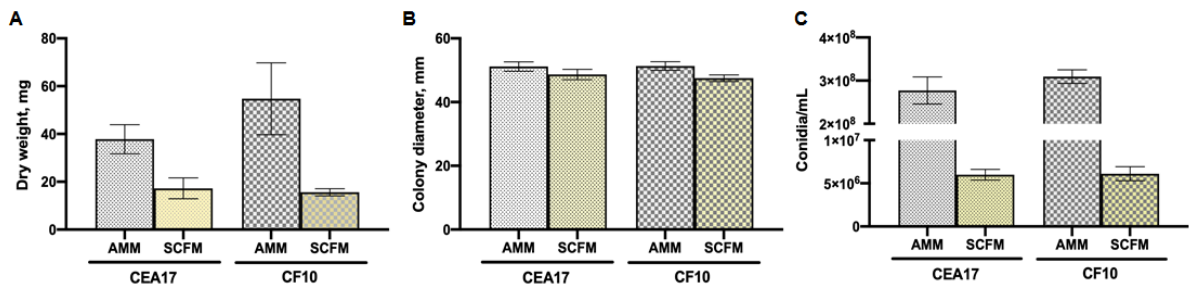


Figure 5. Phenotypic characteristics of *A. fumigatus* CEA17 Δ *akuB* and CF10 grown in liquid SCFM2. (A) Both strains of the fungus exhibit reduced biomass formation in SCFM2 broth in comparison to cultures grown in AMM. (B) Radial growth of both tested strains is comparable between colonies on SCFM2 agar and AMM agar. (C) *A. fumigatus* did not produce conidia when grown on SCFM2 agar. In comparison to cultures grown on AMM agar, a remarkable reduction in recovered conidia count of almost two orders of magnitude was observed.

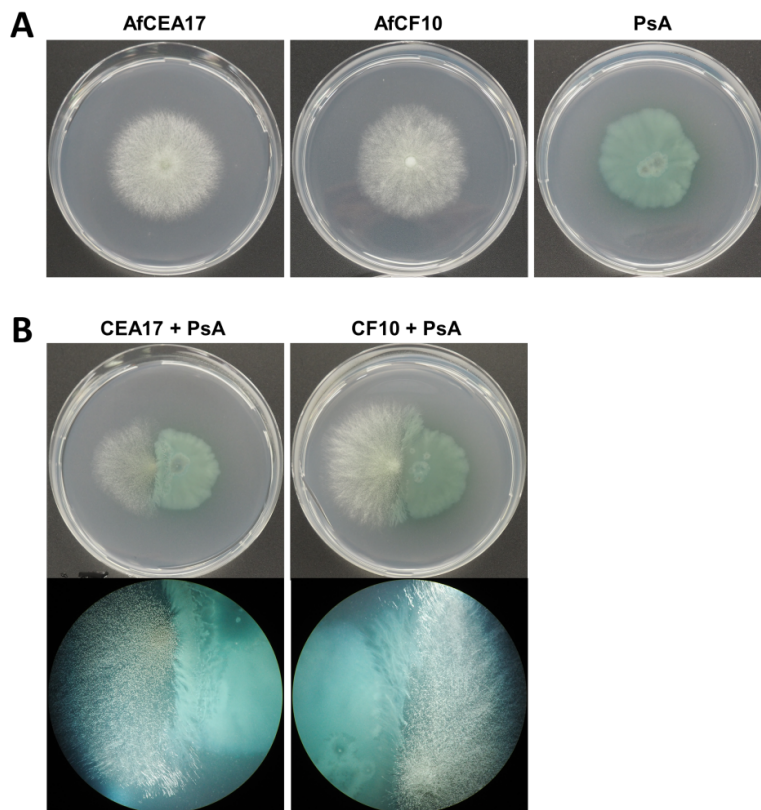


Figure 6. SCFM2 supports a balanced growth of *A. fumigatus* and *P. aeruginosa* alike. (A) Both strains of the fungus and the bacterium exhibit a similar fitness on SCFM2 agar in monoculture. (B) When cultivated in close vicinity to each other on SCFM2 agar, both strains of *A. fumigatus* and *P. aeruginosa* overcome any mutual inhibitory effects and grow as a mixed biofilm on the bacterial-fungal interface (top panel). With closer magnification, fungal hyphae covered by the bacterial colony are visible (bottom panel). It is impossible to ascertain which of the organisms is invading the other's space, suggesting a balance in growth on the selected medium.

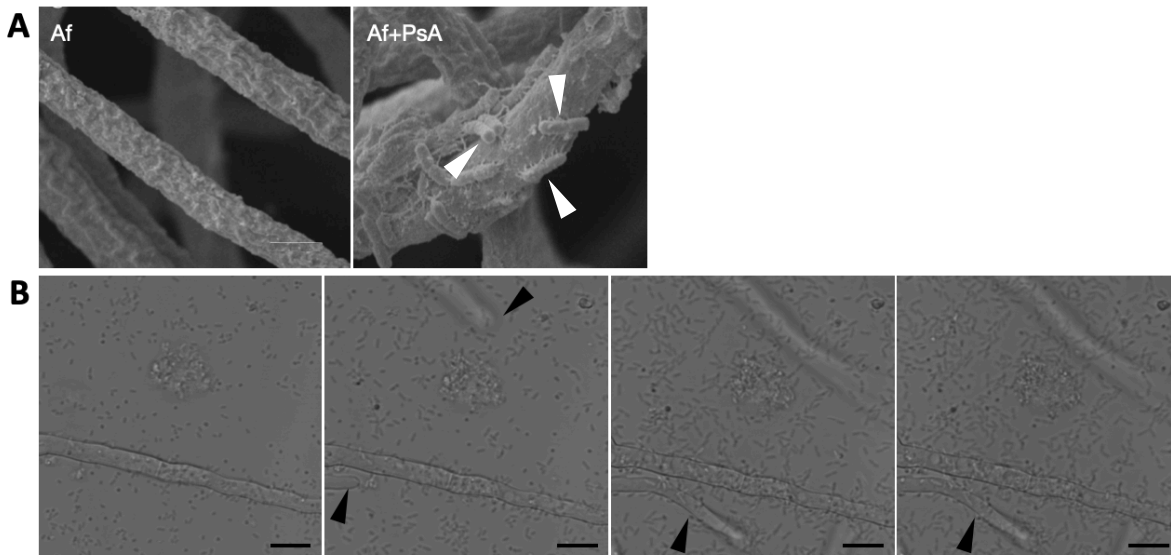


Figure 7. *Pseudomonas aeruginosa* passively adheres to the hyphae of *Aspergillus fumigatus*. (A) Scanning electron micrograph showing *A. fumigatus* (Af) hyphae in monoculture and in co-culture with *P. aeruginosa* (PsA) attached (top panel, *P. aeruginosa* indicated by white arrows; adapted from Keller, 2014). (B) Bottom panel shows a series of consecutive stills from a recording of 2 hours of co-culture of *A. fumigatus* and *P. aeruginosa* in liquid SCFM2 medium. The stills represent 30 min intervals; the black bar represents 10 μm . *P. aeruginosa* was actively proliferating during the cultivation, but remained static. Apparently uninhibited growth of *A. fumigatus* hyphae was also observed (indicated by black arrows).

The penetration of the bacterial colony and the coating of hyphae did not, however, appear to be fundamentally detrimental to the growth of the fungus. Each partner was

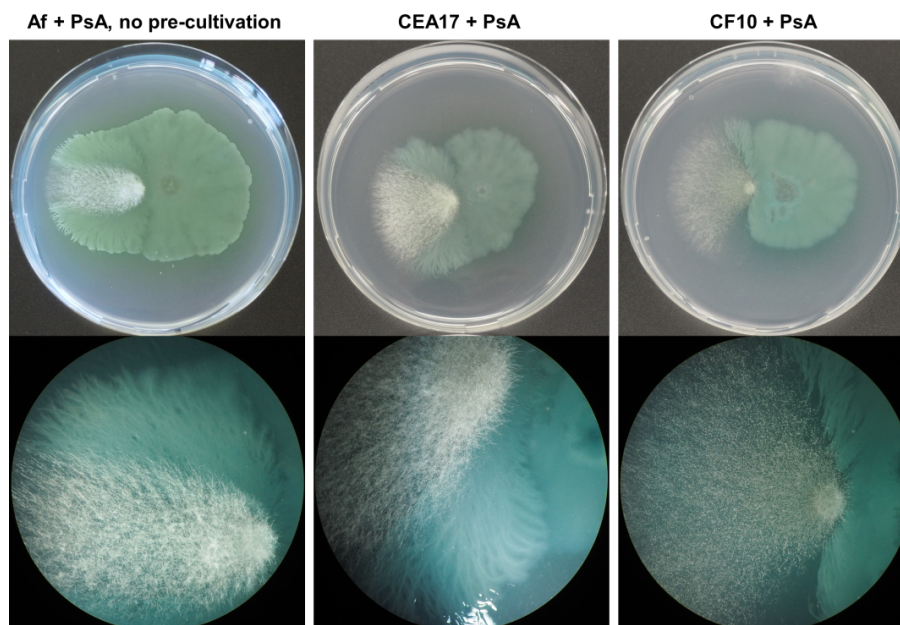


Figure 8. Growth of *Pseudomonas aeruginosa* and *Aspergillus fumigatus* on SFM2 agar under hypoxic conditions. When the two microbes were inoculated simultaneously and cultivated in a controlled atmosphere with 5% (v/v) O_2 , *P. aeruginosa* was better adapted to the hypoxic conditions and showed a mild growth advantage. When, however, *A. fumigatus* was inoculated and allowed to establish colony growth 24 h prior to inoculation of the bacterium, the growth advantage of the latter disappeared and the colonies look comparable to those grown under normoxia.

able to spread in the opposite direction in a proportionate extent. The spread was

contingent upon the rigidity of the medium provided. An agar concentration lower than 1% (w/v) allowed for swimming and swarming motility of *P. aeruginosa* that quickly branched out of the original colony and overgrew the plate (data not shown). Due to the reported rigidity of sputum and sputum plugs recovered from cystic fibrosis patients, as well as the findings that swimming motility is repressed by sputum conditions (Sonawane et al., 2006; Staudinger et al., 2014), the low agar concentration conditions where the bacterium prevails were regarded as unrepresentative of the native CF situation.

1.2 The adherence of *P. aeruginosa* onto *A. fumigatus* is passive and does not support further colonisation

In her dissertation, S. Keller described that *P. aeruginosa* forms a close physical contact with *A. fumigatus* hyphae by passively adhering to the fungal surface (Keller, 2014; Figure 7A). Based on the observation of an interaction zone where the bacterium effectively coats the fungal hyphae, we hypothesised that *P. aeruginosa* can use the mycelial network of *A. fumigatus* as a microbial 'highway', facilitating its own spread, as previously shown for *Bacillus subtilis* (Takeshita 2019). Mixed cultures of pre-grown fungal mycelia and bacterial suspension of various concentrations were prepared in fresh liquid SCFM2 to provide *P. aeruginosa* with the opportunity to swim uninhibited. The co-cultures were monitored and recorded for > 120 min each under a microscope to capture the behaviour of the microbes (Figure 7B). Regardless of the amount of bacteria provided in the medium, the attachment of *Pseudomonas* onto *Aspergillus* hyphae appeared to be a passive, stochastic process, rather than an active movement triggered by trophic tendencies. While the bacteria are multiplying, suggesting vivid metabolic activity, no directed motion is apparent; the bacteria already attached to a hypha remained stagnant, as did those freely suspended in the medium. Furthermore, the video demonstrated that *A. fumigatus* hyphae continued to grow in co-culture despite the active bacterial proliferation.

1.3 Hypoxic conditions favour *P. aeruginosa* growth in static culture

Patient studies indicate a low concentration of oxygen in the CF sputum (Werner et al., 2004), and that dense mucus plugs have a hypoxic gradient (Lambiase et al., 2010), or are entirely anoxic (Cowley et al., 2015). To account for this anaerobic situation in certain portions of the lungs, and thus better simulate the clinical situation, I incubated a co-culture of *A. fumigatus* and *P. aeruginosa* inoculated on SCFM2 agar plates as described above and incubated the plates in a controlled atmosphere with 2% (v/v) O₂. The results obtained in this phenotypic assay support those observed for inhibition of fungal biofilm formation previously (Anand et al., 2017): *P. aeruginosa*, capable of using nitrites and nitrates as alternative final electron acceptors under hypoxic conditions (Costerton, 2002), rapidly overgrew the fungus, whose metabolism is attenuated under hypoxia (Figure 8A). If, however, the fungus was inoculated and allowed to grow 24 h prior to the addition of the bacterium, the situation became more balanced, and the fungal colony was not easily engulfed by the advancing bacterium (Figure 8B). Upon longer cultivation, however, *P. aeruginosa* used the selective advantage of its robust metabolism and outgrew the fungal mass. For subsequent experimentation, I have therefore decided to adopt the conditions that support a more balanced growth and allow for studying the interaction.

2 Transcriptome analysis of *A. fumigatus* and *P. aeruginosa* interaction

Using the CF-sputum mimicking medium SCFM2, *A. fumigatus* (CEA17 \DeltaakuB and CF10) and *P. aeruginosa* PAO1 were confronted in liquid cultures with agitation for 24 h. Total RNA was isolated from the fungus retrieved from the co-culture and RNA sequencing performed. A monoculture of *A. fumigatus* was used as a control sample to assess the transcriptional changes induced in the fungus by exposure to *P. aeruginosa*. The cultivation was performed in triplicates of each culture, RNA isolated individually, and subsequently pooled before sequencing. To verify the credibility of the data, multiple genes were randomly selected to be tested by quantitative real-time PCR (qRT-PCR) performed on cDNA obtained from a different set of biological replicates. The trends in expression detected by qRT-PCR analysis were congruent with the results obtained by RNA sequencing, suggesting that the datasets reflect the reality.

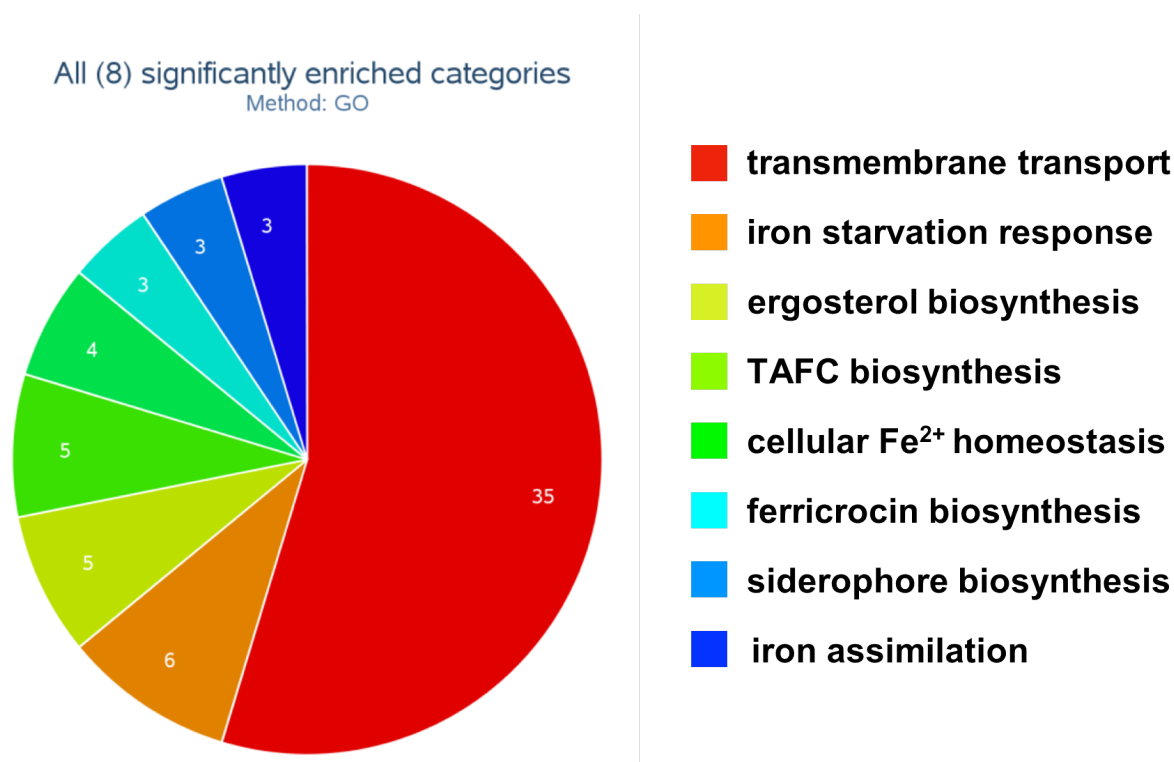


Figure 9. FungiFun analysis of 277 most upregulated genes of *A. fumigatus* in co-cultivation with *P. aeruginosa*. Gene ontology (GO) analysis was performed using the FungiFun web tool (Priebe *et al.*, 2011), selecting biological function, with P-value set at $p = 0.01$. Genes in the upregulated categories are responsible primarily for transmembrane transport and iron metabolism (siderophore biosynthesis, assimilation, homeostasis).

In response to co-cultivation with *P. aeruginosa*, *A. fumigatus* upregulated multiple cellular processes. Gene ontology analysis performed with FungiFun (Priebe *et al.*, 2011) on 280 most highly upregulated genes revealed 8 categories of biological processes as significantly enriched in co-culture ($p < 0.01$, Figure 9). These can be reduced to three categories, namely transmembrane transport, iron acquisition, and ergosterol biosynthesis. In more detail, Table 9 shows a selection of individual upregulated genes sorted by function. Apart from the obvious enrichment of genes in the aforementioned categories, differential regulation can be observed for genes encoding enzymes for

primary metabolism, in particular polysaccharide, lipid, and amino acid catabolism, as well as multiple stress response proteins. These results indicate an adaptive reaction of *A. fumigatus* to the presence of *P. aeruginosa*, in an attempt to secure nutrients for further growth. Additionally, the high upregulation of several enzymes involved in polysaccharide catabolism, it can be postulated that, as previously recorded by Briard *et al.*, the exposure of the fungus to a close physical contact with *P. aeruginosa* and its metabolites triggered a reorganisation of the cell wall (Briard *et al.*, 2017), for which polysaccharide-modulating enzymes are crucial.

Table 9. List of selected genes from the 280 most highly upregulated genes of *A. fumigatus* CEA17 \DeltaakuB co-cultured with *P. aeruginosa*. Differential regulation is expressed as log₂ fold change in TPM count between CEA17 \DeltaakuB + PsA/CEA17. Listed genes are sorted according to assigned biological function.

Gene accession number	Function	log ₂ (FC)
<i>Saccharide metabolism</i>		
AFUB_000160	putative alpha-L-rhamnosidase	2.51
AFUB_006940	hydrolase activity, O-glycosyl compounds	2.66
AFUB_049500	putative glyceraldehyde 3-phosphate dehydrogenase	2.48
AFUB_061880	betaglucanase	1.80
AFUB_090610	rhamnosidase B	2.66
AFUB_096950	glycosyl transferase family 8 family protein	3.15
AFUB_100920	hydrolase activity, O-glycosyl compounds	1.95
<i>Transmembrane transport</i>		
AFUB_003700	transmembrane transport protein	2.54
AFUB_005210	transmembrane transport protein	2.35
AFUB_012160	ABC multidrug transporter	2.54
AFUB_016830	putative high-affinity nitrate transporter	2.51
AFUB_028420	transmembrane transport protein	2.35
AFUB_046340	transmembrane transport protein	3.72
AFUB_046860	transmembrane transport protein	2.55
AFUB_048240	transmembrane transport protein	2.51
AFUB_048880	transmembrane transport protein	2.87
AFUB_049420	transmembrane transport protein	2.87
AFUB_052310	putative high-affinity iron permease	2.33
AFUB_062170	transmembrane transport protein	2.34
AFUB_081040	transmembrane transport protein	3.40
AFUB_081190	amino acid transport protein	3.34
AFUB_084720	transmembrane transporter; solute:proton antiporter	2.13
AFUB_086840	transmembrane transport protein	2.56
AFUB_095220	Putative MDR1 family ABC transporter	2.17
AFUB_096480	transmembrane transport protein	2.51
AFUB_099620	transmembrane transporter, nitrate transport	2.35
AFUB_100800	transmembrane transport protein	2.37
AFUB_035520	siderochrome-iron transporter	1.92
AFUB_071880	putative Zn transporter	1.92

Iron metabolism		
AFUB_016560	putative alpha-ketoglutarate-dependent taurine dioxygenase	2.26
AFUB_016570	pyridine nucleotide-disulphide oxidoreductase	4.12
AFUB_016580	triacylfusarinine C (TAFC) biosynthetic enoyl-CoA hydratase, putative	6.96
AFUB_016590	fusarinine C NRPS	2.92
AFUB_016610	putative secreted polygalacturonase GH-28	2.13
AFUB_016660	metalloreductase involved in response to iron starvation	3.69
AFUB_044470	ABC multidrug transporter with a predicted role in iron metabolism	5.76
AFUB_044480	putative esterase with a predicted role in iron metabolism	6.00
AFUB_044490	putative acetyltransferase with a role in iron metabolism	8.24
AFUB_044500	putative siderophore iron transporter	5.59
AFUB_044810	putative siderophore transporter	6.46
AFUB_044820	ABC multidrug transporter SitT	5.64
AFUB_044830	NRPS	7.54
AFUB_044840	enoyl-CoA hydratase/isomerase family protein	6.90
AFUB_044850	siderophore biosynthesis acetylase AceI	9.13
AFUB_044860	siderophore biosynthesis lipase/esterase	7.85
AFUB_044870	acetyltransferase activity	4.34
AFUB_052300	putative ferroxidase	3.61
AFUB_052310	putative high-affinity iron permease	2.33
AFUB_052420	hapX	2.94
Stress response		
AFUB_034690	putative 30-kilodalton heat shock protein	2.62
AFUB_072390	integral plasma membrane heat shock protein	2.03
AFUB_081810	integral plasma membrane heat shock protein	5.04

An analysis of downregulated *A. fumigatus* genes in co-cultivation provides more insight into the processes concerning the secondary metabolic response of the fungus. Surprisingly, when 277 most downregulated genes were analysed by FungiFun (Priebe et al., 2011) gene ontology tool, eleven significantly enriched categories were identified ($p < 0.01$, Figure 10). Of these, nine are directly associated with secondary metabolism (secondary metabolite biosynthesis (unspecified), mycotoxin biosynthesis, fumitremorgin B biosynthesis, asperthecin biosynthesis, verruculogen biosynthesis, endocrocin biosynthesis, monodictyphenone biosynthesis, melanin biosynthesis, and pigment biosynthesis (unspecified)), and the remaining two (oxidation-reduction process, metabolic process) are wide enough to encompass further secondary metabolic genes. Table 10 provides a more detailed look into the genes downregulated in response to *P. aeruginosa*. Multiple biosynthetic gene clusters, including that encoding for gliotoxin biosynthetic enzymes, belong to the most highly downregulated genes under the given conditions; this even despite the fact that gliotoxin is likely the most important antipseudomonadal metabolite that *A. fumigatus* can produce (Reece et al., 2018). Summarily, it appears that instead of exploiting its secondary metabolic potential, *A. fumigatus* turns the expression of a large proportion of its secondary metabolites off. This finding may appear counterintuitive, but the effects are unsurprising, when the

balanced growth of *A. fumigatus* and *P. aeruginosa* that can be observed in SCFM2 medium is considered.

All (11) significantly enriched categories
Method: GO

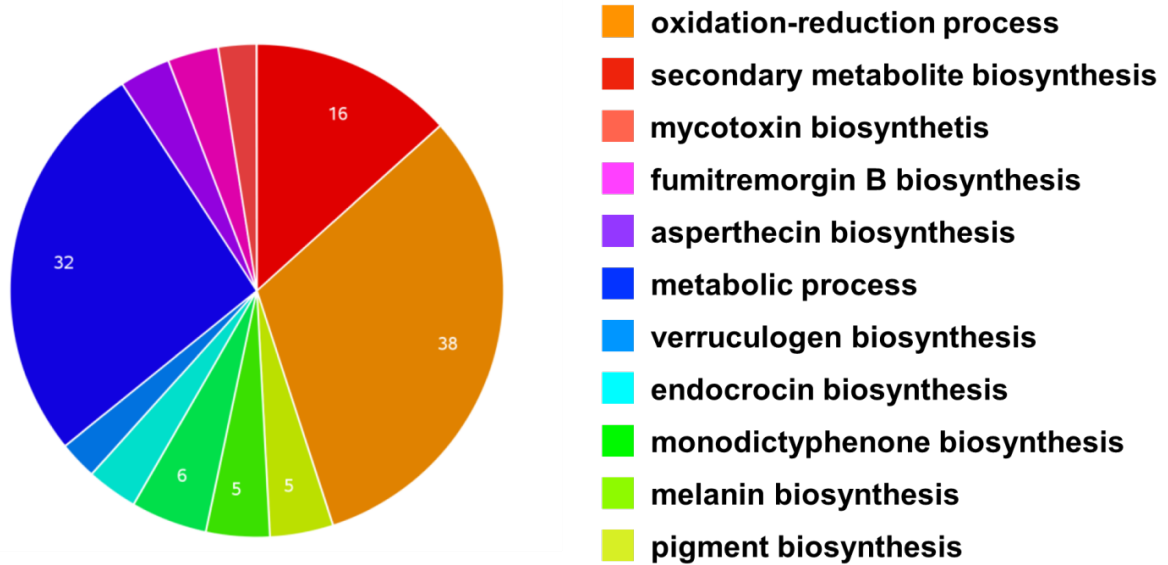


Figure 10. FungiFun analysis of 280 most downregulated genes of *A. fumigatus* in co-cultivation with *P. aeruginosa*. Gene ontology (GO) analysis was performed using the FungiFun web tool (Priebe *et al.*, 2011), selecting biological function, with P-value set at $p = 0.01$. Most downregulated categories represent genes with a function in secondary metabolism, both metabolite-specific and unspecified (red) as well as other metabolic functions.

Table 10. List of selected genes from the 280 most highly downregulated genes of *A. fumigatus* CEA17 Δ *akuB* co-cultured with *P. aeruginosa*. Differential regulation is expressed as \log_2 fold change in TPM count between CEA17 Δ *akuB* + PsA/CEA17. Listed genes are sorted according to assigned biological function.

Gene accession number	Function	$\log_2(\text{FC})$
<i>Sugar metabolism</i>		
AFUB_001130	endo-1.4-beta-xylanase, secreted	-2.25
AFUB_020300	alpha-amylase activity, calcium ion binding	-3.16
AFUB_028400	alpha-L-arabinofuranosidase	-2.46
AFUB_029100	alpha-amylase activity	-2.15
AFUB_066600	endo-1.4-beta-xylanase activity	-3.75
AFUB_080950	beta-1.4-glucanase	-4.36
AFUB_096700	extracellular arabinase	-2.21
<i>Fumagillin/pseurotin biosynthesis</i>		
AFUB_085990	glutathione transferase <i>psoE</i>	-3.87
AFUB_086010	P450 monooxygenase <i>psoD</i>	-2.24
AFUB_086020	O-methyltransferase <i>psoC</i>	-3.81
AFUB_086060	P450 monooxygenase	-1.96

AFUB_086070	putative acetate-CoA ligase	-3.89
AFUB_086090	non-heme iron-dependent dioxygenase	-2.46
AFUB_086120	unknown	-2.18
AFUB_086140	hypothetical protein	-2.51
AFUB_086190	acyltransferase fumagillin	-2.83
Fumitremorgin/verruculogen/brevianamide biosynthesis		
AFUB_086310	verruculogen synthase <i>ftmF</i> (from fumitremorgin)	-5.82
AFUB_086320	cytochrome P450	-5.59
AFUB_086330	brevianamide F prenyltransferase	-5.44
AFUB_086340	O-methyltransferase <i>ftmD</i>	-4.10
AFUB_086350	cytochrome P450	-3.24
AFUB_086360	NRPS	-6.02
Gliotoxin biosynthesis		
AFUB_075710	gliotoxin NRPS <i>gliP</i>	-4.69
AFUB_075720	P450 monooxygenase <i>gliC</i>	-2.36
AFUB_075760	efflux transporter <i>gliA</i>	-10.23
AFUB_075780	P450 monooxygenase <i>gliF</i>	-5.73
AFUB_075790	thioredoxin reductase <i>gliT</i>	-7.53
AFUB_075810	heme binding protein, electron carrier	-2.04
AFUB_075820	geranylgeranyl diphosphate synthase	-2.17
Melanin biosynthesis		
AFUB_033220	laccase <i>abr2</i>	-5.15
AFUB_033230	multicopper oxidase <i>abr1</i>	-3.83
AFUB_033240	heptaketide hydrolase <i>ayg1</i>	-6.92
AFUB_033270	scytalone dehydratase <i>arp1</i>	-1.97
Hexahydroastechrome biosynthesis		
AFUB_036240	FAD-binding domain protein	-2.22
AFUB_036260	DMAT synthase, prenyltransferase	-3.96
AFUB_036270	hexahydroastechrome NRPS	-3.67
AFUB_036280	O-methyltransferase	-5.91
AFUB_036290	transporter protein	-7.44
AFUB_036300	C6 transcription factor <i>hasA</i>	-4.08
Fumiquinazoline A biosynthesis		
AFUB_078040	fumiquinazoline A NRPS	-5.96
AFUB_078050	FAD monooxygenase	-6.29
AFUB_078060	flavoprotein amide oxidase <i>fmqD</i>	-7.72
Endocrocin biosynthesis		
AFUB_100730	endocrocin A PKS <i>encA</i>	-2.88
AFUB_100740	metallo-beta-lactamase <i>encB</i>	-4.62
AFUB_100750	anthrone oxzgenase <i>encC</i>	-6.30
AFUB_100760	2-oxoglutarate-Fe(II) type oxidoreductase	-3.12

<i>Asperthecin biosynthesis</i>		
AFUB_101110	oxidoreductase activity	-2.04
AFUB_101120	transporter protein	-1.66
AFUB_101130	uncharacterised, asperthecin biosynthetic process	-2.04
AFUB_101140	uncharacterised, asperthecin biosynthetic process	-4.78

3 Secondary metabolism of *A. fumigatus* confronted with *P. aeruginosa*

A. fumigatus harbours an extensive arsenal of secondary metabolites. As is the case for all secondary metabolites, usually studied in an artificial environment, their function remains a contentious issue (Macheleidt et al., 2016; Stroe et al., 2020; Netzker et al., 2018). Tentative roles for some compounds produced by the fungus have been elucidated, and it has been demonstrated that a number of them are deployed during infection of a host (Bignell et al., 2016), while others have been studied on the backdrop of environmental interactions and are recognised as antagonistic agents (Raffa & Keller, 2019). Growth of *A. fumigatus* in a cystic fibrosis lung combines these two aspects: the fungus interacts with the host and other microbes simultaneously.

Using the SCFM2-based CF lung mimicry model, I performed a comprehensive study of the changes to the secondary metabolome expressed by *A. fumigatus* alone and in interaction with *P. aeruginosa*. Each culture was homogenised, extracted with ethyl acetate, and analysed by LC-MS to yield insights into the types of metabolites produced in simulated sputum, *i.e.* those that might be relevant in the CF context, and the ways in which *A. fumigatus* modulates the production of these metabolites when confronted with the bacterium. The interpretable results are summarised in Figure 11.

Perhaps the most striking finding is the almost complete disappearance of the biosynthetic products of the metabolic supercluster on chromosome 8 (Wiemann et al., 2013). This supercluster, essentially combining two different metabolic clusters, both under control of a single transcription factor, produces a large array of metabolites of two classes: fumagillin and its congeners, and pseurotin and its congeners. Fumagillin is a meroterpenoid polyketide toxin with immunomodulatory and amoebicidal properties, and one of the virulence determinants for *A. fumigatus* (Fallon et al., 2010; Guruceaga et al., 2018). The compound was found as one of the major peaks in the extract of *A. fumigatus* monoculture grown on SCFM2. In co-culture with *P. aeruginosa*, however, the peak is drastically reduced (CF10) or completely disappeared (CEA17) (Figure 11a). Similarly, pseurotin, an antibacterial hybrid NRPS-PKS product (Pinheiro et al., 2013) and the other major product of the supercluster, disappeared completely when *P. aeruginosa* was present (Figure 11b). These data are supported by the transcriptional profile of the constituent genes of the supercluster, most of which were heavily downregulated in CEA17 \DeltaakuB co-culture (Figure 12). Surprisingly, some of the cluster genes of the CF10 strain showed upregulation in the RNA sequencing data; however, given the low amount of both, fumagillin and pseurotin detected in co-culture supernatants, it is safe to assume that those data are a technical artefact, and the realistic situation is better represented by the transcriptional profile of the CEA17 \DeltaakuB strain in

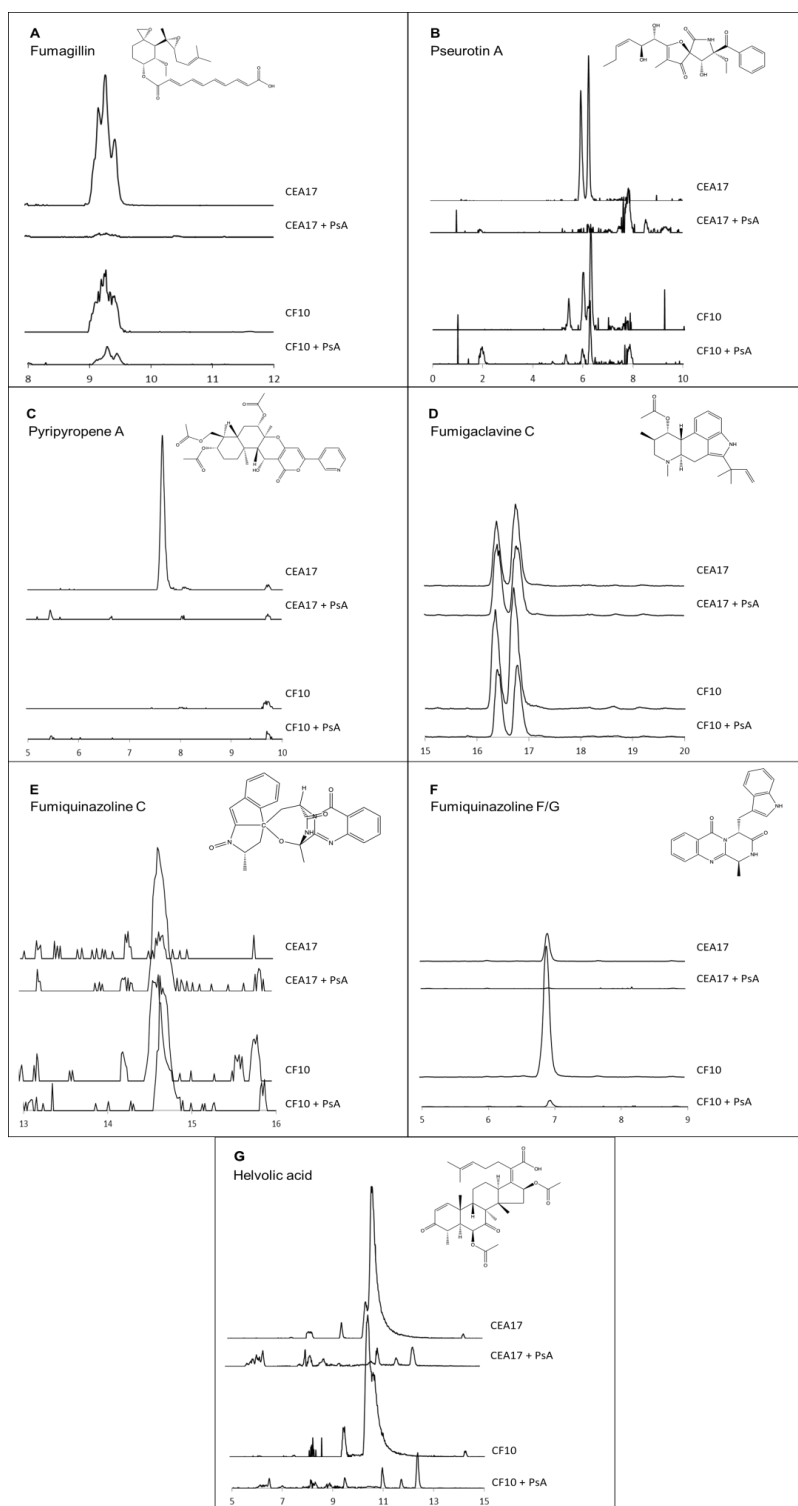


Figure 11. LC-MS-based analysis of secondary metabolites of *A. fumigatus* in co-culture with *P. aeruginosa*. Multiple metabolites with differential abundance patterns could be identified, some in a strain-specific manner. Data are presented as extracted ion chromatograms (EIC) representing each compound. (A) fumagillin (m/z 457); (B) pseurotin A (m/z 431); (C) pyripyropene A (m/z 583); (D) fumigaclavine C (m/z 366); (E) fumiquinazoline C (m/z 443); (F) fumiquinazoline F/G (m/z 358); (G) helvolic acid (m/z 568).

co-culture. Intermediate and shunt products of the biosynthesis of either of the toxins (*e.g.* ovalicin, β -transbergamotene) were not detected.

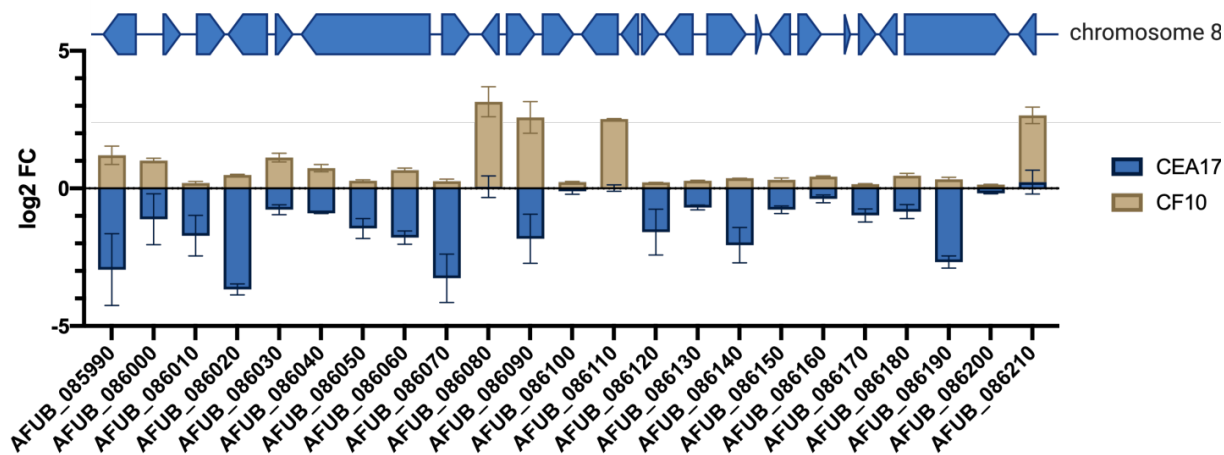


Figure 12. Fumagillin and pseurotin-producing supercluster on chromosome 8 and its expression pattern in *A. fumigatus* CEA17 Δ *akuB* and CF10 in co-culture with *P. aeruginosa*. For simplicity, gene identifiers are only given for the CEA17 Δ *akuB* strain. The downregulation of the cluster genes evident from the transcriptome data, shown here as log₂ fold change, correlates well with the absence of the metabolites from co-culture supernatants. In *A. fumigatus* CF10, the cluster gene expression appears unchanged in relation to the control group, and several genes even show upregulation. Given that fumagillin is completely absent from the co-culture supernatant and pseurotin is present in a drastically reduced amount, this is believed to be an artefact of the measurement.

Pyripyropene A underlines one of the small phenotypic differences observed between the two *A. fumigatus* strains. While no detectable pyripyropene A was produced by CF10, a clear peak could be observed in the supernatant extract of CEA17 Δ *akuB* (Figure 11c). Furthermore, pyripyropene A is yet another compound to be completely absent from co-culture. This polyketide was discovered serendipitously as an acyl coenzyme A:cholesterol acyltransferase inhibitor (Omura et al., 1993) and its natural role in microbial communication or infection remains unknown.

Fumigaclavine C is an ergot alkaloid produced by a dimethylallyl tryptophan synthase and has been described as a virulence determinant for *A. fumigatus*, inhibiting the host pro-inflammatory cytokine response (Du et al., 2011; Panaccione & Arnold, 2017). Furthermore, an inhibitory effect of the compound on a spectrum of Gram-positive and Gram-negative bacteria was observed, including *P. aeruginosa* (MIC 31.25 μ g/mL) (Pinheiro et al., 2013). The amount of fumigaclavine C (and a possible isomer with a slightly different retention time) remained almost constant between strains and conditions (axenic or co-culture; Figure 11d), suggesting that fumigaclavine C is produced by the fungus and might exert a weak antipseudomonadal effect during interaction, but is not actively upregulated and deployed to challenge *P. aeruginosa*.

Two different putative fumiquinazolines were observed in low amounts in the extracts. These tryptophan-derived peptidic mycotoxins usually accumulate in conidia, but have also been reported from culture supernatants (Larsen et al., 2007). In the present experiment, fumigaclavine C and fumigaclavine F/G were detected in an incongruous manner. The former could be observed in low amounts in co-culture of CEA17 Δ *akuB* and *P. aeruginosa*, but not in the monoculture, while it was present in both monoculture and co-culture of the CF10 strain (Figure 11e). The latter, however,

was produced only in monocultures of each strain, and attenuated in the co-cultures, in the same fashion as fumagillin or pseurotin (Figure 11f). The precise effect these alkaloids have on the host or bacteria is unknown.

In addition to NRPS and PKS products, *A. fumigatus* can produce helvolic acid, a fusidane-type triterpenoid antibiotic. Helvolic acid belongs among the compounds for which activity has been described both in the environment, and the host. In the latter, helvolic acid suppresses ciliary movement in respiratory epithelium (Amitani et al., 1995). Chromatographic analysis revealed that helvolic acid is prominently produced by the fungus in synthetic sputum medium (Figure 11g), thus making it potentially important in patients, in whom mucociliary clearance is impaired to begin with. In co-culture with *P. aeruginosa*, however, the compound disappeared from the supernatant entirely. Helvolic acid has an antibacterial effect on the Gram-positives *Streptococcus agalactiae* and *Staphylococcus aureus* (Lv et al., 2017; Kong et al., 2018); here, however, the production was attenuated, suggesting that in a mixed infection, helvolic acid is present at a level too low to be detrimental to either the bacterium, or the patient.

Furthermore, a number of fungal compounds with toxic properties, usually found in *A. fumigatus* culture supernatants grown on minimal media, such as, brevianamides, fumigatin, hexadecyloastechrome derivatives, or verruculogen (data not shown), were not detected at all in cultures grown in liquid SCFM2 medium, even after longer cultivation periods. Similarly, there was a pronounced absence of gliotoxin, both from axenic and mixed cultures, challenging the previously asserted claim that the metabolite plays a role in the interaction between *A. fumigatus* and *P. aeruginosa* in CF lung (Reece et al., 2018). Both of these results support the findings of the transcriptome analysis of *A. fumigatus* discussed above. Summarily, the analysis demonstrates that multiple prominent mycotoxins produced by *A. fumigatus* either decrease in quantity or are completely absent from co-culture with the bacterium. With reference to the RNA sequencing data, it is likely that these compounds are attenuated in expression as a reaction to the presence of *Pseudomonas* or a *Pseudomonas*-generated signal, rather than degraded by bacterial activity.

3.1 *A. fumigatus* CF10 produces a xanthocillin derivative in co-culture with *P. aeruginosa*

I compared the secondary metabolic profiles of *A. fumigatus* monocultures with those of *A. fumigatus* / *P. aeruginosa* mixed cultures between strains, as analysed by LC-MS and high resolution LC-MS. While no differentially produced new peaks attributable to the fungus could be found in the secondary metabolic profile of *A. fumigatus* CEA17 Δ *akuB* in co-culture with *P. aeruginosa*, the CF10 strain demonstrated a clear activation of expression of a secondary metabolite completely absent in the axenic culture control (Figure 13a). In the monoculture, at retention time (RT) 13.4 min, the chromatographic analysis showed a double peak with UV maxima at 335 and 350 nm, characteristic for fumagillin (Figure 13b) (Wiemann et al., 2013). However, at the same retention time, the extract of Af CF10 and PsA co-culture showed a different peak, with a single shoulder and an UV absorption maximum at about 354 nm.

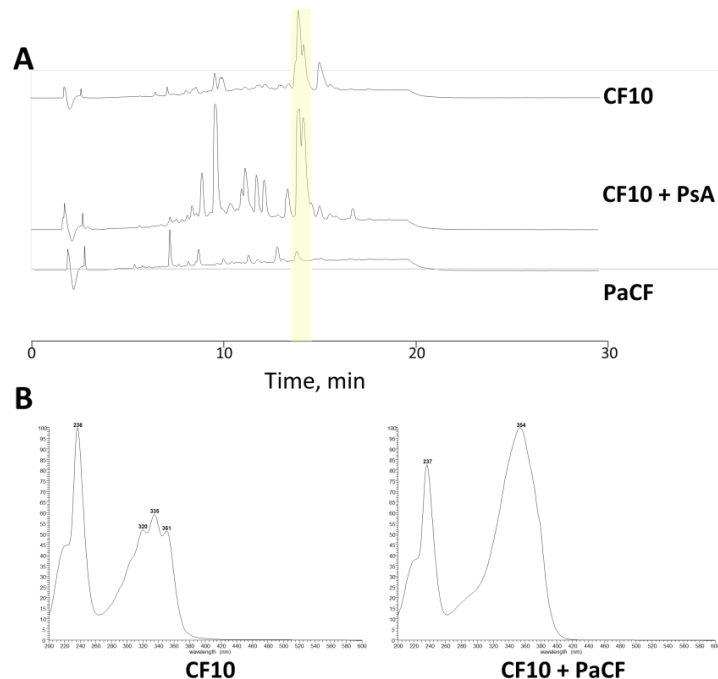


Figure 13. A novel peak appears in the LC-MS analysis of the organic extract of *A. fumigatus* CF10 and *P. aeruginosa* co-culture. (A) A new peak was observed in the chromatogram of the *A. fumigatus* CF10 and *P. aeruginosa* co-culture extract analysis, overlaying the original peak of fumagillin in monoculture. (B) PDA analysis revealed that the absorption spectra of the aforementioned peak are indicative of a new compound, with absorption maxima at 237 and 354 nm. In contrast, the compound with the same retention time in monoculture shows multiple absorption maxima indicative of fumagillin.

High resolution mass spectrometry of the peak in question determined a mass-to-charge ratio m/z 381.0554 $[M-H]^-$, with a predicted elemental composition of $C_{19}H_{13}N_2O_5S$ (calculated mass for $C_{19}H_{13}N_2O_5S$ 381.0551). Interrogation of available mass spectral databases (MassBank, ChemEBI) revealed a compound with a corresponding mass and molecular formula, BU-4704 (Figure 14a).

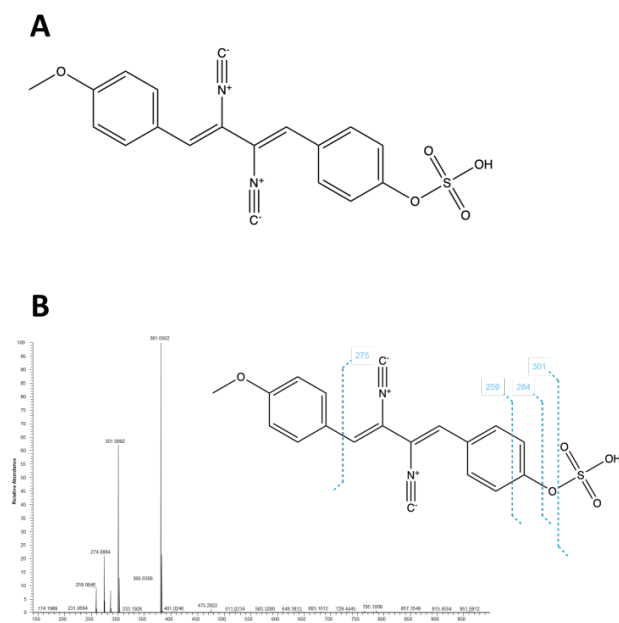


Figure 14. BU-4704, an isonitrile alkaloid, is the novel compound produced by *A. fumigatus* CF10 (A) Structure of BU-4704 (Tsunakawa *et al.*, 1993). (B) Proposed fragmentation pattern of BU-4704 correlates with the fragmentation pattern observed in HRESIMS for the newly identified compound found in co-culture.

This isonitrile-containing xanthocillin derivative was previously reported as a product of *Aspergillus* sp., whose production was triggered by a specific rich medium (Tsunakawa et al., 1993), and, along with other *N*-formylated isonitrile compounds, by interaction with the Gram-positive actinobacterium *Streptomyces peucetius* (Zuck et al., 2011). The identity of the compound was further confirmed by analysing the fragmentation pattern, with characteristic losses of sulphonate and sulphate moieties, as well as an aromatic ring cleavage at the other pole of the molecule (Figure 14b).

Furthermore, a second, heretofore unidentified BU-4704 congener (here designated as BU-4704B) is synthesised by *A. fumigatus* during co-cultivation, lacking the double bond adjacent to the isonitrile function of sulphated tyrosine (Figure 15).



Figure 15. A previously unidentified compound, BU-4704B, is produced by *A. fumigatus* CF10 alongside BU-4704. (A) Structure of BU-4704B, as proposed by HRESI-MS analysis. (B) EIC for m/z 383 (+) shows that BU-4704 is produced exclusively in co-culture of *A. fumigatus* CF10 confronted with *P. aeruginosa*. (C) Proposed fragmentation pattern of BU-4704B correlates with the fragmentation pattern observed in HRESI-MS for the newly identified compound.

3.1.1 BU-4704 and BU-4704B are produced by an uncharacterised gene cluster of *A. fumigatus*

Structurally, BU-4704s are nitrilated aryl sulphate alkaloids with a tail-to-tail joined dityrosine backbone. It was therefore hypothesised that the compounds are produced by a non-ribosomal peptide synthetase and/or an isonitrile synthase. As indicated in Section 2.2.2 of Introduction to the present work, the latter group of enzymes is relatively well-studied in bacteria, but the fungal isonitrile synthases had not been functionally characterised at the time of the study. To identify the biosynthetic enzymes responsible for the production of BU-4704 and its saturated derivative, I therefore explored the bacterial isonitrile synthase counterparts producing a structurally similar compound.

Incidentally, the *pvc* operon of *P. aeruginosa*, canonically associated with the production of pseudoverdine and the pyoverdine chromophore, produces paerucumarin, an additional iron-chelating molecule with an isonitrile-containing dihydroxycumarin structure (Clarke-Pearson & Brady, 2008). In the first step of the biosynthetic process, PvcA (isonitrile synthase) functionalises the amino group of a tyrosine into a nitrile, and the intermediate is subsequently oxidised by PvcB to yield an intermediate unsaturated bond at the α -carbon, effectively creating a monomeric part of the xanthocillin backbone (Figure 16).

Acknowledging the expected differences between the prokaryotic and eukaryotic secondary metabolic enzymes, the sequence of the pseudomonadal *pvcA* gene (PA2254) and its protein product were used in a BLAST analysis against the annotated *A. fumigatus* genome sequences in an attempt to find an orthologous sequence. The search led to the identification of multiple isonitrile synthase domain-containing genes:

Afu3g13690/13700, Afu4g01420, and Afu5g02660 (N.B. given that *A. fumigatus* CEA17 \DeltaakuB did not produce the xanthocillin derivative in co-culture, BLAST search results of *A. fumigatus* Af293 were taken into consideration). Of the identified candidates, only the former is part of canonical biosynthetic gene cluster, with an adjacent NRPS gene (Afu3g13730), and Afu5g02660 shows a higher sequence similarity with both *pvcA* and *pvcB* than Afu4g01370 (30.24% and 23.74% identity, respectively).

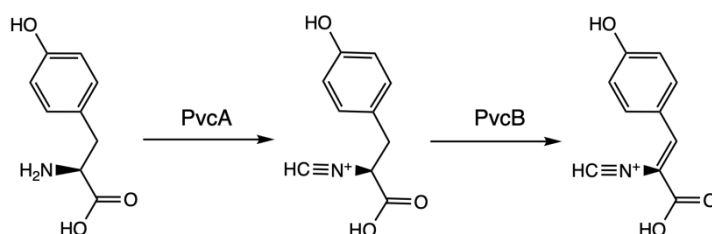


Figure 16. First two steps of the proposed biosynthesis pathway of paerucumarin. PvcA converts the amine function of tyrosine into an isocyanide, and PvcB oxidises the adjacent bond between α and β carbons (Clarke-Pearson and Brady, 2008)

Hypothesising that Afu5g02660 is the fungal gene encoding the isocyanide synthase responsible for the biosynthesis of BU-4704, its sequence homologue was found in *A. fumigatus* CF10 genome to be CF10_04996. The DNA and amino acid sequences of CF10_04996, a suspected isocyanide synthase, were analysed using the CD-search tool to verify the presence of an isocyanide synthase domain. The analysis showed that the protein contains a DIT1/PvcA domain conserved among nitrilated dityrosine synthases, as well as an additional taurine dioxygenase domain, presumably responsible for oxidising the bond between the α and β carbon atoms of tyrosine (Marchler-Bauer et al., 2017) (Figure 17).

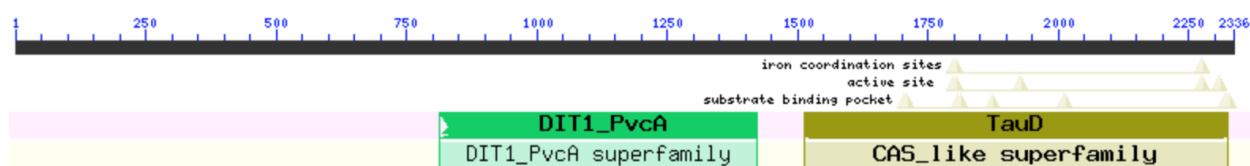


Figure 17. Conserved domain analysis of the DNA sequence of CF10_04996, a suspected isocyanide synthase. The analysis was performed using the CD-search web tool (<https://www.ncbi.nlm.nih.gov/Structure/cdd/wrpsb.cgi>). A Dit1/PvcA-like isocyanide domain and a TauD-like dioxygenase domain were found to be present in CF_04996.

Additionally, the genomic context of CF10_04996 was characterised. Owing to the provisional format and annotation of the CF10 strain, the genome of *A. fumigatus* Af293 and the genomic context of Afu5g2660 were also used as a proxy to identify genes associated with the biosynthetic gene cluster. Based on the results of another function prediction analysis by CD-search, the series of five genes clustered directly upstream of CF10_04996 encode a Dit2-like oxidoreductase (CF10_4991), a hypothetical protein (CF10_04992), a putative *O*-methyltransferase (CF10_04993), a protein of unknown function (CF10_04994), and a basic leucine zipper transcription factor; similarly, the adjacent downstream gene encodes a protein similar to a pseudomonadal isocyanide hydratase (CF10_04997) (Figure 18). The transcriptome analysis of the data support the

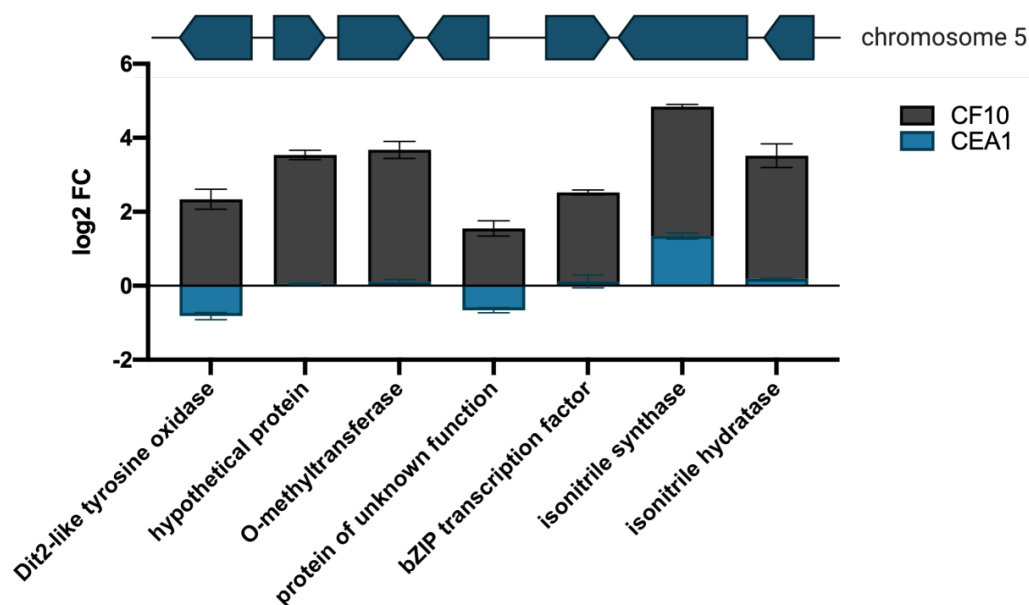


Figure 18. Gene composition and expression pattern of the BU-4704-producing biosynthetic gene cluster. The genes correlate with the *xan* biosynthetic gene cluster described by the group of Keller (Lim *et al.*, 2019). In *A. fumigatus* CF10, a clear upregulation of the cluster genes was observed in RNA sequencing data in response to co-cultivation with *P. aeruginosa*.

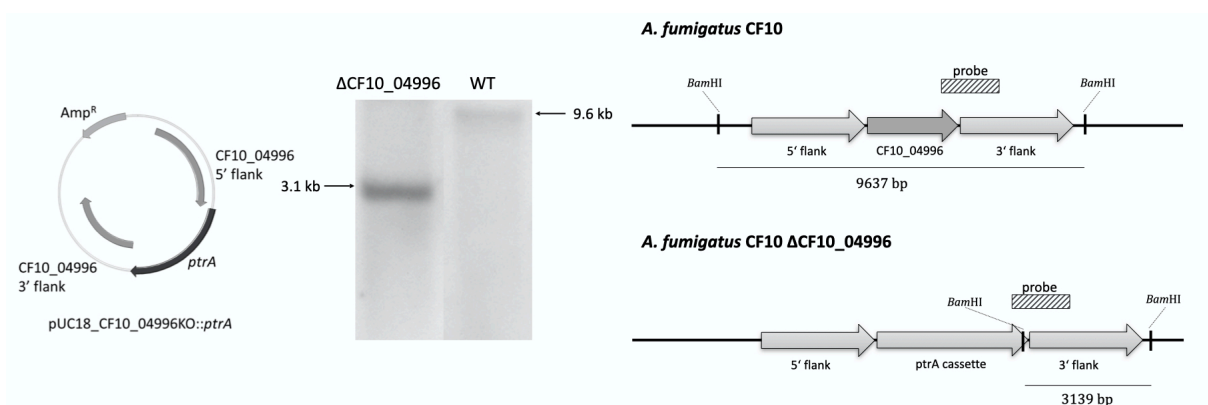


Figure 19. Generation of *A. fumigatus* Δ CF10_04996 mutant. The plasmid pUC_CF10_04996KO::ptrA was assembled by ligating *Hind*III-linearised pUC18 plasmid backbone with PCR-amplified DNA fragments: 1.5 kb flank upstream of the CF10_04996 ORF (CF10_04996 5' flank), *ptrA* resistance cassette, and 1.5 kb flank downstream of the CF10_04996 ORF (CF10_04996 3' flank). The gene deletion was achieved by homologous recombination of the gene-flanking sequences with the genomic sequence, substituting the *ptrA* cassette for *chtA*. Southern blot was used to verify the mutant, where a *Bam*HI restriction site was added due to the insertion of the *ptrA* cassette. A dig-dUTP-labelled probe was directed to a sequence overlapping the *ptrA* cassette and the 3' flank. Expected wild-type band was at 9.6 kb, expected mutant band was at 3.1 kb.

involvement of the listed genes. In CF10, all these genes were upregulated after 24 h in response to co-cultivation with *P. aeruginosa* (Figure 18). Interestingly, each of the constituent genes of the suggested cluster has a homologue in the *A. fumigatus* CEA17 Δ *akuB* (AFUB_015150 - AFUB_015210). However, the production of a xanthocillin-type compound by this strain was never detected in axenic or mixed cultures. This correlates well with the RNA sequencing results: the expression of the cluster genes in CEA17 Δ *akuB* remained baseline regardless of the tested conditions. The

reason behind this discrepancy remains unknown. There are, for example, numerous sequence differences between the cluster transcription factors of each strain; however, any potential inactivation of a cluster by mutation of its native regulatory element fails to explain the transcriptional inactivity of all genes in CEA17 \DeltaakuB .

Assuming that the CF10_04995 gene encodes the dityrosine/isocyanide synthase essential for the production of BU-4704, the loss of this gene should lead to the loss of compound production in the mutant strain. The gene was therefore deleted in *A. fumigatus* CF10 by homologous recombination and replaced by the pyrithiamine resistance *ptrA* cassette, and the deletion mutant verified by Southern blotting (Figure 19). Subsequently, the mutant was co-cultivated with *P. aeruginosa* in agitated liquid cultures, and the organic extract of the culture analysed by LC-MS for the presence of BU-4704 and its reduced congener (m/z 383 [M-H]⁻). As shown before, the wild-type strain produced both compounds when triggered by interaction with the bacterium, but not in an axenic culture. In contrast, the *A. fumigatus* CF10 Δ CF10_04996 mutant strain lost the ability to synthesise the compounds, irrespective of the presence of the bacterium (Figure 20), confirming that CF10_04996 indeed encodes the isonitrile synthase producing the xanthocillin derivatives.

It has been indicated that the presence of the isonitrile moiety in various isonitrile- and *N*-formyl-functionalised secondary metabolites often imparts biological activity (Section 2.2.2 of Introduction). Due to the clear activation of biosynthesis of BU-4704 and its saturated derivative in response to the presence of *P. aeruginosa* in the culture, I hypothesised that the compound might act as an antibiotic agent, limiting the growth of the bacterium. To test the hypothesis, *A. fumigatus* CF10 and the Δ CF10_04996 mutant were confronted with *P. aeruginosa* on SCFM2 agar plates, where the interaction could be

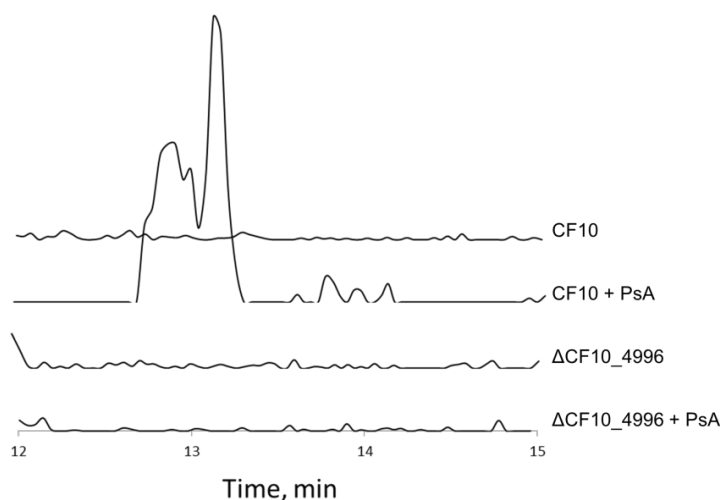


Figure 20. BU-4704 and BU-4704B are not produced by *A. fumigatus* CF10 Δ CF10_04996. EIC for m/z 381 - 383 is shown. Both compounds are induced by co-cultivation of *P. aeruginosa* with the CF10 wild-type strain. In Δ CF10_04996, lacking the isonitrile synthase gene, no metabolites were detected, irrespective of the presence of the bacterium in the culture.

observed. Confirming the results suggested by Tsunakawa *et al.*, (1993) when the xanthocillin derivative was first published, BU-4704 did not appear to have a noticeable antibiotic effect on *P. aeruginosa*. On the confrontation plates, the wild-type and the mutant strains had an identical phenotype, with the wild type displaying no obvious selective growth advantage in the interaction zone that could be ascribed to the production of the BU-4704 (Figure 21).

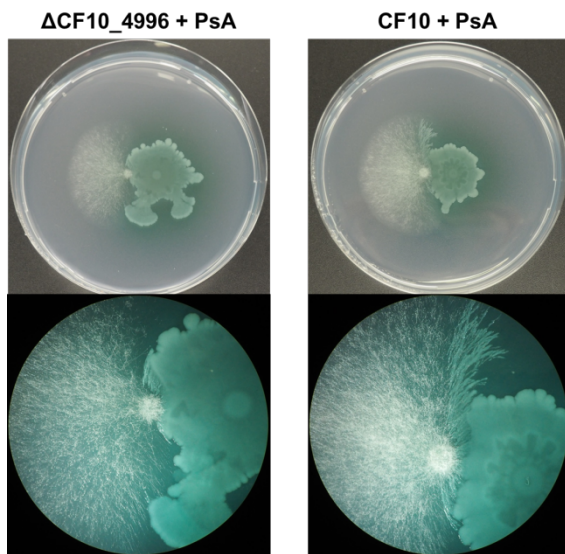


Figure 21. BU-4704 and BU-4704B triggered by *P. aeruginosa* do not confer a selective advantage in interaction on the producing *A. fumigatus* CF10 strain. Both CF10 and Δ CF10_04996 showed the same phenotype when confronted with *P. aeruginosa*. The mild antibiotic effect of BU-4704 (Tsunakawa *et al.*, 1993) does not translate into an inhibitory effect on the bacterium.

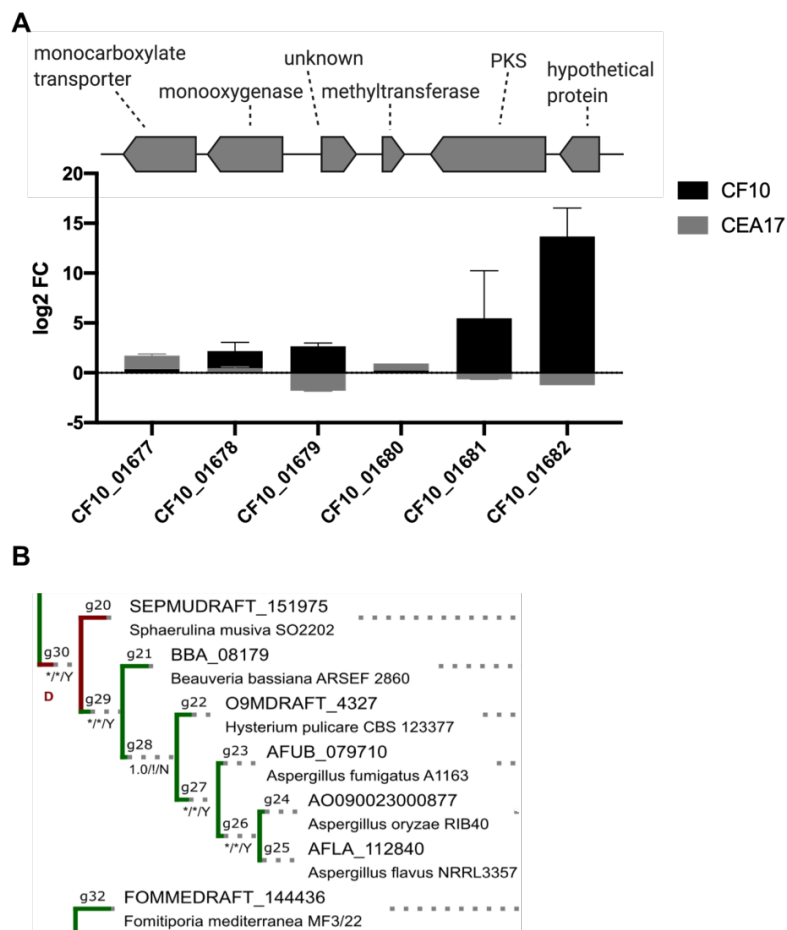


Figure 22. Inactive PKS biosynthetic gene cluster in *A. fumigatus*. (A) Gene composition and expression pattern of the constituent gene in the PKS cluster. Upregulation of expression of the PKS gene and an adjacent predicted hypothetical protein were observed in the CF10 strain. In CEA17 Δ akuB, the expression profile is unchanged in co-culture. Absolute amounts of transcripts were close to zero. (B) Orthologues of the PKS gene can be found in multiple other fungi. To the best of our knowledge, neither has been characterised in detail or attributed with production of a metabolite.

Thus, the biosynthesis of xanthocillin-type antibiotics by *A. fumigatus* does not represent any apparent role in the interaction of the fungus with *P. aeruginosa*. Concomitantly with the experimental part of the present work, the group of Keller published a comprehensive characterisation of isonitrile synthases of *A. fumigatus*, their regulation in response to copper and their chalkophore properties (Lim et al., 2018). This study corroborates the findings of a previously uncharacterised, xanthocillin-producing cluster presented here.

3.2 *A. fumigatus* CF10 harbours a non-functional PKS cluster

Among the most highly upregulated genes of the cystic fibrosis isolate strain CF10 in co-cultivation with *P. aeruginosa* belongs a putative biosynthetic gene cluster with a polyketide synthase backbone enzyme, CF_01677 - CF10_01681 (Figure 22a). The cluster has a homologue in *A. fumigatus* CEA17 \DeltaakuB (AFUB_045420 - AFUB_045460), as well as multiple other species (Figure 22b). However, the RNA sequencing data of the CEA17 \DeltaakuB strain suggest that *P. aeruginosa* does not elicit transcriptional activation of the cluster. Since this cluster has not been described before and was highly upregulated in one of the strains in response to *P. aeruginosa*, it was of interest to characterise the cluster, identify the associated secondary metabolite produced by the PKS, and elucidate its role in the interaction with the bacterium.

The identified biosynthetic gene cluster does not contain a native transcription regulator that could be manipulated to artificially induce expression of the cluster genes. Thus, the predicted PKS gene from the cystic fibrosis isolate, CF10_01681, was deleted instead, assuming that removal of the producing enzyme would result in the lack of a compound, which could be detected by LC-MS analysis. To this effect, the Δ CF10_01681 mutant was co-cultured with *P. aeruginosa* to induce cluster activation, secondary metabolites extracted from the culture supernatant, and the extract analysed. Surprisingly, despite the pronounced upregulation of all the genes within the cluster, no compound was detected that could be attributed to the cluster, *i.e.* in chromatographic and spectrometric analyses, the CF10 wild type and the Δ CF10_01681 mutant produced identical results (data not shown). Later, it was discovered that the fungus likely secretes the PKS enzyme, as it was found to be among the most enriched proteins in the secretome analysis of *A. fumigatus* and *P. aeruginosa* co-culture. It was therefore concluded that the cluster, despite the promising upregulation during interaction, was dysfunctional.

3.3 MALDI-IMS analysis

In addition to chemical analysis of liquid co-cultures, *A. fumigatus* and *P. aeruginosa* were cultivated on solid SCFM2 agar at a 1 cm distance from one another and the interaction zone was analysed by matrix-assisted laser desorption ionisation imaging mass spectrometry (MALDI-IMS, Figure 23). Apart from providing insight into the chemistry of microbial interaction, this method enables spatial resolution of the individual compounds. Simultaneous pinpointing of the location and abundance of metabolites in the interaction, be it directly the confrontation zone, or on the poles, where the microbes are not in contact, contributes to understanding the metabolites' role in the process. Precise compound identification, however, can become difficult due to the lack of fragmentation spectra, and identification of compounds relies on exact mass measurements.

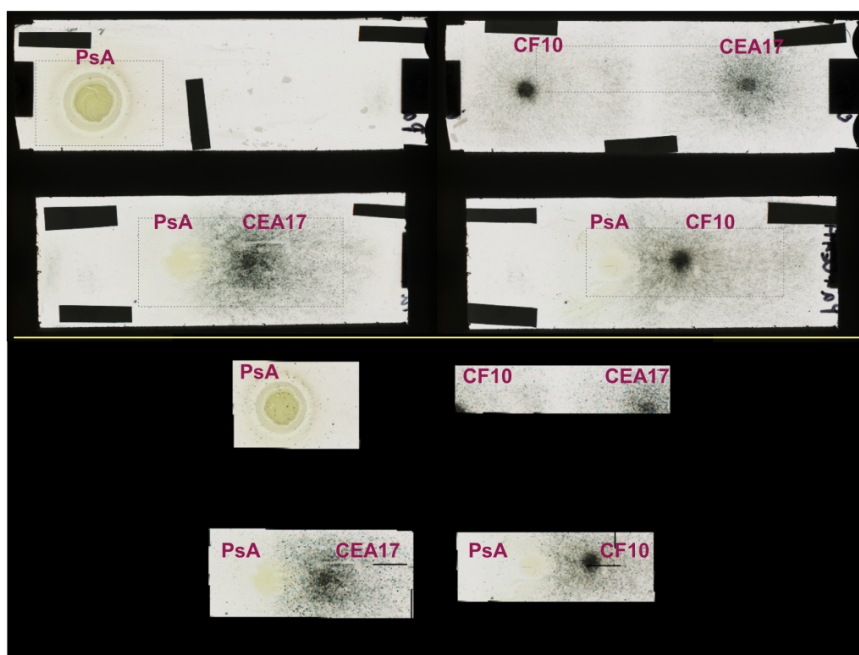


Figure 23. Layout of the samples used for MALDI-IMS. The pictures of cultures of *A.fumigatus* CEA17 and CF10, and *P.aeruginosa* (PsA) grown on SCFM2 agar deposited on ITO slides following desiccation. Representative portions of each of the axenic cultures and both co-cultures (bottom panel) were selected for measurements. This layout was used in all the analysed images in the following section.

The most prominent chemical interaction observed on solid SCFM2 agar plates is the differential production of relatively large compounds, with molecular weight ranging between 700 and 1,000 Da (Figure 24a). Interrogating the MassBank database, the compounds could be identified as rhamnolipids, synthesised by *P.aeruginosa*. These pseudomonadal biosurfactants belong to the class of glycolipids, and incorporate a single or double rhamnose glycosyl moiety linked to a 3-(3-hydroxyalkanoyloxy)alkanoate (HAA) fatty acid chain by means of an ether or an ester bond (Cabrera-Valladares et al., 2006). Rhamnolipids are diverse, with the structural heterogeneity underpinned by length and degree of branching of the HAA function, depending on growth media and culture conditions (Desai & Banat, 1997; Mulligan, 2005). They have long been recognised as quorum sensing-dependent virulence factors of *P.aeruginosa* (Zulianello et al., 2006), which, furthermore, also possess antimicrobial activity against multiple bacterial species (ITO et al., 1971). More recently, it was shown that rhamnolipids are also antifungal agents, effective against the environmental *Fusarium solani*, *Penicillium funiculosum* (Haba et al., 2002), but also *A.fumigatus* (Briard et al., 2017). It was therefore interesting to find that while there is a set of dirhamnolipids produced by the bacterium directly in the interaction zone or within the bacterial colony subjected to *A.fumigatus* (m/z 770.7 [M+H]⁺ or 792.6 [M+Na]⁺; 778.5 [M+Na]⁺ or 794.5 [M+K]⁺; 804.5 [M+Na]⁺ or 820.3 [M+K]⁺; 984.7 [M+Na]⁺ or 1000.7 [M+K]⁺; Figure 24b). These masses are not found, or only found in low amounts, in the axenically grown colony of *P.aeruginosa*. Conversely, another set of rhamnolipids was found in the bacterial monoculture (m/z 675.1 [M+H]⁺; 711.6 [M+H]⁺; 776.3 [M+H]⁺; 824.7 [M+H]⁺; Figure 24c). Detection of such structurally diverse rhamnolipids further supports the findings of both, the structure dependency, as well as the deployment of dirhamnolipids in interaction with *A.fumigatus*. Given the lack of overlap between the two sets of rhamnolipids described above, these findings also suggest that *P.aeruginosa* adjusts the biosurfactant production to reflect the environmental situation and uses different types of rhamnolipids when grown alone, as opposed to a co-culture.

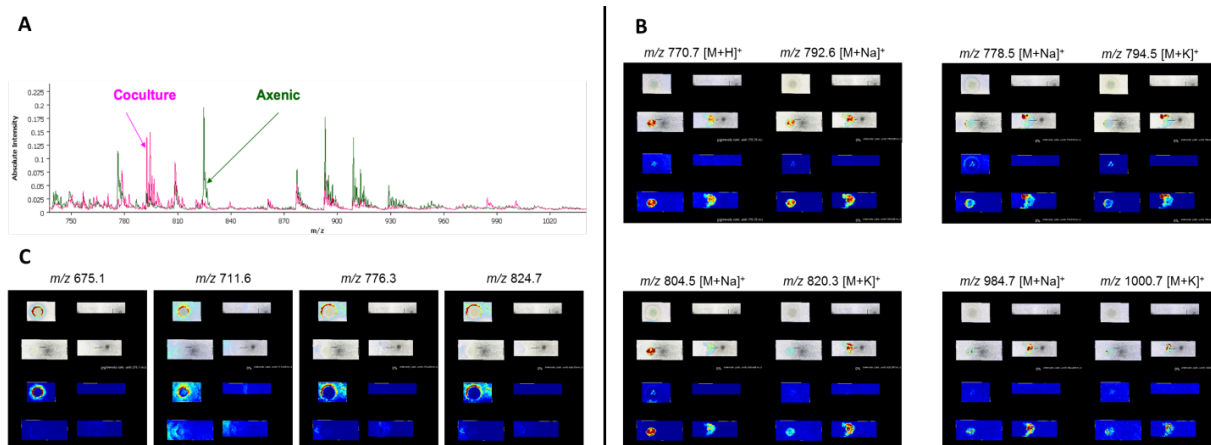


Figure 24. Rhamnolipids produced by *P. aeruginosa* alone and in co-culture with *A. fumigatus*. (A) Total ion content of the analysed cultures, displaying differences in the chemistries of axenic cultures (green) and co-cultures (pink), in the range of 700 - 1000 Da. (B) Suspected dirhamnolipids produced by *P. aeruginosa* when co-cultivated with *A. fumigatus*, irrespective of the strain. The distribution pattern within the samples is the same for all compounds. (C) Structurally different dirhamnolipids with different molecular masses are produced by *P. aeruginosa* grown axenically. The same compounds do not occur co-culture, or are only present as faint signals distal to the bacterial-fungal interface zone.

Another pseudomonadal compound found to be produced in different abundance between axenic and mixed cultures is pyoverdine, a high-affinity siderophore. *P. aeruginosa* produces three pyoverdine congeners, pyoverdines C, D, and E (Briskot et al., 1986). In the present analysis, I found three masses, correlating to pyoverdine E and its sodiated and potassiated ions (m/z 1333.9 [M+H]⁺; 1356.4 [M+Na]⁺; 1372.5 [M+K]⁺; Figure 25). Sass *et al.* asserted that through pyoverdine sequestration, pyoverdine is the main pseudomonadal inhibitor of *A. fumigatus* growth (Sass et al., 2019). This claim is based on the treatment of developing *A. fumigatus* biofilm by extract of *P. aeruginosa* monocultures. Here, however, the apparent abundance of pyoverdine E was

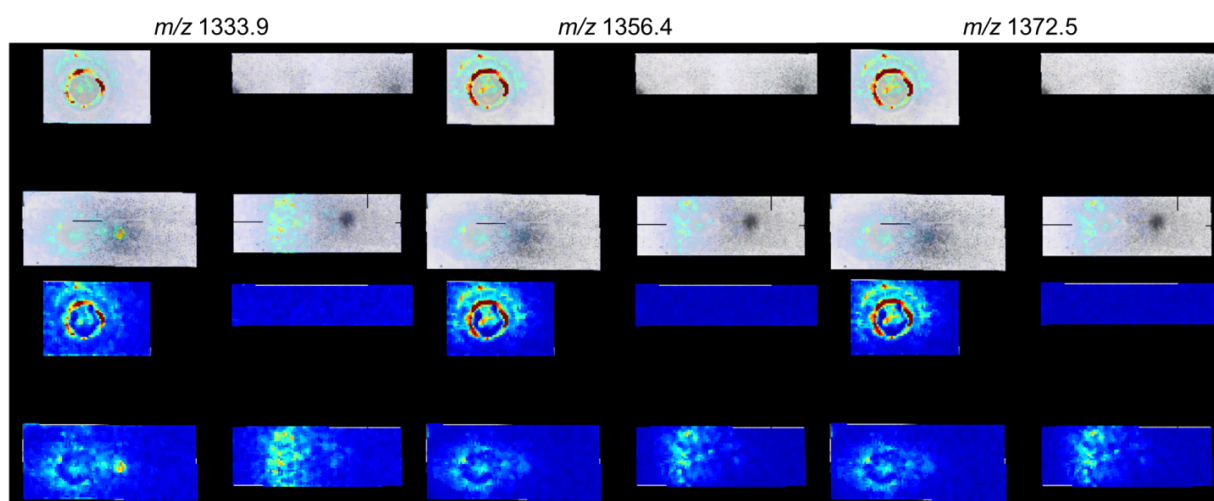


Figure 25. Abundance and distribution of pyoverdine produced by *P. aeruginosa* in monoculture and co-culture with the fungus. Pyoverdine E was detected in three forms, as a simple dehydrogenated cation, m/z 1333.9 [M+H]⁺; a sodiated ion, m/z 1356.4 [M+Na]⁺; and a potassiated ion, m/z 1372.5 [M+K]⁺. Surprisingly, the abundance of the ions was higher in bacterial monocultures than in bacterial-fungal co-cultures, suggesting that the inhibitory role of pyoverdine (Sass *et al.*, 2019) might not be as relevant to the interaction in CF sputum as formerly assumed.

considerably lower than in monoculture, and the signal present in the colony co-cultured with the fungus did not show a directional tendency, *i.e.* the production is general, rather than directed against *A. fumigatus*. This resembles the changing expression profile of fumagillin, pseurotin A, or fumiquinazoline F/G toxins in the fungus in co-cultivation with *P. aeruginosa* (Figure 11). Thus, these results shed new light on the communication between the fungus and the bacterium, and challenge the reductionist approach to studying of microbial interactions; the fact that a compound produced by one partner shows an inhibitory effect on the other does not invariably mean that the compound is, indeed, really used in the suggested manner when the two microbes are in close proximity to each other. Furthermore, none of the products of biotransformation of phenazines suggested by the group of Dorrestein (Moree et al., 2012) were reliably detected. In the study, the authors grew *A. fumigatus* and *P. aeruginosa* in close proximity on yeast malt agar plates, which could explain the different phenotype in comparison to SCFM2.

Several unidentified ions were found to be produced by *A. fumigatus* exclusively in response to co-cultivation with the bacterium, in a strain-dependent fashion (Figure 26). A compound with m/z 162.5 (+) (potential diketopiperazine), m/z 204.3 (+), and m/z 296.4 (+) were both produced in high abundance in CEA17 \DeltaakuB selectively in co-culture with *Pseudomonas*, while being completely absent in the CF10 strain, independent of the conditions. Two ions specific for CF10 were m/z 586.2 (+) and m/z 664.3 (+). These ions were, however, not exclusive to co-culture, and were also found in high abundance in monoculture (Figure 26). Further study and identification were impossible due to the fact that none of these ions were detected again in extracts analysed by conventional LC-MS method. Additionally, in a preliminary uncontrolled experiment, with measurement carried out in negative ionisation mode (MALDI-IMS is customarily carried out in positive ionisation mode), the xanthocillin derivative BU-4704 was detected; this compound's chemical structure with nitrile, hydroxide, and sulphate functions precludes positive ionisation.

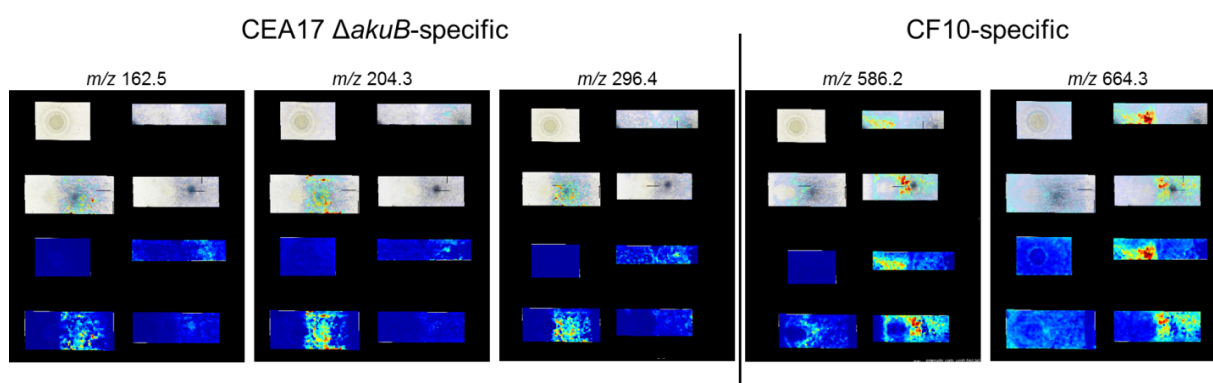


Figure 26. MALDI-IMS revealed the production of unknown strain-specific metabolites triggered by the co-culture. These metabolites were not detected in extracts of liquid cultures of the same strains and thus could not be further characterised within the scope of this work.

4 Fungal and bacterial siderophores in the interaction

4.1 *A. fumigatus* does not disrupt quorum sensing of *P. aeruginosa*

The obvious downregulation of pyoverdine, pseudomonadal high-affinity siderophore, during co-cultivation of *P. aeruginosa* with *A. fumigatus* on solid SCFM2 agar inspired the question whether *A. fumigatus* is capable of causing siderophore dysregulation in the bacterium by disrupting quorum sensing (QS)-dependent signalling. Pyoverdine biosynthesis is a costly process triggered under iron starvation conditions; thus, it is heavily regulated through a quorum sensing signalling network (Stintzi et al., 1998). Since this network is complex, interconnected, and contains multiple compensatory mechanisms in case of inactivation of a constituent part (Lee & Zhang, 2014), I decided to use a proxy system to evaluate potential disruptions to QS by the fungus. The LasR-LasI QS system uses *N*(3-oxododecanoyl)homoserine lactone (C12-HSL) to feed into the RhlR-RhlI system, communicating environmental hypoxia, starvation, and low iron conditions, and the disruption of this system results in a 2-fold decrease of pyoverdine

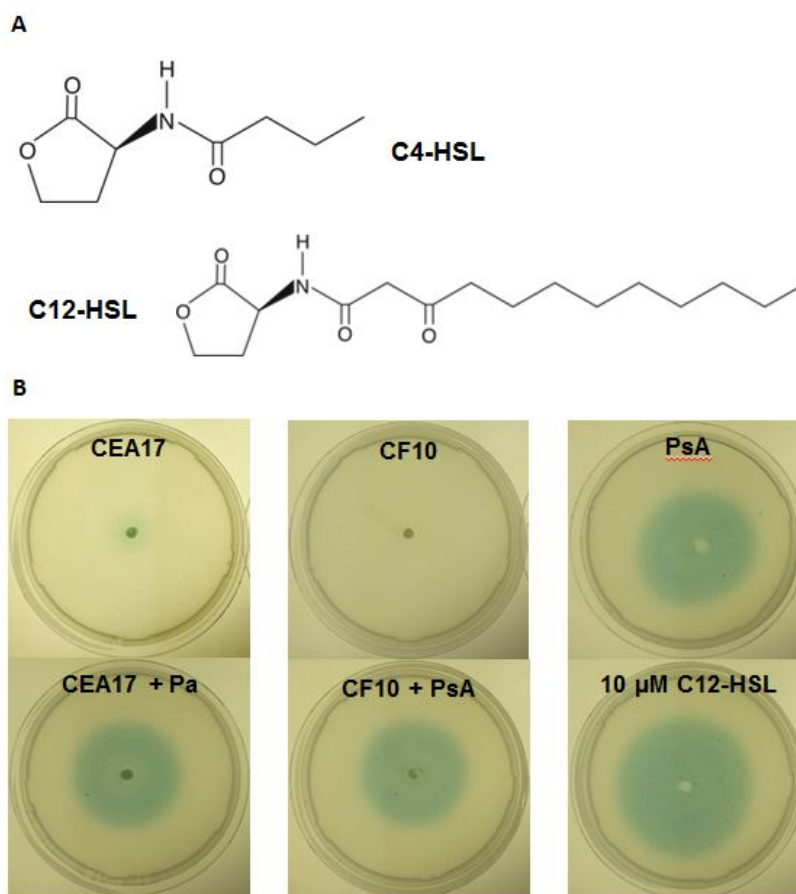


Figure 27. Quorum sensing of *P. aeruginosa* in SCFM2-based co-culture with *A. fumigatus*. (A) Structures of *N*-butyrylhomoserine lactone and *N*-(3-oxododecanoyl)homoserine lactone, QS signalling molecules used by the *rhl* and *las* systems, respectively (Lee and Zhang 2015). (B) The bioreporter strain *Agrobacterium tumefaciens* NTL4(pCF218) was treated with concentrated organic extracts of liquid monocultures and co-cultures of *A. fumigatus* CEA17 Δ *akuB* and CF10 with *P. aeruginosa*. 10 μ M pure C12-HSL was used as positive control. While the extracts of the fungal strains did not induce QS-triggered pigment formation, a clear blue halo was visible in samples treated with extracts of *P. aeruginosa*-containing samples. No difference was observed between *P. aeruginosa* monoculture and co-culture, suggesting that *A. fumigatus* does not have an effect on direct *las*-dependent quorum signalling in the bacterium.

production (Stintzi et al., 1998; Lee & Zhang, 2015; Ding et al., 2018). Here, *Agrobacterium tumefaciens* NTL4(pCF218)(pCF372) was used, which produces β -galactosidase upon induction by externally provided acyl homoserine lactones (AHL) and can degrade X-Gal (5-bromo-4-chloro-3-indolyl- β -d-galactopyranoside), forming an insoluble indigo pigment (Kawaguchi et al., 2008). Cultures of the bacterium were prepared by overlaying minimal AB medium agar plates with a 0.5% AB agar suspension of the *Ag. tumefaciens* biosensor strain supplemented with X-Gal (5-bromo-4-chloro-3-indolyl- β -d-galactopyranoside). A hole was bored in the centre of the plate and organic extracts of *A. fumigatus* and *P. aeruginosa* axenic and mixed cultures were deposited in the cavity. The presence of the pseudomonadal C12-HSL activated the β -galactosidase promoter and the consequent formation of a blue halo in the agar was indicative of ongoing QS signalling (Figure 27). The blue halo was observed when an extract of axenic *P. aeruginosa* culture was added. Fungal monocultures extract produced no halo. The faint colour around CEA17 \DeltaakuB supernatant was always present and considered an artefact of a leaky promoter, rather than an indication of an AHL being formed by *A. fumigatus*). The organic extracts of co-cultures produced halos of comparable diameter as that of the bacterial monoculture. This result implies that the concentration of C12-HSL in the cultures is approximately the same, regardless of the presence of *A. fumigatus*. Thus, the homoserine lactone product is not degraded by the fungus and this QS system is still functional in *P. aeruginosa* in co-culture. The RhlR-RhlI system relies on *N*-butyrylhomoserine lactone.

Since the reporter system in *Ag. tumefaciens* responds to AHLs with a longer aliphatic chain, *Chromobacterium violaceum* CV026 reporter strain, responsive to short-chain AHLs, was used to investigate the presence of C4-HSL. In this biosensor, the production of the purple pigment violacein is conditioned by the presence of exogenous AHL. Similarly to the *Ag. tumefaciens* setup, *C. violaceum* CV026 was seeded in semi-solid LB agar and overlaid on an agar plate. Like before, samples of fungal and bacterial cultures were added into a hole bored in the centre of the plate. In this instance, however, no colour formation was observed at all, even in a positive control, where the bacterium was treated with 10 μ M C4-HSL standard (data not shown). The reporter strain was exclusively responsive to higher (>20 μ M) concentrations of C4-HSL, leading to the conclusion that in SCFM2, *P. aeruginosa* produces C4-HSL in low abundance only. During the study, no reporter strains were available to test for the interference of *A. fumigatus* with the other two *Pseudomonas* QS systems, namely PQS (*Pseudomonas* quinolone signal) and IQS (integrated quinolone signal) (Lee & Zhang, 2015).

4.2 *P. aeruginosa* is likely capable of using TAFC as a xenosiderophore

The evident drop in abundance of the main iron siderophore of *P. aeruginosa* in co-culture with *A. fumigatus* leads to the conclusion that the bacterium must rely on other means of acquisition of this essential nutrient. As outlined in Section 3.1.1 of Introduction, *P. aeruginosa* has other means of iron sequestration available, namely through coordination by pyochelin, by haem-binding proteins, and *via* phenazine-mediated reductive assimilation (Caza & Kronstad, 2013). Furthermore, *P. aeruginosa* is an accomplished siderophore pirate, importing iron-chelating molecules produced by other species (Cornelis & Dingemans, 2013). I therefore hypothesised that *P. aeruginosa* is also capable of using the main siderophore of *A. fumigatus*, *N,N,N'*-triacetylfusarinine, to obtain iron for its own growth. This hypothesis was tested by seeding iron-deficient M9 minimal medium with a defined inoculum of *P. aeruginosa*, which was pre-washed in physiological saline to remove traces of iron carried over from the previous cultivation

medium. Beside the PAO1 wild type, a siderophore-deficient mutant $\Delta pvdD\Delta pchEF$ was used as a control group, which, by definition, relies on provision of an accessible exogenous iron source. The cultures were then supplemented with an iron source in a final concentration of 10 μM . Iron was provided in form of iron (III) chloride, ferric pyoverdine (commercial; added as an equimolar mixture of pyoverdine and FeCl_3), and purified ferric TAFc. The cultures were incubated for 24 h at 37°C and following the incubation, optical density of the culture measured at $\lambda = 600 \text{ nm}$. A stark difference could be observed between all the treated samples with ferric siderophores, ferripyoverdine and ferriTAFc alike, and those treated with iron-deficient siderophores (Figure 28). The OD_{600} values measured in cultures treated with ferripyoverdine and ferric TAFc resembled those of the positive control, treated with ferric chloride. In contrast, treatment with either of the empty siderophores resulted in stunted planktonic growth in the culture, reaching OD_{600} resembling that of the negative control. This low amount of growth in iron-limited conditions was presumably maintained due to carryover iron from pre-culture, as well as iron contamination brought in through medium components. This simple experiment confirmed that *P. aeruginosa* does have the capability of supporting its own growth by using TAFc as iron source if no other sources are available.

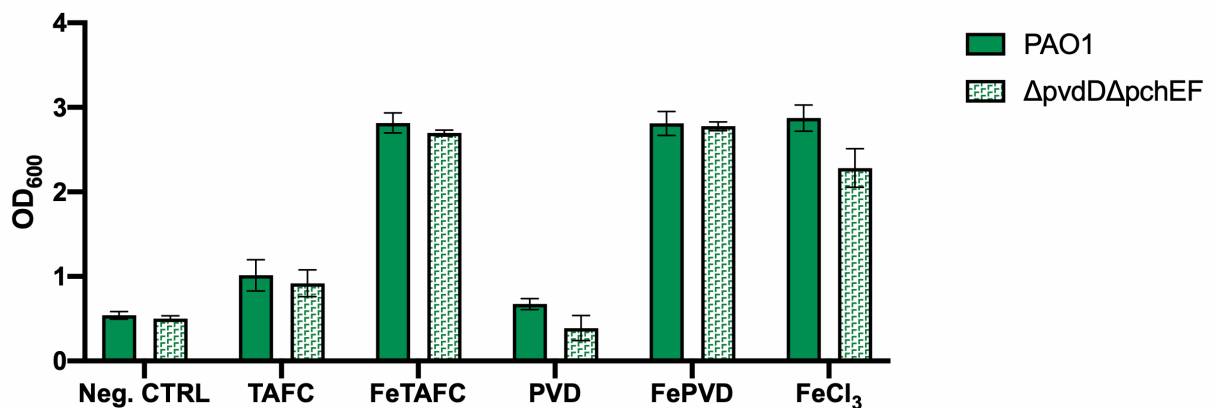


Figure 28. Growth of *P. aeruginosa* PAO1 and a siderophore-deficient mutant $\Delta pvdD\Delta pchEF$ in minimal medium with ferric TAFc as the sole iron source. *P. aeruginosa* strains were grown in M9 minimal medium and provided with ferric TAFc (FeTAFc), ferric pyoverdine (FePVD) and ferric chloride (FeCl_3) as iron sources. Iron-free siderophores were used as control. When treated with FeTAFc as the sole iron source, both wild-type and siderophore-lacking strains restore normal growth in minimal medium, suggesting that *P. aeruginosa* is capable of using FeTAFc as a xenosiderophore for iron acquisition. The rudimentary growth in the negative control group is likely caused by a carry-over of iron from previous cultivation, as well as contamination of medium with trace iron.

4.2.1 Radioactive labelling of TAFc indicates internalisation of the siderophore by *P. aeruginosa*

Next, I set out to investigate the implied internalisation of TAFc by *P. aeruginosa*. The testing was performed by feeding *P. aeruginosa* wild type and $\Delta pvdD\Delta pchEF$ strains with TAFc where iron was substituted by gallium-68. ^{68}Ga is a positron-emitting radioactive gallium isotope which forms trivalent cations and has a similar atomic radius as iron. Gallium-68 can therefore be used to radioactively label TAFc, where it is coordinated with a high efficiency and forms a radiochemically pure (Figure 29) chemically stable complex (Petrik et al., 2010). Iron-starved *P. aeruginosa* was supplemented with the radioactive siderophore complex and allowed time for internalisation; hydrogen

peroxide-inactivated *P. aeruginosa* at the same CFU number was used as control. Supernatant containing excess free ^{68}Ga -TAFc was removed and the radioactivity measured. The positron emitted during the radioactive decay of ^{68}Ga nuclide almost immediately annihilates with an adjacent electron and two 511 keV gamma photons of opposite directions are emitted, which are recorded by a gamma counter.

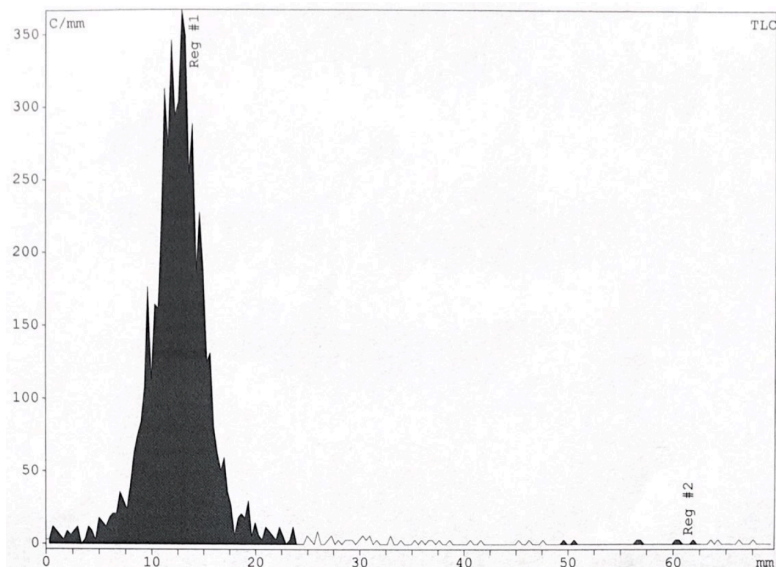


Figure 29. TLC-based analysis of radiochemical purity of ^{68}Ga -TAFc. The single steep peak is generated by the pure radioactively labelled siderophore, meaning that the major proportion of radioactivity within the tested sample is present as the desired ^{68}Ga -TAFc.

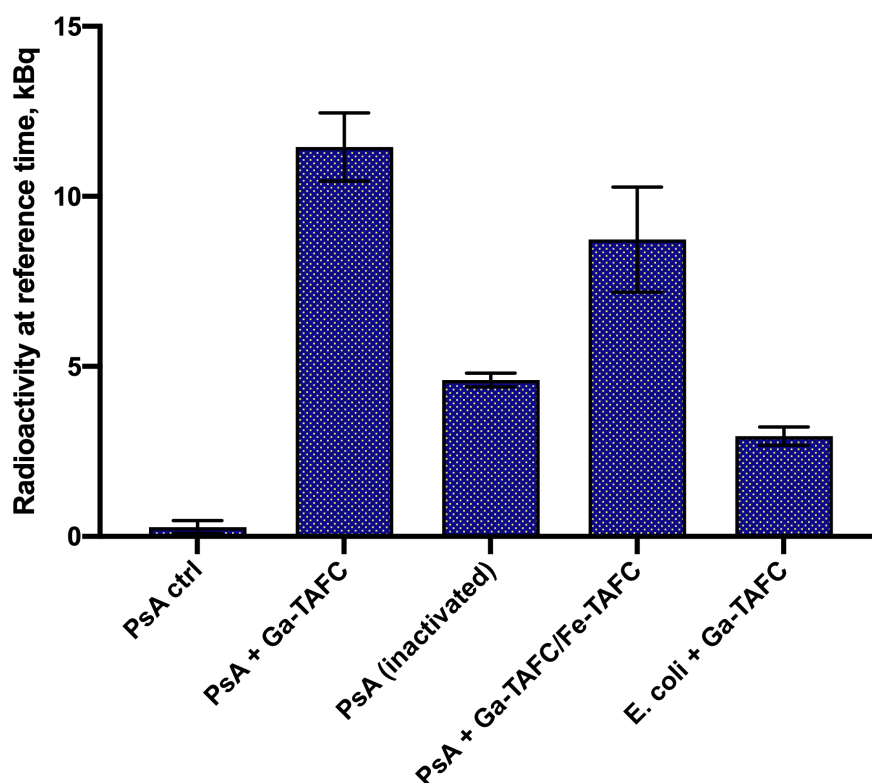


Figure 30. Radioactivity measured within *P. aeruginosa* caused by ^{68}Ga -TAFc internalisation. Iron-starved *P. aeruginosa* treated with ^{68}Ga -TAFc emitted radioactivity detectable by a gamma counter, which can be interpreted as siderophore internalisation. The detectable radioactivity in hydrogen peroxide-inactivated *P. aeruginosa* and *E. coli* is presumably caused by free ^{68}Ga coordinated by LPS on the bacterial surface. Like in the fungus, ferric TAFc serves as a competitive uptake inhibitor of the radioactively labelled TAFc, as evidenced by a drop in detected radioactivity in samples treated with both molecules simultaneously.

The bacterial biomass with internalised ^{68}Ga -TAFC is gamma radiation-active, and is expected to emit radiation; conversely, if no or little internalisation occurred, detected radioactivity should be low. As seen in Figure 30, the untreated *Pseudomonas* control shows no gamma activity. Peroxide-killed *P. aeruginosa* and *E. coli* used as control organism show a low but substantial level of radioactivity - it is presumed that this is caused by adherence of uncoordinated ^{68}Ga that remained after chelation by TAFC. Both *P. aeruginosa* and *E. coli* are Gram-negative bacteria, with surfaces covered with lipopolysaccharide (LPS). The glycan polymer of the O-antigen part of LPS contains multiple hydroxyl groups, each carrying a negative net charge. Thus, the surfaces of even dead bacteria or bacteria unable to internalise TAFC will still form coordination complexes with free positively charged transition metals, effectively acting as “mops” for cations. It is believed that the radioactivity observed in ^{68}Ga -TAFC-treated inactivated *P. aeruginosa* and *E. coli* is caused by the passive “mopping” effect, rather than active uptake of the labelled compound. In metabolically intact *P. aeruginosa*, however, the detected radioactivity is more than double that of the dead control, reaching up to about 12 kBq, which is indicative of an active internalisation of the radioactively labelled siderophore (Figure 30). Research of the group of Decristoforo indicated that ferric TAFC is a competitive uptake inhibitor of the gallium-coordinated form in *A. fumigatus* (Petrik et al., 2010). To investigate whether this metal-specific preference is maintained in *Pseudomonas*, I provided the bacterial sample with equimolar amounts of Fe-TAFC and ^{68}Ga -TAFC. Indeed, the radioactivity measured in these samples was decreased in relation to those treated by ^{68}Ga -TAFC only, but not as low as that detected in inactivated *P. aeruginosa* or *E. coli*. Summarily, these results suggest that *P. aeruginosa* is capable of internalising the *A. fumigatus* siderophore *N,N,N'*-triacetylfusarinine C and liberating iron for its own use. Further investigation into the internalisation process is warranted to validate the claim, including an addition of a metal chelator such as diethylenetriamine pentaacetic acid (DTPA), and elucidation of the pseudomonadal membrane protein responsible for the xenosiderophore uptake. It is worth noting that these results merely indicate the capability of *P. aeruginosa* to use the fungal siderophore for its own growth. This does not, however, mean that it is the preferred, or even commonly used manner of iron acquisition in the environment or a CF patient's lung.

5 LC-MS-based secretome analysis of *A. fumigatus* and *P. aeruginosa* co-culture

Many types of interactions have been described between *A. fumigatus* and *P. aeruginosa* (see Section 4 of Introduction). The interactions observed to date are commonly mediated through microbial communication by various secondary metabolites produced by either of the partners, *e.g.* gliotoxin of the fungus, or phenazines of the bacterium. Beyond their secondary metabolic potential, filamentous fungi are also known for using secreted effector proteins for communication with other organisms; this model has been particularly well described in plant-pathogenic fungi (Rep, 2005; Djamei et al., 2011). Likewise, plant-associated bacteria are known to use protein secretion for communication at the plant-microbe interface (De la Peña et al., 2008). Section 1.2 of Results describes the passive attachment, as well as close proximity and movement arrest of *P. aeruginosa* in presence of *A. fumigatus* hyphae during co-cultivation. It is therefore conceivable that the interplay between these microbes in a CF lung

environment, in addition to direct contact, also happens *via* secreted effectors over a certain distance. I have therefore analysed the total proteins secreted by *A. fumigatus* during co-cultivation in SCFM2 medium. For the purposes of secretome analysis, mucin was omitted from the cultivation medium, as it is impossible to remove from culture supernatant prior to the sample preparation, and its proteinaceous nature and high concentration would render the subsequent analysis impossible.

A gel-free, high resolution LC-MS analysis of secreted proteins present in *A. fumigatus*/*P. aeruginosa* co-culture supernatants was performed. The co-cultivation was carried out in triplicates, proteins extracted from each culture supernatant individually and pooled before analysis. The results of the analysis are presented in Tables 11 and 12.

Table 11. Most highly upregulated proteins in co-culture of *A. fumigatus* and *P. aeruginosa* carried out in SCFM2 medium; change expressed as fold change of abundance ratio Af + PsA/Af

Gene accession number	Function	Abundance ratio
AFUB_095310	Probable exopolygalacturonase	740.57
AFUB_045790	Polyketide synthase, putative	436.60
AFUB_036620	Allantoicase Alc, putative	191.61
AFUB_033190	Cyanide hydratase	117.95
AFUB_011660	Uncharacterized protein	95.96
AFUB_076000	Uncharacterized protein	41.42
AFUB_047290	MFS multidrug transporter, putative	35.66
AFUB_004010	Probable glucan 1,3-beta-glucosidase A	28.17
AFUB_034600	Extracellular dioxygenase, putative	27.29
AFUB_018280	Actin polymerization protein Bzz1, putative	27.28
AFUB_077630	Probable 1,4-beta-D-glucan cellobiohydrolase B	24.69
AFUB_041450	Pectin methylesterase, putative	19.37
AFUB_078380	Cell wall glucanase (Scw4), putative	12.97
AFUB_002490	Phospho-2-dehydro-3-deoxyheptonate aldolase	10.62
AFUB_089920	Alcohol dehydrogenase, putative	8.19
AFUB_091450	Proteasome subunit alpha	7.87
AFUB_081790	Dehydrogenase, putative	7.65
AFUB_072430	Extracellular triacylglycerol lipase, putative	6.67
AFUB_040170	Proteasome regulatory particle subunit (RpnL), putative	6.48
AFUB_003290	Uncharacterized protein	5.73
AFUB_084630	Uncharacterized protein	5.36
AFUB_018330	Extracellular serine carboxypeptidase, putative	4.94
AFUB_088030	Ribosomal protein S5	4.68
AFUB_028320	Uncharacterized protein	4.49
AFUB_086950	Uncharacterized protein	4.36
AFUB_085520	Uncharacterized protein	3.95
AFUB_014370	Uncharacterized protein	3.70
AFUB_015970	Ribonuclease T2, putative	3.67
AFUB_049070	NPP1 domain protein, putative	3.59
AFUB_045510	FAD binding domain protein	3.42
AFUB_084480	133-beta-glucanosyltransferase	3.37
AFUB_080770	Mannan endo-1,4-beta-mannosidase F	3.34

AFUB_077620	Endoglucanase, putative	3.26
AFUB_080630	Uncharacterized protein	2.90
AFUB_018320	Beta-fructofuranosidase, putative	2.82

Surprisingly, the interaction between *A. fumigatus* and *P. aeruginosa* resulted in many more fungal proteins being downregulated than upregulated. Among 36 most highly enriched proteins (Table 11), a quarter are extracellular enzymes with a carbohydrate catabolic processing function (AFUB_095310, exopolygalacturonase; AFUB_004010, β -1,3-glucan glucosidase; AFUB_077630, β -1,4-glucan cellobiohydrolase; AFUB_041450, pectin methylesterase; AFUB_078380, cell wall glucanase (Scw4); AFUB_084480, 1,3- β -glucanosyltransferase; AFUB_080770, endo-1,4- β -mannosidase F; AFUB_077620, endoglucanase, AFUB_018320, β -fructofuranosidase). In contrast, a number of proteins with the same or a similar function were found among the most downregulated proteins, effectively missing from the co-culture supernatant (AFUB_080950, endo-1,4- β -glucanase; AFUB_081740, cellobiose dehydrogenase, AFUB_072510, phosphomannomutase; AFUB_052050, class III chitinase; AFUB_084070, glycosyl hydrolase). This suggests that the confrontation of the fungus with *P. aeruginosa* elicited large-scale fungal cell wall architecture modification processes, during which the fungus actively regulated the various cell-wall modifying enzymes to adapt to the presence of the bacterium. While not all these enzymes were secreted *per se*, it is assumed that their association with the cell wall became disrupted at some point during the process of cultivation or sample handling. Furthermore, two of the top upregulated enzymes are involved in protein degradation processes (AFUB_091450, proteasome subunit alpha; AFUB_040170, proteasome regulatory particle subunit (RpnL)), with further unspecified function. Additionally, AFUB_049070, whose protein product contains an NPP1 domain, showed enrichment in co-culture with *Pseudomonas*. Proteins with this domain are known from other pathogenic fungi, oomycetes, and bacteria to cause necrosis in host tissues and trigger host defence responses especially in plants (Gijzen & Nürnberger, 2006). Nonetheless, little is known about their implication in interaction with animal hosts and other microbes.

Table 12. Most highly downregulated proteins in co-culture of *A. fumigatus* and *P. aeruginosa* carried out in SCFM2 medium; change expressed as fold change of abundance ratio Af + PsA/Af

Gene accession number	Function	Abundance ratio
AFUB_006960	High expression lethality protein Hel10, putative	-2433.02
AFUB_061630	Hsp90 binding co-chaperone (Sba1), putative	-1895.92
AFUB_049980	Allergen, putative	-1871.29
AFUB_091050	Electron transfer flavoprotein alpha subunit, putative	-1654.68
AFUB_025910	60S acidic ribosomal protein P2	-1437.98
AFUB_040130	Threonine synthase Thr4, putative	-1266.74
AFUB_003510	ATP synthase delta chain, mitochondrial, putative	-1036.28
AFUB_085960	Cell surface protein Mas1, putative	-896.72
AFUB_020670	40S ribosomal protein S21	-770.44
AFUB_083470	Choline oxidase (CodA), putative	-719.09
AFUB_097390	Dihydrodipicolinate synthetase family protein	-617.84
AFUB_086140	Uncharacterized protein	-612.38

AFUB_054050	Acyl-CoA dehydrogenase family protein	-587.22
AFUB_025880	Carbamoyl-phosphate synthase, large subunit	-543.55
AFUB_040790	4-nitrophenylphosphatase	-489.81
AFUB_025750	Fatty acid activator Faa4, putative	-479.86
AFUB_065800	Short chain dehydrogenase, putative	-471.47
AFUB_073360	Isocitrate dehydrogenase LysB	-443.88
AFUB_020360	14-3-3 family protein ArtA, putative	-438.61
AFUB_080950	Probable endo-beta-1,4-glucanase D	-422.11
AFUB_081740	Cellobiose dehydrogenase, putative	-419.20
AFUB_023120	Actin cortical patch component, putative	-401.80
AFUB_087780	Aspergillopepsin, putative	-399.04
AFUB_019010	Glutaminyl-tRNA synthetase	-389.21
AFUB_051640	Histone acetyltransferase type B subunit 2	-363.17
AFUB_042850	Phosphoribosyl-aminoimidazole-succinocarboxamide synthase	-362.34
AFUB_036860	60S ribosomal protein L22, putative	-354.94
AFUB_063280	Branched-chain-amino-acid aminotransferase	-350.35
AFUB_012570	Multifunctional tryptophan biosynthesis protein	-338.63
AFUB_011540	Glycine cleavage system H protein	-322.17
AFUB_015390	Coatomer subunit delta, putative	-314.58
AFUB_097160	DUF453 domain protein	-312.30
AFUB_091290	Acetyltransferase component of pyruvate dehydrogenase complex	-310.85
AFUB_076740	Chaperonin, putative	-303.79
AFUB_072510	Phosphomannomutase	-303.11
AFUB_035880	40S ribosomal protein S0	-298.11
AFUB_005670	Disulfide isomerase, putative	-296.50
AFUB_007210	60S acidic ribosomal protein P1	-295.56
AFUB_059490	U1 small nuclear ribonucleoprotein, putative	-294.74
AFUB_101540	Uncharacterized protein	-285.25
AFUB_034740	Ketol-acid reductoisomerase	-271.88
AFUB_049500	Glyceraldehyde-3-phosphate dehydrogenase	-268.60
AFUB_082130	Extracellular matrix protein, putative	-267.40
AFUB_084070	Glycosyl hydrolase family 43 protein	-264.46
AFUB_018110	1-aminocyclopropane-1-carboxylate deaminase, putative	-259.06
AFUB_051530	60S ribosomal protein L4, putative	-258.54
AFUB_030040	Cutinase	-257.51
AFUB_055620	Pyridoxine biosynthesis protein	-249.35
AFUB_072380	Fumarylacetoacetate hydrolase family protein	-247.13
AFUB_042100	60S ribosomal protein L21, putative	-244.73
AFUB_052050	Class III chitinase, putative	-237.45
AFUB_053920	Adenosine kinase, putative	-222.61
AFUB_038850	Galactokinase	-218.44
AFUB_027050	Orotate phosphoribosyltransferase	-216.31

Among the 60 most downregulated proteins listed in Table 12, those with annotated biological function in amino acid metabolic processes are the most enriched (*e.g.* AFUB_040130, threonine synthase Thr4; AFUB_025880, carbamoyl phosphate

synthase; AFUB_034740, ketol-acid reductoisomerase; AFUB_012570, multifunctional tryptophan biosynthesis protein; AFUB_073360, isocitrate dehydrogenase LysB). However, when a more extensive list of downregulated proteins is considered, a slightly different result emerges, indicating an attenuation in carbon and organonitrogen metabolism (data not shown).

During the isolation of fungal proteins from co-culture, it is not possible to avoid extracting secreted bacterial proteins, too. Thus, while it was not the objective of the analysis, many proteins secreted by *P. aeruginosa* were co-isolated and detected by LC-MS. Based on their scaled abundance in the protein extract, Table 13 lists the top 50 most abundant pseudomonadal proteins found in co-culture and provides insight into the physiological state of the bacterium. Bacteriophage proteins (PA0616 - 0626) and exotoxin A (PA1922) dominate the spectrum. The genome of *P. aeruginosa* PAO1 hosts the filamentous Pf4 phage, highly transcribed under conditions encountered in CF lungs (Secor et al., 2015), and previously shown to coordinate and sequester ferric iron, thus capable of starving *A. fumigatus* of the nutrient (Penner et al., 2016). The effects of exotoxin on other microbes are not known. A gene ontology analysis performed on a higher number of *Pseudomonas* proteins (700 most highly abundant) revealed an enrichment of proteins involved in membrane transport, siderophore trafficking, peptidoglycan synthesis, flagellum-dependent movement, and amino acid catabolism. The latter might be caused by the composition of the medium, with its high amino acid content. It is uncertain whether (and/or which of) these proteins are constitutively expressed during growth on the SCFM2 medium, and which ones are produced in reaction to the presence of *A. fumigatus* in the culture. However, the co-isolated proteins with their varying amounts afford a valuable gauge of the other side of the interaction context.

Table 13. Most highly abundant co-isolated proteins of *P. aeruginosa* present in supernatant of co-culture of *A. fumigatus* and *P. aeruginosa* carried out in SCFM2 medium

Gene accession number	Function	Scaled abundance
PA0620	Probable bacteriophage protein	748.75
toxA	Exotoxin A	743.71
PA0619	Probable bacteriophage protein	725.88
PA0622	Probable bacteriophage protein	715.28
PA2451	Uncharacterized protein	710.90
PA4625	Uncharacterized protein	703.99
chiC	Chitinase	701.69
aprA	Serralysin	693.78
flgK	Flagellar hook-associated protein 1 FlgK	688.67
fliD	B-type flagellar hook-associated protein 2	674.08
PA5033	Uncharacterized protein	673.80
PA0628	Uncharacterized protein	664.57
PA0781	Uncharacterized protein	664.03
PA1922	Probable TonB-dependent receptor	662.38
PA0618	Probable bacteriophage protein	658.58
eddB	Extracelullar DNA degradation protein, EddB	653.71
PA2452	Uncharacterized protein	653.64
exaA	Quinoprotein alcohol dehydrogenase (cytochrome c)	642.57

PA0617	Probable bacteriophage protein	638.14
ampDh3	AmpDh3	628.53
PA0366	Probable coniferyl aldehyde dehydrogenase	625.89
cbpD	Chitin-binding protein CbpD	623.88
PA3800	Outer membrane protein assembly factor BamB	621.16
hasAp	Heme acquisition protein HasAp	619.93
PA0626	Uncharacterized protein	618.17
PA0616	Uncharacterized protein	611.61
PA1874	Uncharacterized protein	611.27
retS	RetS (Regulator of Exopolysaccharide and Type III Secretion)	610.00
PA3383	Binding protein component of ABC phosphonate transporter	609.00
PA1934	Uncharacterized protein	587.40
PA0623	Probable bacteriophage protein	584.62
PA3332	Uncharacterized PhzA/B-like protein PA3332	583.92
PA4972	Uncharacterized protein	583.06
PA1923	Uncharacterized protein	582.16
PA3734	Uncharacterized protein	577.04
PA0007	Uncharacterized protein	573.86
PA1401	Uncharacterized protein	573.47
PA5103	Uncharacterized protein	572.83
PA2433	Uncharacterized protein	568.79
PA0080	Uncharacterized protein	568.36
PA0688	Alkaline phosphatase L	567.64
PA0388	Uncharacterized protein	566.64
pvdN	PvdN	565.96
antB	Anthranilate dioxygenase small subunit	565.82
PA0227	Probable CoA transferase, subunit B	565.71
PA0144	Uncharacterized protein	559.11
fptA	Fe ³⁺ -pyochelin receptor	559.03
PA3619	Uncharacterized protein	558.81
PA2024	Uncharacterized protein PA2024	555.87
cupA4	Fimbrial subunit CupA4	555.61
hmgA	Homogentisate 1,2-dioxygenase	554.08

5.1 A. *fumigatus* produces a putative cyanide hydratase in co-cultivation with *P. aeruginosa*

A heretofore uncharacterised *A. fumigatus* protein showed one of the highest positive changes in abundance among differentially regulated proteins, increasing from 3.2 in fungal monoculture to 659.5 in co-cultivation with *P. aeruginosa* (scaled abundance, $p < 0.001$). Orthologues of this protein found in other fungi were characterised as nitrilases/cyanide hydratases, enzymes catalyzing the hydration of cyanide into formamide (Figure 31a). Fungal cyanide hydratases are wide-spread among plant pathogenic fungi, where they detoxify phytogenic cyanide, used by plants as a defence

mechanism (Kobayashi & Shimizu, 1994; Basile et al., 2008). A cyanide hydratase conserved in the genome of *A. fumigatus*, a plant saprophyte and an opportunistic animal pathogen, is therefore a surprising finding. The protein sequence of the putative cyanide hydratase was analysed using CD-search, confirming the presence of a nitrilase/cyanide hydratase domain in the protein, as well as the interface for the characteristic homodimer formation (Figure 31b). Furthermore multiple sequence alignment revealed that the protein sequence of the *A. fumigatus* cyanide hydratase (AfCHT) shares a high level of homology with previously characterised fungal cyanide hydratases: 84.93% identity with *A. nidulans*; 67.42% identity with *N. crassa* (Basile et al., 2008); 65.17% identity with *F. solani* (Barclay et al., 1998); 64.07% identity with *G. sorghi* (Wang & VanEtten, 1992) (Figure 31c). The enzyme contains the highly conserved catalytic triad of a glutamic acid, a lysine, and a cysteine residue that nucleophilically attacks the nitrile group (Kobayashi et al., 1998), leading to the conclusion that AFUB_033190 encodes an *A. fumigatus* variant of a cyanide hydratase, hereafter designated the gene *chtA*.

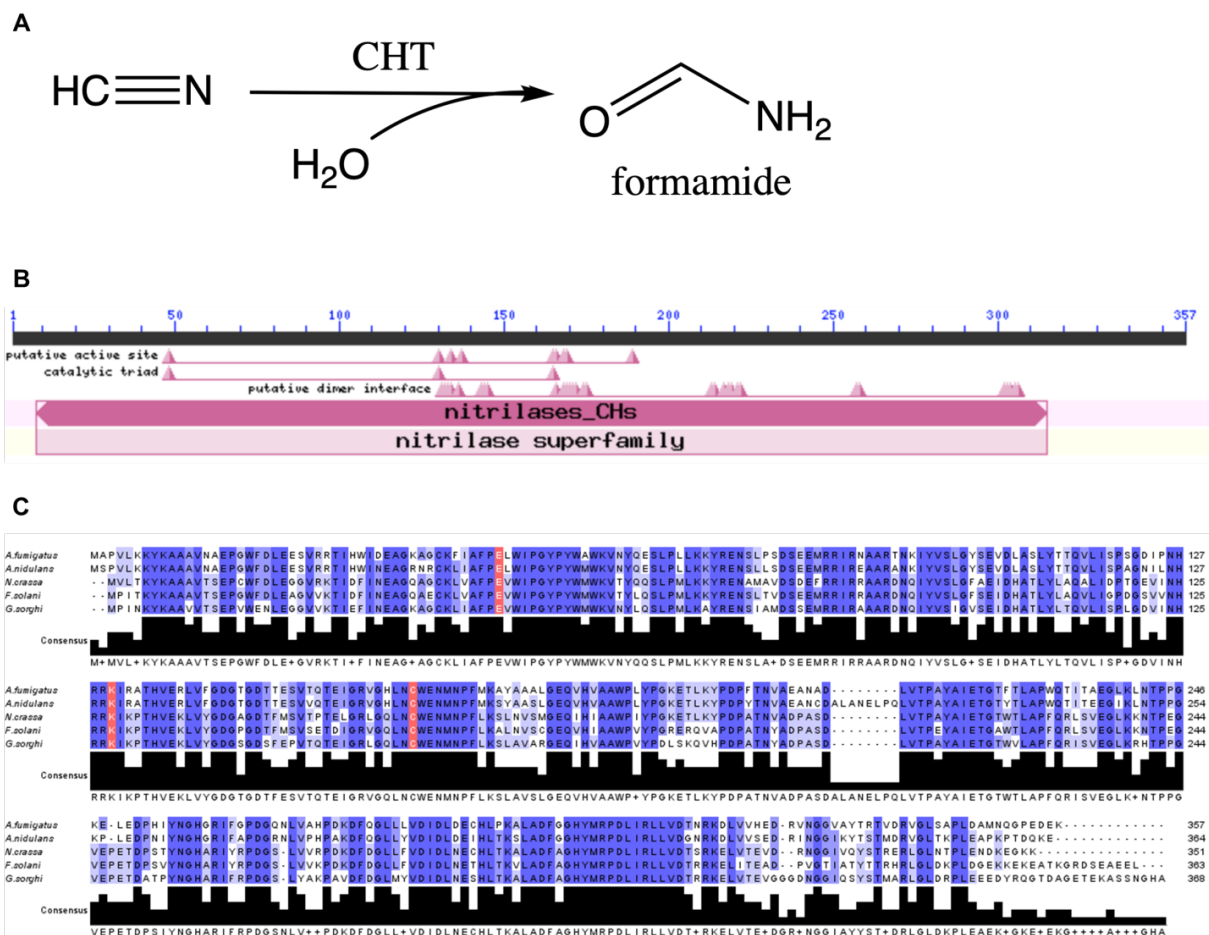


Figure 31. Cyanide hydratase of *A. fumigatus*. (A) Cyanide detoxication reaction catalysed by cyanide hydratases (Basile et al., 2008). (B) CD-search analysis of the DNA sequence of AFUB_033190, a suspected cyanide hydratase of *A. fumigatus*, revealed the presence of a nitrilase/cyanide hydratase domain. (C) Alignment of *A. fumigatus* cyanide hydratase sequence with those from fungal species where the enzyme has been characterised. The highly conserved catalytic triad (Kushawaha et al., 2018) is highlighted in red.

5.1.1 The expression of *chtA* is contingent on the presence of cyanide

Quantitative RT-PCR was used to determine the transcriptional response of the wild type *A. fumigatus* CEA17 \DeltaakuB to the presence of exogenous cyanide. To this effect, pre-grown fungal mycelia were suspended in fresh AMM supplemented with potassium cyanide, ranging in concentration from 50 μM (very low) to 500 μM (high), with a cyanide-free culture used as control. The analysis demonstrated that *chtA* expression in *A. fumigatus* under untreated, cyanide-free conditions was only baseline, with the log₂ relative quantity being about 5 times lower than that of the housekeeping gene (*cox5*, cytochrome oxidase subunit 5; data not shown). Upon treatment with cyanide, however, the expression levels of *chtA* spike. A highly significant level of upregulation ($\log_2(\text{FC}) > 8$) of *chtA* transcription was detectable already at low cyanide concentration (50 μM), which increased with progressively higher concentrations (100 μM , 300 μM , 500 μM) to $\log_2(\text{FC}) \cong 10$ (Figure 32).

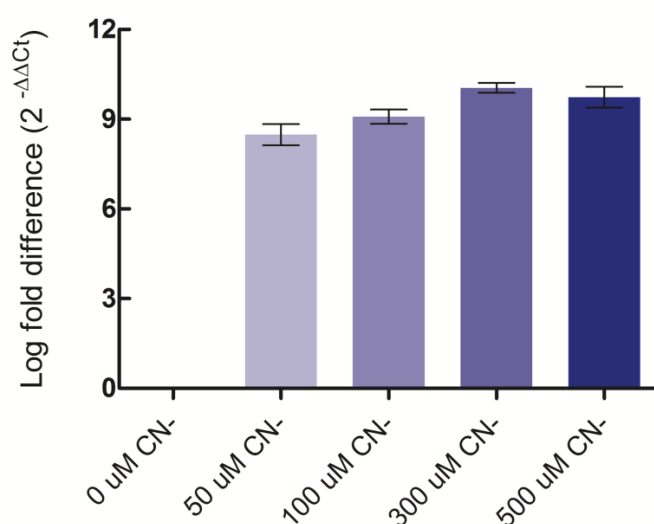


Figure 32. Expression profile of *chtA* (AFUB_033190) in response to exogenous HCN in the culture. Addition of even low amounts of HCN into the fungal culture induced a strong transcriptional response in *chtA*. This response did not appear to be dose-dependent.

5.1.2 AfCHT is essential for growth in presence of cyanide and rapidly detoxifies exogenous KCN

The CHT-encoding gene, designated *chtA* (Afu2g17500) was deleted to ascertain its function in cyanide metabolism. The deletion mutant, $\Delta chtA$ (Figure 33), showed a severe growth defect in AMM supplemented with 300 μM KCN (a concentration slightly higher than the physiologically relevant range detected in cystic fibrosis lungs; Neerincx et al., 2015) in comparison with the wild type (Figure 34). The parental strain treated with cyanide formed the same amount of biomass as the untreated control; meanwhile, the mutant, showing a similar phenotype as the WT in the untreated control, formed no recoverable biomass in the culture supplemented with KCN. The experimental setup involved a 6 h germination period before treatment to allow for formation of metabolically active biomass that could produce the catabolic enzyme. If this step was omitted, the germination was slowed down even in wild type spores. Under those conditions, the growth recovered with a delay and a comparable amount of biomass was only observed after additional 24 hours of cultivation (data not shown). Strikingly, the phenotypic difference was not observed on agar plates, where, regardless of the

concentration of cyanide added to agar, both the wild type and the cyanide metabolism-deficient mutant exhibited the same growth pattern.

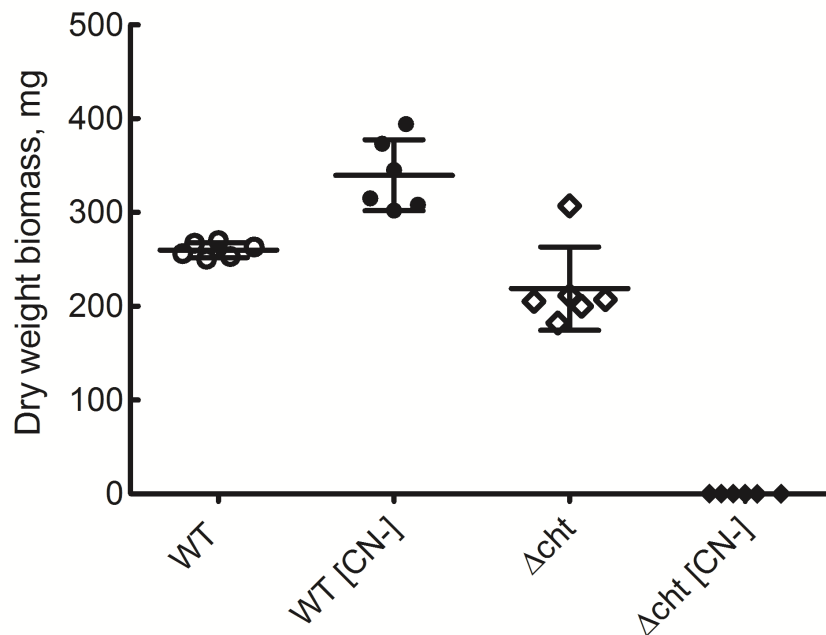
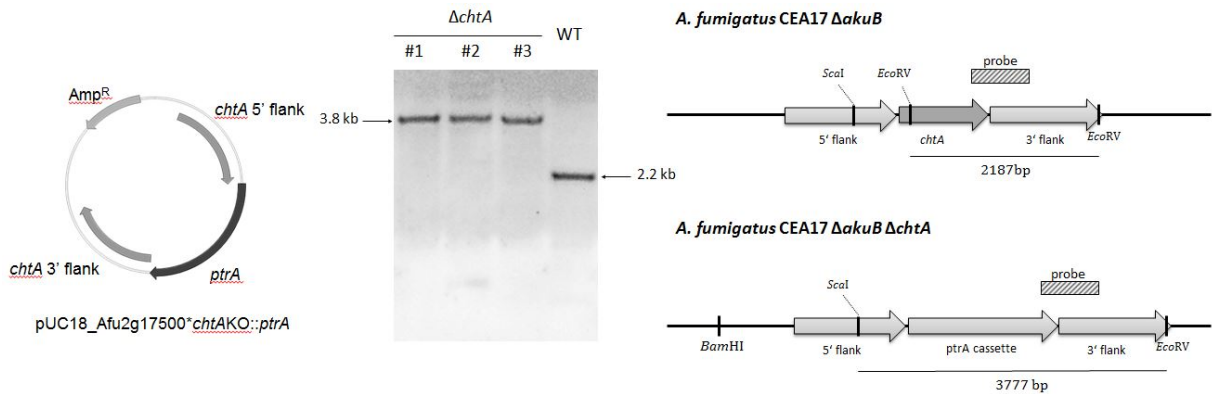


Figure 34. Biomass formation of *A. fumigatus* grown in presence of 300 μ M HCN. While the wild-type strain displayed a paradoxical boost in growth when treated with hydrogen cyanide and incubated for 72 h, the Δ *chtA* mutant, incapable of detoxifying cyanide, formed almost no biomass at all when treated.

To estimate the catalytic capacity of *A. fumigatus* to detoxify CN⁻, mycelia were suspended in AMM supplemented with a high concentration of KCN (1 mM), and cyanide degradation monitored with a cyanide-specific ion-selective electrode over 6 hours in 90 min intervals. The response of the wild-type fungal biomass to exogenous cyanide was remarkably rapid, with the concentration decreasing from the apparent 1 mM CN⁻ to ca 800 μ M (20%) already after the initial 90 min, and plummeting sharply to less than 50 μ M (> 90%) in the following 4.5 hours (Figure 35). This was in stark contrast to the Δ *chtA* mutant, incapable of producing cyanide hydratase. The concentrations of CN⁻ ions measured in treated Δ *chtA* cultures coincided with the treated medium controls, remaining almost unchanged from the initial concentration. The slight decrease in CN⁻ concentration detectable in the treated mutant samples can be attributed to the evolution of HCN gas from the cultures, caused by the low pH medium (pH 6.5).

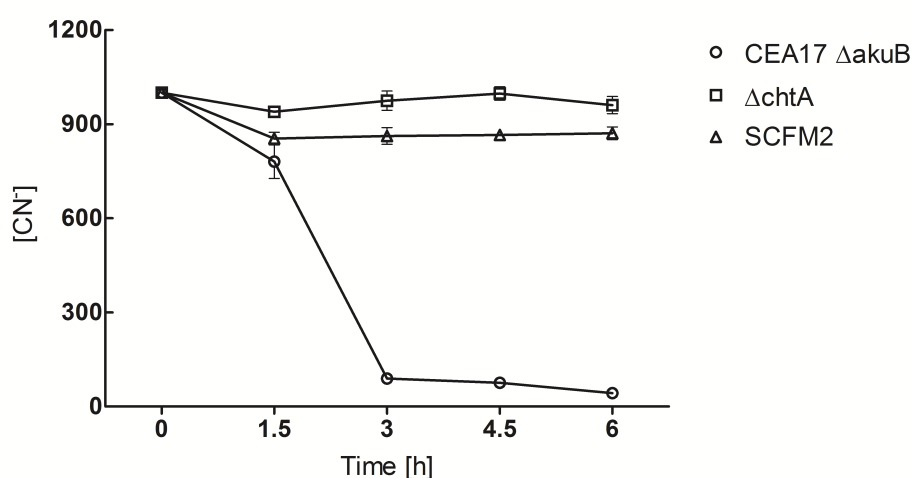


Figure 35. Cyanide detoxication by *A. fumigatus*. At the initial time point, cultures were treated with a final concentration of 1 mM KCN, and CN⁻ concentration monitored with a CN-specific ion-selective electrode. The wild-type strain of *A. fumigatus* as shown to be capable to rapidly detoxify cyanide, with CN⁻ concentration dropping to less than 50 μ M in 3 hours. The concentrations of cyanide in the Δ *chtA* mutant, however, remained near the initial value.

5.1.3 Cyanide detoxication during co-cultivation with *P. aeruginosa*

The experimental setup that led to the discovery of the *A. fumigatus* cyanide hydratase involved an interaction with *P. aeruginosa*. Building on the previously asserted observation that there is only baseline expression of *chtA* in cyanide-free conditions, the high abundance of the protein product in co-cultivation implies the presence of cyanide produced by *Pseudomonas* (*A. fumigatus* itself is acyanogenic (Neerincx et al., 2015)). As described in Section 3.1.2 of Introduction to the present work, bacterial cyanogenesis is carried out by the *hcnABC* operon, which is tightly regulated at the transcriptional level (Blumer & Haas, 2000). It was postulated that if *A. fumigatus* triggers cyanide production in *P. aeruginosa*, then the Δ *chtA* mutant should be susceptible to inhibition when confronted with *P. aeruginosa* wild type. Additionally, an acyanogenic strain of *P. aeruginosa* Δ *hcnB* was generated (Figure 36) to serve as a control, next to which the fungal cyanide hydratase mutant should grow without impediment.

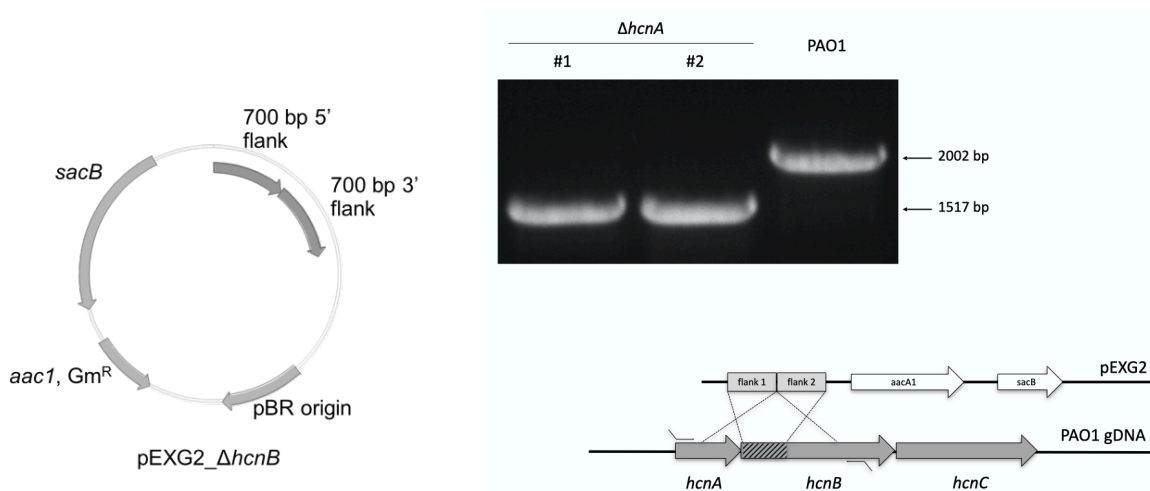


Figure 36. Construction of an acyanogenic $\Delta hcnB$ mutant. Plasmid pEXG2, was linearised with *Hind*III and *Eco*RI, and ligated with end-to-end joined PCR-amplified DNA fragments of *P. aeruginosa* flanking the 0.5 kb target portion of the *hcnB* gene, to create pEXG2_Δ*hcnB*. *P. aeruginosa* PAO1 was electroporated to facilitate plasmid uptake. Following recombination and selection of merodiploids on gentamicin-containing medium, the transformants were transferred to sucrose-containing NSLB medium for *sacB* counterselection. Correct mutants were identified by PCR using primers binding outside of the flank sequences, yielding a shorter PCR product (1.5 kb) than the wild-type strain (2 kb).

The wild-type and mutant strains of each respective microbe were then inoculated on a plate of SCFM2 agar, which was incubated in a hypoxic atmosphere (O_2 5% (v/v)) at 37°C to stimulate cyanide production in *P. aeruginosa*. Surprisingly, after 24 hours of incubation, all pairwise combinations demonstrated the same growth phenotype, and no difference could be seen between the wild-types and mutants (Figure 37). As an alternative approach, planktonic cultures were prepared by inoculating fresh SCFM2 with pre-grown fungal mycelium and bacterial suspension, and incubated in sealed flasks at 37 °C with the hypoxic gradient created by shaking for 16 - 24 h. After incubation, the fungal $\Delta chtA$ mutant was expected to show inhibited growth when incubated with *P. aeruginosa* wild type, and normal growth in co-culture with the acyanogenic $\Delta hcnB$ strain. The concentration of cyanide was also expected to be high in the culture supernatant of PAO1 wild type alone and in combination with $\Delta chtA$, and low for PAO1 wild type with CEA17 $\Delta akuB$, which can detoxify cyanide. However, the measurement of $[CN^-]$ revealed that even in PAO1 axenic cultures, where cyanogenesis

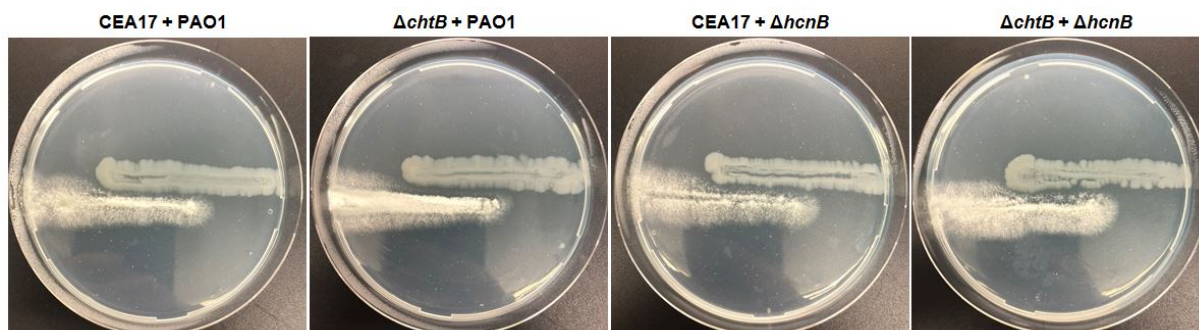


Figure 37. Interaction of *P. aeruginosa* and *A. fumigatus* cyanide-producing and -degrading mutants grown on SCFM2 agar. No difference could be observed between pairwise combinations of *A. fumigatus* wild type and $\Delta chtA$ mutant, and *P. aeruginosa* wild type and $\Delta hcnB$ mutant. The lack of a phenotypic difference could be caused by a lack of cyanide production by *P. aeruginosa* PAO1, due to unfavourable conditions.

should be happening in an uninhibited fashion, the concentration of CN⁻ ions was beyond the reliable linear range of measurement of the device (<25 μM). An attempt to prove ongoing cyanogenesis by proxy, *via* expression analysis of the *hcnA* gene by qRT-PCR, only supported the previous findings of a lack of differential gene expression and cyanogenesis in *P. aeruginosa* cultures, axenic or mixed. The *hcnA* gene was, in fact, found to be mildly downregulated (Figure 38). It was therefore concluded that the discovery of the fungal cyanide hydratase was serendipitous, depending on a particular set of conditions that favoured cyanogenesis. Replicating these conditions has, however, proved elusive, and the extremely tight regulation of *P. aeruginosa* physiology renders certain parts of its secondary metabolism recalcitrant to study in this particular model of interaction.

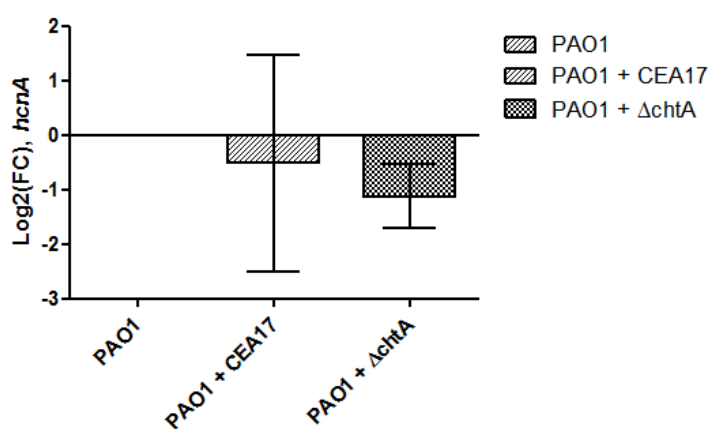


Figure 38. Expression profile of *hcnA* in *P. aeruginosa* PAO1 in co-cultivation with *A. fumigatus* wild type and Δ*chtA* mutant. The presence of the fungus itself did not trigger cyanide production in *P. aeruginosa*, as evidenced by a lack of induction of the *hcnA* gene. The stringent regulation of cyanogenesis in the bacterium is presumably responsible for the unsuccessful attempts to replicate the situation where the fungal cyanide hydratase expression was triggered by bacterial cyanide in the medium.

6 Mutual detoxication of *A. fumigatus* and *P. aeruginosa*

Thus far, most results obtained during this study indicate virulence attenuation and a multitude of detoxication mechanisms being at work during the co-cultivation of *A. fumigatus* and *P. aeruginosa* on SCFM2 medium. To realistically determine the impact that the interaction may have, a cell proliferation assay was performed on A549 human pulmonary basal epithelial cells. The cells were treated with filter-sterilised supernatants and organic extracts of axenic cultures of each of the *A. fumigatus* strains (CF10 and CEA17 Δ*akuB*) and *P. aeruginosa*, as well as those of co-cultures of each fungus with the bacterium, all grown in liquid SCFM2. Interestingly, neither of the supernatants exhibited any significant antiproliferative effect on the cell line (data not shown). Concentrated organic extracts suspended in DMSO, on the other hand, were more potent inhibitors of proliferation of the epithelial cells. Most strikingly, however, it was the extracts of *A. fumigatus* monocultures that showed the highest antiproliferative effect, with CF10 strain being slightly more inhibitory than CEA17 Δ*akuB* (Figure 39). The GI₅₀ for CF10 organic extract was determined to be 0.5% concentration of the extract, while it was higher for all other extracts. This included the monoculture of *P. aeruginosa*, as well as the co-cultures of the bacterium with either of the *A. fumigatus* strains. SCFM2 does not negatively affect proliferation of A549 epithelial cells.

It is conceivable that the cytostatic effect of extracts from mixed fungal-bacterial cultures is diminished by the suspected mutual detoxication during co-culture. Transcriptome data, as well as chemical analyses, suggest that the production of *A. fumigatus*-derived mycotoxins is decreased or completely abolished in presence of *P. aeruginosa*. This lack of secondary metabolites in co-culture and, implicitly, their presence in the *A. fumigatus* monocultures, could explain why the co-culture extracts lose the cytostatic activity, while the extracts of monocultures retain it. As to the differences between CF10 and CEA17 \DeltaakuB , it could be speculated that the absolute amounts, as well as ratios of different secondary metabolites vary, causing CF10 to be more antiproliferative than CEA17 \DeltaakuB . Since no different metabolites were detected in axenic cultures of CF10 than CEA17 \DeltaakuB , it is unlikely that the different potency in antiproliferative activity could be attributed to an additive effect caused by a differential, CF10-specific metabolite. The low cytostatic effect of axenic *P. aeruginosa* extracts on pulmonary epithelia is also surprising. It could be speculated that SCFM2 provides conditions that attenuate the virulence traits of the bacterium.

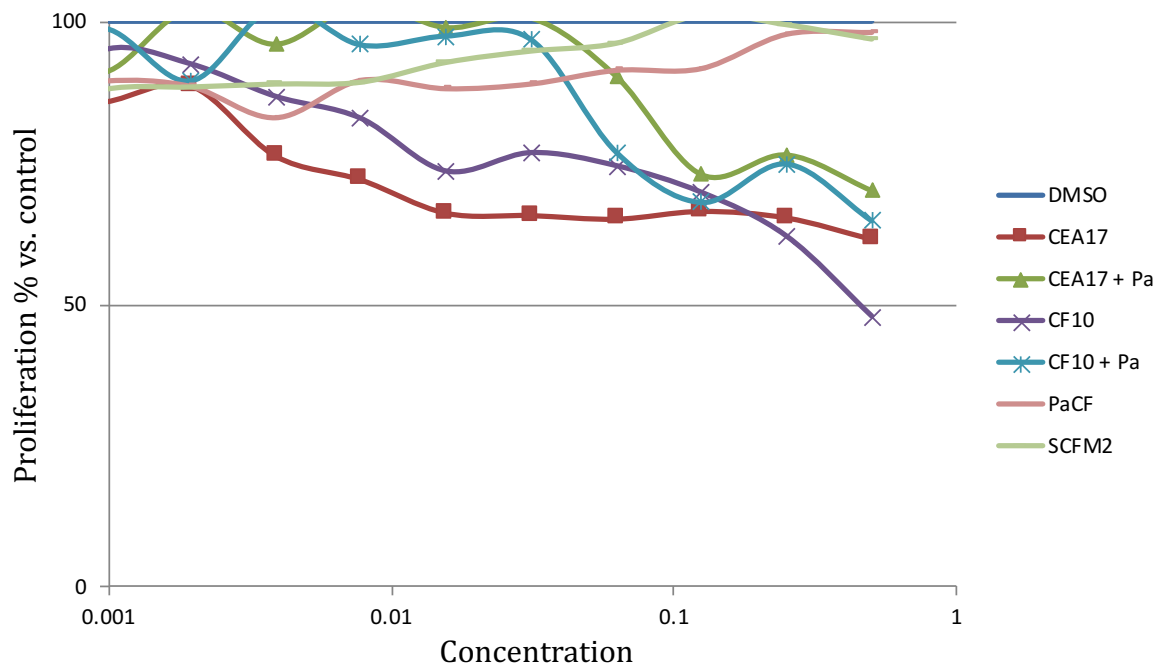


Figure 39. Analysis of antiproliferative effects exhibited by extracts of *P. aeruginosa* and *A. fumigatus* co-cultures carried out in SCFM2. Human adenocarcinoma pulmonary epithelial cells A549 were treated with various concentrations of extracts from monocultures of *P. aeruginosa* and *A. fumigatus* CEA17 \DeltaakuB and CF10, and from co-cultures of each fungal strain with the bacterium. Only the extract of CF10 monoculture was found to be significantly antiproliferative, followed by the extract of CEA17 \DeltaakuB . The antiproliferative effects are, however, not additive, and each co-culture extract had a less potent inhibitory effect, hinting at a mutual detoxication between *A. fumigatus* and *P. aeruginosa*.

C Discussion

1 Studying the ecology of microbial interactions relevant to human infections

Contrary to the conventional laboratory *in vitro* model of a microbial culture, microorganisms inhabiting natural habitats, including clinically relevant niches, *e.g.* human tissues and surfaces during an infection process, seldom live in isolation. Rather, they co-exist in consortia with other species and strains, constituting small ecosystems where the members of the community interact with each other and their physical environments (Brogden et al., 2005). Often, these milieus of growth of pathogenic and avirulent microbes alike are formed on mucosal or abiotic surfaces in the human body as combined microbial biofilms. Although the appreciation of the existence and co-inhabitation of human tissues by diverse microbes at a time came with the first microscopes, it was only recently that the notion of polymicrobial infections has started gaining traction and garnering interest of researchers as relevant to the process and outcome of infection (Peters et al., 2012). Our understanding of the interactions within such communities is still rather limited, and clinically relevant microbes commonly continue being investigated in isolation. This leads to the erroneous assumption that polymicrobial infections can be disintegrated into, and treated as, individual components (de Vos et al., 2017). This concept, however, defies two different aspects of the reality. On one hand, the evolutionary notion that microbes co-inhabiting the same available spaces for millions of years have developed physical and chemical communication pathways to facilitate synergistic, mutualistic, or antagonistic relations, and, on the other hand, the clinical observation that the interaction between bacteria, fungi, viruses, and parasites modulates the severity of the disease progression, as well as its outcome (Brogden et al., 2005; Short et al., 2014; Byrd and Segre, 2016). Thus, studying microbial interactions on the backdrop and in interplay with the host environment with their added level of complexity might provide invaluable insights into communication mechanisms and form a basis for novel diagnostic and therapeutic approaches.

The context of cystic fibrosis with its complex environment, heterogeneous microbiome and various modes of clinical demonstrations of the disease (Rogers et al., 2003; Flight et al., 2015; Quinn et al., 2016) offers a challenging mosaic of microbe-microbe and microbe-host interactions. Working with the most prevalent bacterial and fungal pathogens in cystic fibrosis-related infections, the present work has proposed that multiple microbe-microbe interactions asserted as relevant to the disease are heavily contingent on the environmental conditions used during the study, and underlined the importance of approximating native disease conditions before such assertions are made. These concepts, as well as new findings and their importance will be discussed.

1.1 The effects of growth media and mimicking host environment

Microbial pathogenesis and, implicitly, the ongoing interactions between colonising microbes are conditioned by the environment of the host body (Brown et al., 2008). The network of interactions is dynamic and often dependent on each individual microbe's strategy to cope with the host responses, available nutrients, population density of own and other present strains, or reliance on virulence factors (Gallagher et al., 2002; Diggle et al., 2003; Munoz-Elias and McKinney, 2006; Shiner et al., 2006). Despite this acknowledged dependency, the representation of native-like environment in studies of infection or infection-related microbial communication is poor.

In cystic fibrosis, mucus secretion is impaired due to a genetic aberration, resulting in hypersecretion of thick, viscous mucus, which becomes colonised by bacteria and fungi (Lyczak et al., 2002), and the ensuing inflammation turns mucus into a mucopurulent secretion called phlegm, biochemically resembling pus (Rubin, 2009). When expectorated, the phlegm is called sputum. In contrast to normal mucus, whose viscous properties are dictated predominantly by MUC5AC and MUC5B mucins (Henke et al., 2007), phlegm/sputum additionally contains breakdown products of necrotic inflammatory lymphocytes and epithelial cells, bacteria, cell debris, and complexes of neutrophil-derived DNA and F-actin co-polymers, which further thicken the secretion (Lethem et al., 1990; Sanders et al., 2000; Dawson et al., 2003). The composition of cystic fibrosis sputum, with respect to free amino acids, cations, anion, glucose, and lactate was defined by the group of Whiteley, who formulated a synthetic cystic fibrosis sputum medium (SCFM) based on average concentrations of each component measured in 14 CF sputum samples (Palmer et al., 2007). This formulation was later improved upon by addition of relevant amounts of DNA, lipid (1,2-dioleoyl-sn-glycero-3-phosphocholine, DOPC), and mucin to yield SCFM2, mimicking native sputum conditions more closely (Turner et al., 2015). Both of these media were developed to study the nutritional effects of CF environment specifically on *P. aeruginosa*; the present work, however, suggests that the SCFM2 medium is also suitable as a representative background on which interkingdom microbial interactions can be studied, perhaps better representative of the processes happening during an interaction directly within the human host.

The growth and physiology of *P. aeruginosa* were closely studied directly on sputum and on the SCFM2 medium at multiple instances. Each study identified major differences between sputum-based media and other media, conventionally used to grow bacteria *in vitro*. Sputum and SCFM2 support bacterial growth by providing primarily amino acids (proline, alanine, arginine, glutamate) rather than glucose as a preferred carbon source (Palmer et al., 2005; Palmer et al., 2007). Carbon, as well as nitrogen, utilisation profiles were linked to changes in *P. aeruginosa* virulence and biofilm formation through endotoxin formation (Raetz and Whitfield, 2002), type III secretion systems (Rietsch et al., 2004), rhamnolipid production (Santos et al., 2002), and quorum sensing (Shrout et

al., 2006; Mund et al., 2017). The identification of *P. aeruginosa* transcriptome during human CF infection using SCFM2 medium confirmed a global downregulation of primary anabolism (and, inversely, upregulation of degradation pathways) of carbohydrates and amino acids, as well as of genes involved in the TCA cycle, which was contrary to the regulation observed in *in vitro* cultures (Cornforth et al., 2018). These findings are mirrored in *Stenotrophomonas maltophilia* (Willsey et al., 2019) and *Mycobacterium abscessus* (Miranda-CasoLuengo et al., 2016), two other important bacterial CF pathogens, when grown in SCFM2. Furthermore, the same study proposed that quorum sensing-regulated genes, in particular those regulated by LasR/LasI as the 'core *las* QS regulon' using C12-HSL (Chugani et al., 2012), were consistently expressed at a lower level in human infection. Previously, however, the *Pseudomonas* quinolone signal (PQS)-dependent signalling had been found to be induced specifically by growth on human sputum (Palmer et al., 2005). These findings are important premises to build upon when considering the participation of *P. aeruginosa* in interaction with *A. fumigatus* on the SCFM2 medium.

The results presented here suggest that the CF sputum-mimicking conditions of SCFM2 are also suitable for cultivation of the fungal pathogen *Aspergillus fumigatus*, supporting its growth in liquid, as well as solid cultures. In general, the selection of cultivation media for *A. fumigatus* is guided by convention, most commonly using *Aspergillus* minimal medium (AMM) (Pontecorvo et al., 1953), Sabouraud medium (Guinea et al., 2005), or other complete media. Authors attempting to elucidate mechanisms of microbial communication relevant to cystic fibrosis have long relied on using media designed for cell line culture (*e.g.* supplemented RPMI-1640 (Granillo et al., 2015; Briard et al., 2017), or for cultivation of fungi (*e.g.* Sabouraud glucose broth (Manavathu et al., 2014) or malt extract medium (Briard et al., 2016)). None of these conditions are, however, fully representative of, or convergent with, those encountered in the CF lung. Furthermore, little is known about how *A. fumigatus* adjusts its physiology when cultivated under various conditions, with perhaps the most comprehensive study to date uncovering merely the phenotypic variation in sporulation and germination in different media and under various stress factors (Momany and Kang, 2019).

A single study addressed the possible differences in interaction between *A. fumigatus* and *P. aeruginosa* (Ferreira et al., 2015) depending not only on the bacterial strain, but also on the growth conditions of each of the partners. In the study, both microbes were grown in RPMI-1640 medium, and *A. fumigatus* inhibition was observed to be higher by live *P. aeruginosa* or sterile culture filtrate from biofilms, than that of a planktonic culture. The authors emphasise the possible adaptations of the bacterium to prolonged exposure to the polymicrobial CF lung environment; however, the role of active interaction between the bacterium and the fungus was not acknowledged.

It was shown here that in SCFM2, *A. fumigatus* exhibited similar radial growth on solid agar plates as on AMM. Sporulation and biomass production in liquid culture were, however, not as high as in AMM. Still, SCFM2 proved to support a balanced growth of *A.*

fumigatus and *P. aeruginosa*, fulfilling the rationale of finding a medium representative of native conditions in CF lung, which does not favour (or suppress) the growth of one of the interaction partners. Like in previously documented instances, *A. fumigatus* and *P. aeruginosa* grown in SCFM2 media, solid and liquid alike, form close physical association, where the bacteria adhere to fungal hyphae (Keller, 2014; Briard et al., 2017). In addition to Keller's finding that the adhesion process was passive, I have shown that *P. aeruginosa* did not exhibit an active trophic tendency to move towards or along the fungal hyphae. Such behaviour was, however, previously observed between fungi and bacteria. The group of Takeshita described a dispersal mechanism of *Bacillus subtilis*, where the bacterium in a mutualistic relationship with *Aspergillus nidulans* delivers thiamine to the fungus, using it as toll to travel along the mycelial networks like highways (Takeshita, 2019). It remains unknown whether *P. aeruginosa* deploys this dispersal strategy at a later time during colonisation. Other CF-relevant bacteria, such as *Stenotrophomonas maltophilia*, *Staphylococcus aureus*, or *Burkholderia cenocepacia* complex adhere to the fungal hyphae, and environmental *Burkholderia spp.* were shown to translocate using fungal hyphae, but no movement has been described to date in CF sputum or simulating media (Ramírez et al., 2015; Kaur et al., 2015; Melloul et al., 2016; Lightly et al., 2017). Similarly, based on the multiple antagonistic mechanisms described for the interaction between *A. fumigatus* and *P. aeruginosa* and biofilm growth in the lung, it seems unlikely that the dispersal of fungal conidia within sputum would take place by swarming of the bacterium, like it does with *Paenibacillus vortex* (Ingham et al., 2011).

Using SCFM medium has shown to have a diminishing effect on antifungal activity of other bacteria. *B. cenocepacia* complex cultivated on SCFM agar plates in interaction loses its antifungal potency, which is retained on potato dextrose agar (Lightly et al., 2017).

2 Fungal cell wall remodelling in response to co-cultivation with *P. aeruginosa*

A number of differentially expressed genes found in the transcriptome analysis, both up- and downregulated, encode for enzymes with polysaccharide modulatory activity, suggesting that a reorganisation of the fungal cell wall is triggered by co-cultivation of *A. fumigatus* with *P. aeruginosa*. The secretome analysis further hints at fungal cell wall restructuring processes being elicited during co-cultivation. Five extracellular polysaccharide-degrading enzymes (exopolygalacturonase, β -1,3-glucanase, β -1,4-glucan cellobiohydrolase, pectin methylesterase, cell wall glucanase scw4), one protease (extracellular serine carboxypeptidase), and one lipase (extracellular triacylglycerol lipase), showed a significant increase in abundance in co-culture. This is not a solitary finding, and major fungal cell wall restructuring has been described in *A. fumigatus* in response to the presence and adherence of *P. aeruginosa* (Briard et al., 2017). According to the study, *P. aeruginosa* adheres to hyphal surface by becoming attached onto galactosaminogalactan in the cell wall, and causing cell wall thickening by dirhamnolipid-

mediated inhibition of β -1,3-glucan synthesis, increased branching, and melanisation of hyphae. Here, the melanisation was not evident, and melanin biosynthesis genes are downregulated in *P. aeruginosa*-exposed *A. fumigatus* in SCFM2 medium. Similar thickening of the cell wall and hyperbranching of hyphae was observed in *A. fumigatus* in association with *S. aureus* (Granillo et al., 2015) and *S. maltophilia* (Melloul et al., 2016; Melloul et al., 2018). It was suggested that the hyphal deformations could be caused by high enzymatic activity in the apical region caused by the presence of bacterial metabolites (Momany, 2004; Granillo et al., 2015). Similarly, the hyphae of *Aspergillus nidulans* in co-cultivation with *S. rapamycinicus* exhibit a similar hyphal hyperbranching phenotype in response to the presence of the bacterium (Schroeckh et al., 2009). Dynamic cell wall reorganisation is a well-documented stress response strategy of filamentous fungi and yeasts with filamentous morphology (Hopke et al., 2018) employed during instances of biotic and abiotic stress, alike (Ene et al., 2015; Ellett et al., 2017). It is therefore conceivable that upon close physical association of a potentially antagonistic bacterium, *A. fumigatus* undergoes a major restructuring of hyphal cell wall as a mode of adaptation to the biotic stress. Interestingly, however, the expression of the cell wall integrity pathway genes of *A. fumigatus* in co-culture (Valiante et al., 2015) was not significantly different from monoculture after 24 h, suggesting that signalling for cell wall reorganisation might be an early response to the presence of *P. aeruginosa* and its secreted factors, and does not last.

3 Secondary metabolism in the interaction of *A. fumigatus* and *P. aeruginosa*

3.1 Secondary metabolites of *P. aeruginosa*

The ecological role of microbial secondary metabolites remains a matter of dispute - some have evolved as communication devices, while the biological function of many other microbially-produced compounds as determined by *in vitro* experiments may be circumstantial, rather than intentional (Macheleidt et al., 2016; Keller, 2019). Thus, when drawing conclusion about biological function, it is important to consider secondary metabolism directly in the relevant context. In the interaction between *P. aeruginosa* and *A. fumigatus*, secondary metabolites of the bacterium have stolen the spotlight and been most extensively studied. Pyoverdine, the high-affinity siderophore of *P. aeruginosa*, has been pinpointed as the single most important factor in inhibition of the fungus in co-culture (Sass et al., 2018), postulated to sequester available iron in the environment, effectively starving the fungus. This claim was further supported by the findings that exogenous pyoverdine triggers increased siderophore production in *A. fumigatus* and that the inhibitory effect of pyoverdine can be salvaged by supplementation with fungal siderophores (Sass et al., 2019). Both of these studies were performed using RPMI-1640 as culture medium. However, MALDI-IMS experiments performed on co-cultivation of *A. fumigatus* and *P. aeruginosa* grown here on CF sputum-

mimicking medium showed that the production of pyoverdine by the bacterium was lower in co-culture than in an axenically grown colony of the bacterium. It is unknown whether the decrease in pyoverdine production is simply an adjustment to the presence of the fungus or a result of an active inhibition strategy of *A. fumigatus*. Such an active attenuation of *Pseudomonas* virulence through suppression of siderophore production has previously been shown in *Candida albicans* in a gastrointestinal colonisation model (Lopez-Medina et al., 2015). The hypoxic environment of the CF lungs (Anand et al., 2017) and the presence of blood-derived haem in the lungs (Ochsner et al., 2000) further advocate the notion that pyoverdine might not be instrumental in the interaction of *P. aeruginosa* and *A. fumigatus*. While this does not disqualify the previous findings of the potency of pyoverdine to inhibit the fungus, it casts a light on the possible relevance of this inhibition strategy with respect to CF sputum context.

Rhamnolipid production was detected by MALDI-IMS in *P. aeruginosa* both in axenic and mixed cultures with *A. fumigatus*. Dirhamnolipids produced by the bacterium are structurally dependent on the culture conditions (Desai and Banat, 1997; Mulligan, 2005). Increased production of these biosurfactants was elicited by the interaction between *P. aeruginosa* and *A. fumigatus* grown in RPMI-1640 (Briard et al., 2017). The authors further suggest that dirhamnolipids inhibit the fungal β -1,3-glucan synthase activity, eliciting a cell wall restructuring with major chitin compensation and cell wall thickening (Briard et al., 2017). Here, production of rhamnolipids by *P. aeruginosa* could also be observed. Surprisingly, mass spectrometry imaging revealed that different sets of biosurfactant molecules is deployed by the bacterium alone and in co-culture, with no overlap between them, suggesting a highly specialised reaction of *P. aeruginosa* to the presence of *A. fumigatus*. Furthermore, the exposure of the fungus to the bacterium led to architectural changes within the cell wall, presumably triggered by the rhamnolipid moieties. The transcriptome, as well as secretome data presented here support this finding: dynamic changes in the expression of polysaccharide-metabolic enzymes can be seen in the fungus exposed to *P. aeruginosa*. This effect, however, does not appear to be specific to only one bacterium. *S. maltophilia* grown in a combined biofilm with *A. fumigatus* on SCFM2 medium also elicits significant cell wall thickening (Melloul et al., 2016), although the effect might be achieved through a different mechanism (Li et al., 2009).

Phenazines have also been implicated in the purported inhibitory activity of *P. aeruginosa* on *A. fumigatus*, affecting hyphal development through production of reactive oxygen and reactive nitrogen species (ROS, RNS) (Briard et al., 2015; Zheng et al., 2015). At high concentrations, reduced phenazines penetrate the hyphal surface, are oxidised by intracellular oxygen and NADPH, and trigger a NapA-dependent oxidative stress response, which poisons the mitochondria by ROS and RNS (Briard et al., 2015). Interestingly, although phenazines could be found in extracts of liquid co-cultures of *P. aeruginosa* and *A. fumigatus*, the same compounds were not detected by MALDI-IMS. Furthermore, phenazine detoxication by *A. fumigatus* was proposed by the group of

Dorrestein, where the bacterial metabolites were biotransformed into less toxic derivatives by *A. fumigatus* (Moree et al., 2012). When the microbes were grown in SCFM2 liquid medium, phenazines themselves were present, but the modified products (phenazine-1-sulphate, 1-methylphenazine, 1-hydroxyphenazine) could be detected, suggesting that either sufficient production of these compounds by the bacterium, or their biotransformation by the fungus (through an undefined mechanism) depend directly on the cultivation conditions.

3.2 Secondary metabolites of *A. fumigatus*

The transcriptome analysis performed on *A. fumigatus* indicated that in co-cultivation with *P. aeruginosa*, the secondary metabolism of the fungus is attenuated. It was therefore unsurprising to find that some mycotoxins, traditionally associated with infection, such as fumagillin, pseurotin, fumitremorgin, or helvolic acid (Bignell et al., 2016) were not detected, or detected in lower amounts in co-cultivation.

Fumagillin and pseurotin are two bioactive mycotoxins produced by a biosynthetic supercluster (Wiemann et al., 2013). Fumagillin is an inhibitor of methionine aminopeptidases (Ehlers et al., 2016), affecting a multitude of cellular signalling pathways dependent on these enzymes, leading to growth and proliferation arrest in host cells (Guruceaga et al., 2019). It also protects *A. fumigatus* from host phagocytosis by inhibiting lymphocyte function (Fallon et al., 2010). Pseurotin has not been implicated in host tissue damage, but has been shown to have antibacterial properties against Gram-positive as well as Gram-negative bacteria (Pinheiro et al., 2013), and an immunomodulatory effect by inhibiting IgE production (Ishikawa et al., 2009). These metabolites are usually produced in high abundance, forming prominent peaks in chromatograms of *A. fumigatus* extracts. The production was detected in monoculture of the fungus grown in SCFM2 medium. However, the transcription of the supercluster, and thus also the biosynthesis of the toxins was attenuated when *A. fumigatus* was co-cultured with *P. aeruginosa*. A similar scenario was observed for helvolic acid, a toxin proved to have potent cilioinhibitory effect (Amitani et al., 1995), as well as potent antibacterial properties against Gram-positive bacteria, while being ineffective against Gram-negative ones (Ratnaweera et al., 2014; Kong et al., 2018).

It was interesting to observe that gliotoxin, an archetype of mycotoxins, and a reported inhibitor of *P. aeruginosa* growth (Reece et al., 2018), was also not detected either in *A. fumigatus* monocultures or mixed cultures with *P. aeruginosa*. Although Reece *et al.*, clearly showed that fungal culture supernatant containing gliotoxin antagonised the growth of *P. aeruginosa* biofilm and implicates gliotoxin in the interaction of the microbes in CF lung, gliotoxin was not found to be present in the culture supernatant of *A. fumigatus* SCFM2 monoculture, or in co-cultivation with *P. aeruginosa*, nor was it detected during cultivation on solid SCFM2 medium. Previously, the presence of lipopolysaccharide in potato dextrose broth medium, mimicking the presence of Gram-negative bacteria, significantly induced the production of gliotoxin in *A.*

fumigatus culture (Svahn et al., 2014). Here the induction effect could not be reproduced by the presence of *P. aeruginosa*, independent of the length of cultivation. The downregulation of the gliotoxin biosynthetic gene cluster was also evident from the transcriptome data, further supporting the veracity of this finding. The presence of gliotoxin likely contributes to virulence of the fungus in the host (Spikes et al., 2008); therefore, the absence of gliotoxin in simulated CF conditions renders *A. fumigatus* less virulent to the host, and diminishes its antagonistic effect on *P. aeruginosa*. The impact of the differential abundances of other secondary metabolites of *A. fumigatus* on the interaction (*e.g.* pyripyropene, fumisoquine, fumiquinazolines) is undetermined.

3.2.1 Interaction of *A. fumigatus* with *P. aeruginosa* induces the production of isonitrilated compounds in the fungus

One of the strains of *A. fumigatus* tested here, the CF isolate *A. fumigatus* CF10, was found to produce a diisonitrilated dityrosine product, BU-4704, and its previously undescribed saturated congener, here designated as BU-4704B. Simultaneously with the discovery of these compounds in co-culture of *A. fumigatus* and *P. aeruginosa*, the group of Keller comprehensively described isonitrile synthases of *A. fumigatus* and the biosynthetic pathways of fungal isonitrile products (Lim et al., 2018). These xanthocillin-class antibiotics are produced by dimerisation of two tyrosine moieties, catalysed by Dit1-like enzymes (Briza et al., 1996). BU-4704 is produced by the *xan* biosynthetic gene cluster, containing *xanB*, an NRPS-like enzyme with an isonitrile synthase domain (CF10_04996 in *A. fumigatus* CF10)(Lim et al., 2018). Although BU-4704 was shown upon its discovery to have mild antimicrobial properties even against *P. aeruginosa* (Tsunakawa et al., 1993), the deletion of CF10_04996 led to the loss of production of BU-4704(B), but did not result in diminished fitness of *A. fumigatus* CF10 strain in co-culture with *P. aeruginosa*. Furthermore, the induction of isonitrilated and *N*-formylated natural products in *A. fumigatus* by co-cultivation with bacteria was described before. The actinomycete *Streptomyces peucetius* triggers the production of multiple isonitrile- or *N*-formyl-functionalised secondary metabolites when cultivated in vicinity of *A. fumigatus* (Zuck et al., 2011). In fungal monoculture, the same biosynthetic gene clusters can be induced by copper starvation, due to the potential of the alkaloid products to act as fungal chalkophores (Lim et al., 2018). That the copper response trigger is conserved and used when isonitriles are induced by contact with bacteria seems unlikely, due to the fact that no physical contact is necessary for the induction by *S. peucetius* (Zuck et al., 2011), and the fact that despite the copper limitation of SCFM2 medium (no exogenous copper was added, *i.e.* the metal is only present as contaminant), BU-4704 and BU-4704B were detected solely in co-culture, and never in axenic culture of *A. fumigatus* CF10.

4 Siderophore piracy of *P. aeruginosa* extends to fungal siderophores

Over the course of evolution, fungi and bacteria have evolved numerous strategies to improve their fitness through acquisition of iron, one of the limiting essential nutrients (Sheldon et al., 2016; Matthaïou et al., 2018). One such strategy is the production of siderophores, secondary metabolites with a high affinity to the oxidised form of iron, which, upon secretion, chelate ferric ions and are internalised again by microbes (Kramer et al., 2020). However, once secreted, siderophores become public goods and their use is not limited to the producer. *P. aeruginosa* along with other pseudomonads (and, incidentally, many other bacteria) have long been established as accomplished users of xenosiderophores, a strategy sometimes dubbed ‘siderophore piracy’ (Traxler et al., 2012; Galet et al., 2015; Jorth et al., 2020). Previously, *P. aeruginosa* has been shown to pirate ferrioxamine, ferricoelichelin, and ferrichrome (hydroxamate siderophores) from the environmental bacterium *Streptomyces ambofaciens* and fungi (Galet et al., 2015), but also vibriobactin from *Vibrio spp.* (Elias et al., 2011), and enterobactin (catecholate siderophores), produced by multiple species of bacteria, such as *E. coli*, *Salmonella spp.*, *Klebsiella spp.*, or *Shigella spp.* (Caza and Kronstad, 2013). When grown in monoculture, *P. aeruginosa* produced and secreted pyoverdine in abundance. The obvious lack of detectable secreted pyoverdine in co-cultivation with *A. fumigatus* on solid media as analysed by MALDI imaging mass spectrometry, however, led to the notion that siderophore piracy may extend across kingdom boundaries to include TAFC. When ferric triacetylfusarinine C (Fe-TAFC) was provided to the bacterium, both the wild-type strain and the siderophore-free $\Delta pvdD\Delta pchEF$ mutant were capable of growing in iron-limited minimal medium to a similar extent as in a ferripyoverdine-supplied control sample.

To investigate the internalisation of TAFC by *P. aeruginosa*, I drew upon a previously published diagnostic strategy that uses radioactive ^{68}Ga -labelled siderophores as a potential tool for diagnostic imaging (Petrik et al., 2012; Petrik et al., 2013). After treating iron-starved *P. aeruginosa* with the labelled siderophore, the radioactivity measured in live bacteria was higher than in hydrogen peroxide-inactivated samples, as well as in *E. coli* control treated similarly. The inherent drawback of this study is the lack of another negative control where the metal would be coordinated by a chelator such as DTPA that would prevent internalisation of complexing with the negatively charged bacterial surface. Nevertheless, the growth of the bacterium with Fe-TAFC as an exclusive source of iron, as well as the significantly enriched radioactivity in ^{68}Ga -TAFC-treated *P. aeruginosa*, provide a good indication of siderophore piracy. To address the possibility that the TAFC molecule may be degraded by secreted enzymes in the outer environment, the Fe^{3+} ion liberated and subsequently taken up by the bacterium, the siderophore-free $\Delta pvdD\Delta pchEF$ mutant, as well as the lack of any apparent degradation products detected in LC-MS analyses, indicate that this is not a valid possibility.

Moreover, it is important to acknowledge here that the finding was serendipitous and the present study merely indicates that *P. aeruginosa* has the potential to privatise the fungal siderophore for its own use, rather than asserts that this process is routinely ongoing during an interaction in CF lungs. On the contrary, ample evidence suggests that this may not be the case. In the host, the levels of free Fe³⁺ iron are extremely low, reaching under 10⁻²⁴ M (Behnsen and Raffatellu, 2016). In the lower airways, where the impaired mucociliary clearance allows for accumulation of thick mucus, the environment becomes hypoxic or anoxic (Eichner et al., 2014; Montgomery et al., 2017), *i.e.* iron is present in its soluble reduced form (Andrews et al., 2003; Hunter et al., 2013), making the use of Fe³⁺-chelating siderophores obsolete. Indeed, *P. aeruginosa* is capable of adapting its iron acquisition strategies to the situation (Cornelis and Dingemans, 2013). During early stages of infection, *P. aeruginosa* upregulated the transcription of iron acquisition pathways (Cornforth et al., 2018), and pyoverdine was found in expectorated sputa from patients (whether these patients were colonised by *A. fumigatus* is unknown; (Martin et al., 2011). However, pyoverdine-negative mutants accumulate over longer colonisation periods (Vos et al., 2001; Lamont et al., 2009). Furthermore, the chronic inflammation process can lead to impaired vascular function and pulmonary haemorrhaging and haemoptysis (Flume, 2009). It is therefore conceivable that *P. aeruginosa* can take up haem released from haemoproteins (Ochsner et al., 2000). *A. fumigatus*, on the other hand, may need to rely on its poorly studied, low affinity ferrous iron uptake system (Kaplan and Kaplan, 2009; Blatzer et al., 2011), rather than on the preferred siderophore-mediated iron uptake. The physiology of *A. fumigatus* in a prolonged colonisation of a CF lung has, unfortunately, not been studied to date, and the exact adaptations of the fungus to competitive nutrient acquisition during non-invasive growth remain to be investigated.

5 Bacterial cyanogenesis and fungal cyanide degradation

The present study reports an *Aspergillus fumigatus* cyanide hydratase and implies its activation as a response to cyanide presence, as well as its catalytic activity. The gene (*chtA*) encoding the CHT enzyme shares a high percentage of identity with other CHTs in filamentous fungi (Basile et al., 2008), and is solely responsible for the fungus' capacity to detoxify cyanide. The phenotypic characterisation revealed that despite cyanide's potent toxicity profile (Blumer and Haas, 2000; Ryall et al., 2008), the growth of *A. fumigatus* from spores in CN⁻-spiked medium is merely retarded, rather than completely arrested. Upon accumulation of sufficient biomass capable of producing CHT, cyanide was detoxified and normal growth restored.

The presence of cyanide triggered the expression of the *chtA* gene; this activation of transcription was evident from an early and rapid transcriptional reaction of *A. fumigatus*. Such a response follows the mode of regulation exhibited by the cyanide-responsive CHT of *Neurospora crassa*, and is in contrast to that of *A. nidulans*, where the

nitrilase expression levels do not appear to be induced by the addition of cyanide (Basile et al., 2008). The catalytic activity of the AfCht is also remarkably high, capable of reducing 1 mM CN⁻, a concentration higher than the empirically and physiologically relevant concentration measured in CF patients' sputum (approx. 100 - 200 µM) (Ryall et al., 2008; Sanderson et al., 2008; Eiserich et al., 2018). The physiological response and degradation are rapid, with > 95% exogenously provided cyanide converted in 6 hours. In line with the findings of Basile *et al.*, (2008), a single protein product is sufficient to determine the organism's capability to metabolise cyanide.

The production of cyanide by *P. aeruginosa in vitro* is optimised in early stationary phase cultures under microaerobic conditions (O₂ < 5% (v/v)) (Worlitzsch et al., 2002), and temperatures ranging between 34°C and 37°C (Zlosnik and Williams, 2004; Neerincx et al., 2015). Although it has been documented that these conditions occur in the CF lung and bacterial cyanogenesis is present (Sanderson et al., 2008; Eiserich et al., 2018), we were unable to detect sufficient amounts of cyanide in *in vitro* cultures of *P. aeruginosa* grown in SCFM2, whether in mono- or co-culture with *A. fumigatus*. It is thus conceivable that in the human host's sputum context, where the growth and physiology of *P. aeruginosa* are substantially different than in lab conditions (as described elsewhere, *e.g.* dysregulation of quorum sensing (Turner et al., 2015); aggregate formation (Darch et al., 2018); iron homeostasis (Cornforth et al., 2018)), cyanogenesis and its regulation might occur in an altered or delayed fashion.

Cyanogenesis-favouring conditions *per se* are, however, apparently insufficient to elicit the expression of AfCht, and the protein was not detected in secretomes of *A. fumigatus* monocultures cultivated under hypoxic conditions both in minimal and synthetic CF sputum media (data not shown). The production and secretion of cyanide hydratase is, therefore, a specific reaction to the presence of the toxin, rather than a conserved prophylactic defence strategy against *P. aeruginosa*, and presumably other cyanide-producing lung pathogens, such as the *Burkholderia cepacia* complex (Ryall et al., 2008; Neerincx et al., 2015). Furthermore, phagocytosing neutrophils have been reported to produce cyanide *in vitro* (Stelmaszyńska, 1985; Stelmaszyńska, 1986), a situation that could conceivably arise during *A. fumigatus* infection, where such a host defence response would be incapacitated by the fungal enzymatic activity.

6 Mutual detoxication - achieving balance between *A. fumigatus* and *P. aeruginosa*

In light of the results presented here, including the establishment of a CF-representative model that does not favour either of the studied microbes, the attenuation of fungal secondary metabolism as evidenced by RNA sequencing and chemical analyses, decrease of pyoverdine production by *P. aeruginosa* in co-culture with *A. fumigatus*, or fungal degradation of bacteriogenic cyanide, the notion of a mutual detoxication becomes a reasonable explanation to the decreased antiproliferative activity exhibited by the co-

cultivation extracts. The attenuation of antagonistic activity of *A. fumigatus* appears to happen primarily at a transcriptional level, rather than by active enzymatic detoxication of secreted factors present in the environment. Similarly, the decrease of pyoverdine production by *P. aeruginosa* in co-culture may, ultimately, result in reduced virulence (Kang et al., 2019). The influence of the environment on the interaction is also indisputable; indeed, cystic fibrosis sputum, closely modelled by SCFM2, has a profound impact on physiology of *P. aeruginosa* (Turner et al., 2015; Welsh and Blackwell, 2016; Cornforth et al., 2018). A similar environment effect has been shown in *Burkholderia cenocepacia*, which translated directly into a reduced antifungal activity of the bacterium (Lightly et al., 2017). It has previously been proposed that there is a significant positive relationship between bacterial diversity and productivity in CF lung, despite the predominantly negative interactions between individual strains (Morgan et al., 2020). The present work suggests that this relationship may include at least one fungus. Figure 3 outlines the multitude of mechanisms by which *A. fumigatus* and *P. aeruginosa* interact, primarily inhibiting each other's growth. Despite all these mechanisms, the fungus and the bacterium are still capable of forming combined biofilms (Manavathu, 2015; Zheng et al., 2015), and are still co-isolated from expectorated sputa of CF patients (Reece et al., 2017) and can potentially form co-dependencies in the CF host (Baxter et al., 2013).

Figure 40 summarises the main additions of the present work to our understanding of the interactions between *A. fumigatus* and *P. aeruginosa*. I have shown that when given conditions that represent those in CF lungs, and, at the same time, do not unilaterally favour one of the partners, *A. fumigatus* and *P. aeruginosa* can establish a balanced growth without obvious antagonistic tendencies. The secondary metabolism of the fungus was found to be reduced to a level where it had a positive impact on proliferation of a pulmonary epithelial cell line. In light of these results, it is suggested that appropriate representative conditions be used when investigating microbial interactions in the context of cystic fibrosis, and potentially other conditions that facilitate polymicrobial colonisation. Furthermore, the relevance of many findings of antagonistic behaviour between *A. fumigatus* and *P. aeruginosa* to cystic fibrosis ecology ought to be critically reviewed and assessed in defined, CF lung-simulating conditions.

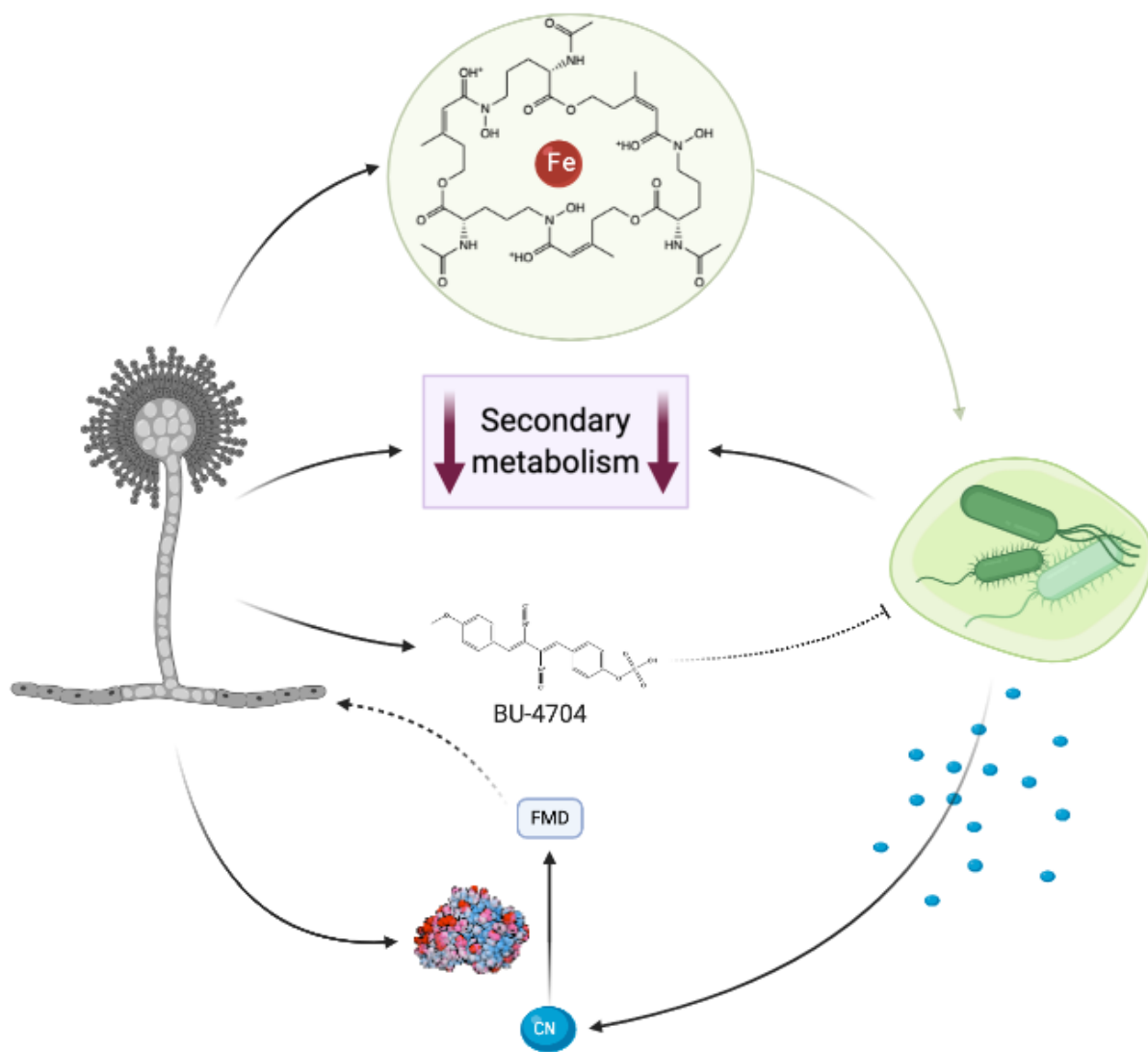


Figure 40. Interactions between *A. fumigatus* and *P. aeruginosa* described in the present work. Top to bottom: *A. fumigatus* produces TAFC, a siderophore that can be privatised by *P. aeruginosa*. Secondary metabolism of both partners was attenuated in co-cultivation. Contact with *P. aeruginosa* triggers the production of an isonitrile alkaloid BU-4704 in *A. fumigatus*; the compound has a negligible inhibitory effect on the bacterium. Under a specific set of conditions, *P. aeruginosa* can produce cyanide, which will be promptly detoxified into formamide by cyanide hydratase of *A. fumigatus*, induced specifically in response to the presence of the toxin in the environment.

References

- ABAD A, FERNÁNDEZ-MOLINA JV, BIKANDI J, et al (2010) What makes *Aspergillus fumigatus* a successful pathogen? Genes and molecules involved in invasive aspergillosis. *Rev Iberoam Micol* 27:155–82. doi: 10.1016/j.riam.2010.10.003
- AKKAN CK, MAY A, HAMMADEH M, et al (2014) Matrix shaped pulsed laser deposition: New approach to large area and homogeneous deposition. *Appl Surf Sci* 302:149–152. doi: 10.1016/j.apsusc.2013.09.061
- AMIN R, DUPUIS A, AARON SD, RATJEN F (2010) The effect of chronic infection with *Aspergillus fumigatus* on lung function and hospitalization in patients with cystic fibrosis. *Chest* 137:171–176. doi: 10.1378/chest.09-1103
- AMITANI R, TAYLOR G, ELEZIS EN, et al (1995) Purification and characterization of factors produced by *Aspergillus fumigatus* which affect human ciliated respiratory epithelium. *Infect Immun* 63:3266–3271. doi: 10.1128/iai.63.9.3266-3271.1995
- ANAND R, CLEMONS K V., STEVENS DA (2017) Effect of anaerobiosis or hypoxia on *Pseudomonas aeruginosa* inhibition of *Aspergillus fumigatus* biofilm. *Arch Microbiol* 199:881–890. doi: 10.1007/s00203-017-1362-5
- ANDREWS SC, ROBINSON AK, RODRÍGUEZ-QUIÑONES F (2003) Bacterial iron homeostasis. *FEMS Microbiol Rev* 27:215–237. doi: 10.1016/s0168-6445(03)00055-x
- ARMSTEAD J, MORRIS J, DENNING DW (2014) Multi-country estimate of different manifestations of aspergillosis in cystic fibrosis. *PLoS One* 9:e98502–e98502. doi: 10.1371/journal.pone.0098502
- AVILÉS E, RODRÍGUEZ AD (2010) Monamphilectine A, a potent antimalarial β -lactam from marine sponge *Hymeniacidon* sp: Isolation, structure, semisynthesis, and bioactivity. *Org Lett* 12:5290–5293. doi: 10.1021/ol102351z
- BALLANCE DJ, TURNER G (1985) Development of a high-frequency transforming vector for *Aspergillus nidulans*. *Gene* 36:321–331. doi: 10.1016/0378-1119(85)90187-8
- BARCLAY M, TETT VA, KNOWLES CJ (1998) Metabolism and enzymology of cyanide/metallo-cyanide biodegradation by *Fusarium solani* under neutral and acidic conditions. *Enzyme Microb Technol* 23:321–330. doi: 10.1016/S0141-0229(98)00055-6
- BASILE LJ, WILLSON RC, SEWELL BT, BENEDIK MJ (2008) Genome mining of cyanide-degrading nitrilases from filamentous fungi. *Appl Microbiol Biotechnol* 80:427–435. doi: 10.1007/s00253-008-1559-2
- BAXTER CG, RAUTEMAA R, JONES AM, et al (2013) Intravenous antibiotics reduce the presence of *Aspergillus* in adult cystic fibrosis sputum. *Thorax* 68:652–657. doi: 10.1136/thoraxjnl-2012-202412
- BEHNSEN J, RAFFATELLU M (2016) Siderophores: More than stealing iron. *mBio* 7:e01906-16. doi: 10.1128/mBio.01906-16
- BIGNELL E, CAIRNS TC, THROCKMORTON K, et al (2016) Secondary metabolite arsenal of an opportunistic pathogenic fungus. *Philos Trans R Soc B Biol Sci* 371:. doi: 10.1098/rstb.2016.0023
- BLATZER M, BINDER U, HAAS H (2011) The metallo-reductase FreB is involved in adaptation of *Aspergillus fumigatus* to iron starvation. *Fungal Genet Biol* 48:1027–1033. doi: 10.1016/j.fgb.2011.07.009
- BLATZER M, SCHRETTL M, SARG B, et al (2011) SidL, an *Aspergillus fumigatus* transacetylase involved in biosynthesis of the siderophores ferricrocin and hydroxyferricrocin. *Appl Environ Microbiol* 77:4959–4966. doi: 10.1128/AEM.00182-11

- BLUMER C, HAAS D (2000) Mechanism, regulation, and ecological role of bacterial cyanide biosynthesis. *Arch Microbiol* 173:170–177. doi: 10.1007/s002039900127
- BONGOMIN F, GAGO S, OLADELE RO, DENNING DW (2017) Global and multi-national prevalence of fungal diseases—estimate precision. *J Fungi* 3:57. doi: 10.3390/jof3040057
- BRAKHAGE AA, VAN DEN BRULLE J (1995) Use of reporter genes to identify recessive trans-acting mutations specifically involved in the regulation of *Aspergillus nidulans* penicillin biosynthesis genes. *J Bacteriol* 177:2781–2788. doi: 10.1128/jb.177.10.2781-2788.1995
- BRAKHAGE A (2005) Systemic fungal infections caused by *Aspergillus* species: epidemiology, infection process and virulence determinants. *Curr Drug Targets* 6:875–886. doi: 10.2174/138945005774912717
- BRAKHAGE AA (2013) Regulation of fungal secondary metabolism. *Nat Rev Microbiol* 11:21–32. doi: 10.1038/nrmicro2916
- BRAKHAGE AA, BRUNS S, THYWISSEN A, et al (2010) Interaction of phagocytes with filamentous fungi. *Curr Opin Microbiol* 13:409–415. doi: 10.1016/j.mib.2010.04.009
- BRAKHAGE AA, LANGFELDER K (2002) Menacing mold: the molecular biology of *Aspergillus fumigatus*. *Annu Rev Microbiol* 56:433–455. doi: 10.1146/annurev.micro.56.012302.160625
- BRANDON M, HOWARD B, LAWRENCE C, LAUBENBACHER R (2015) Iron acquisition and oxidative stress response in *Aspergillus fumigatus*. *BMC Syst Biol* 9:19. doi: 10.1186/s12918-015-0163-1
- BRIARD B, BOMME P, LECHNER BE, et al (2015) *Pseudomonas aeruginosa* manipulates redox and iron homeostasis of its microbiota partner *Aspergillus fumigatus* via phenazines. *Sci Rep* 5:8220. doi: 10.1038/srep08220
- BRIARD B, HEDDERGOTT C, LATGÉ J-P (2016) Volatile compounds emitted by *Pseudomonas aeruginosa* stimulate growth of the fungal pathogen *Aspergillus fumigatus*. *mBio* 7:e00219–e00219. doi: 10.1128/mBio.00219-16
- BRIARD B, MISLIN GLA, LATGÉ JPJP, BEAUVAIS A (2019) Interactions between *Aspergillus fumigatus* and pulmonary bacteria: current state of the field, new data, and future perspective. *J Fungi* 5:48. doi: 10.3390/jof5020048
- BRIARD B, RASOLDIER V, BOMME P, et al (2017) Dirhamnolipids secreted from *Pseudomonas aeruginosa* modify antifungal susceptibility of *Aspergillus fumigatus* by inhibiting β 1,3 glucan synthase activity. *ISME J* 11:1578–1591. doi: 10.1038/ismej.2017.32
- BRISKOT G, TARAZ K, BUDZIKIEWICZ H (1986) Siderophore vom Pyoverdin-Typ aus *Pseudomonas aeruginosa* [1]. *Zeitschrift für Naturforsch - Sect C J Biosci* 41:497–506. doi: 10.1515/znc-1986-5-601
- BRIZA P, KALCHHAUSER H, PITTENAUER E, et al (1996) N,N' bisformyl dityrosine is an *in vivo* precursor of the yeast ascospore wall. *Eur J Biochem* 239:124–131. doi: 10.1111/j.1432-1033.1996.0124u.x
- BROGDEN K, GUTHMILLER J, TAYLOR C (2005) Human polymicrobial infections. *Lancet* 365:253–255. doi: 10.1016/s0140-6736(05)70155-0

- BROWN GD, DENNING DW, GOW NAR, et al (2012) Hidden killers: Human fungal infections. *Sci Transl Med* 4:165rv13-165rv13. doi: 10.1126/scitranslmed.3004404
- BROWN SA, PALMER KL, WHITELEY M (2008) Revisiting the host as a growth medium. *Nat Rev Microbiol* 6:657–666. doi: 10.1038/nrmicro1955
- BRUKNER DABOVIĆ B, RADOJKOVIĆ D, MINIĆ P, et al (1992) Frequency of the Δ F508 deletion and G551D, R553X and G542X mutations in Yugoslav CF patients. *Hum Genet* 88:699–700. doi: 10.1007/BF02265302
- BULLEN JJ, WARD CG, WALLIS SN (1974) Virulence and the role of iron in *Pseudomonas aeruginosa* infection. *Infect Immun* 10:443–450. doi: 10.1128/iai.10.3.443-450.1974
- BYRD AL, SEGRE JA (2016) Adapting Koch's postulates. *Science* (80-) 351:224–226. doi: 10.1126/science.aad6753
- CABRERA-VALLADARES N, RICHARDSON AP, OLVERA C, et al (2006) Monorhamnolipids and 3-(3-hydroxyalkanoyloxy) alkanolic acids (HAAs) production using *Escherichia coli* as a heterologous host. *Appl Microbiol Biotechnol* 73:187–194. doi: 10.1007/s00253-006-0468-5
- CARBERRY S, MOLLOY E, HAMMEL S, et al (2012) Gliotoxin effects on fungal growth: mechanisms and exploitation. *Fungal Genet Biol* 49:302–312. doi: 10.1016/j.fgb.2012.02.003
- CARMODY LA, ZHAO J, KALIKIN LM, et al (2015) The daily dynamics of cystic fibrosis airway microbiota during clinical stability and at exacerbation. *Microbiome* 3:12. doi: 10.1186/s40168-015-0074-9
- CARTERSON AJ, MORICI LA, JACKSON DW, et al (2004) The transcriptional regulator AlgR controls cyanide production in *Pseudomonas aeruginosa*. *J Bacteriol* 186:6837–6844. doi: 10.1128/JB.186.20.6837-6844.2004
- CARTRON ML, MADDOCKS S, GILLINGHAM P, et al (2006) Feo - transport of ferrous iron into bacteria. *BioMetals* 19:143–157. doi: 10.1007/s10534-006-0003-2
- CASSAT JE, SKAAR EP (2013) Iron in infection and immunity. *Cell Host Microbe* 13:509–519. doi: 10.1016/j.chom.2013.04.010
- CASTRIC PA (1975) Hydrogen cyanide, a secondary metabolite of *Pseudomonas aeruginosa*. *Can J Microbiol* 21:613–618. doi: 10.1139/m75-088
- CASTRIC PA (1977) Glycine metabolism by *Pseudomonas aeruginosa*: hydrogen cyanide biosynthesis. *J Bacteriol* 130:826–831. doi: 10.1128/jb.130.2.826-831.1977
- CHAMBERS CE, VISSER MB, SCHWAB U, SOKOL PA (2005) Identification of N-acylhomoserine lactones in mucopurulent respiratory secretions from cystic fibrosis patients. *FEMS Microbiol Lett* 244:297–304. doi: 10.1016/j.femsle.2005.01.055
- CHOTIRMALL SH, MCELVANEY NG (2014) Fungi in the cystic fibrosis lung: Bystanders or pathogens? *Int J Biochem Cell Biol* 52:161–173. doi: 10.1016/j.biocel.2014.03.001
- CHOTIRMALL SH, O'DONOGHUE E, BENNETT K, et al (2010) Sputum *Candida albicans* presages FEV1 decline and hospital-treated exacerbations in cystic fibrosis. *Chest* 138:1186–1195. doi: 10.1378/chest.09-2996

- CHUGANI S, KIM BS, PHATTARASUKOL S, et al (2012) Strain-dependent diversity in the *Pseudomonas aeruginosa* quorum-sensing regulon. *Proc Natl Acad Sci U S A* 109:E2823–E2831. doi: 10.1073/pnas.1214128109
- CLARKE-PEARSON MF, BRADY SF (2008) Paerucumarin, a new metabolite produced by the pvc gene cluster from *Pseudomonas aeruginosa*. *J Bacteriol* 190:6927–6930. doi: 10.1128/JB.00801-08
- CODY WL, PRITCHETT CL, JONES AK, et al (2009) *Pseudomonas aeruginosa* AlgR controls cyanide production in an AlgZ-dependent manner. *J Bacteriol* 191:2993–3002. doi: 10.1128/JB.01156-08
- COHEN TS, PRINCE A (2012) Cystic fibrosis: a mucosal immunodeficiency syndrome. *Nat Med* 18:509–519. doi: 10.1038/nm.2715
- COLEMAN JJ, GHOSH S, OKOLI I, MYLONAKIS E (2011) Antifungal activity of microbial secondary metabolites. *PLoS One* 6:e25321–e25321. doi: 10.1371/journal.pone.0025321
- CONRAD D, HAYNES M, SALAMON P, et al (2013) Cystic fibrosis therapy: a community ecology perspective. *Am J Respir Cell Mol Biol* 48:150–156. doi: 10.1165/rcmb.2012-0059PS
- CORNELIS P, DINGEMANS J (2013) *Pseudomonas aeruginosa* adapts its iron uptake strategies in function of the type of infections. *Front Cell Infect Microbiol* 4:. doi: 10.3389/fcimb.2013.00075
- CORNELIS P, MATTHIJS S (2002) Diversity of siderophore-mediated iron uptake systems in fluorescent pseudomonads: not only pyoverdines. *Environ Microbiol* 4:787–798. doi: 10.1046/j.1462-2920.2002.00369.x
- CORNFORTH DM, DEES JL, IBBERSON CB, et al (2018) *Pseudomonas aeruginosa* transcriptome during human infection. *Proc Natl Acad Sci U S A* 115:E5125–E5134. doi: 10.1073/pnas.1717525115
- COSTERTON JW (2002) Anaerobic biofilm infections in cystic fibrosis. *Mol Cell* 10:699–700. doi: 10.1016/S1097-2765(02)00698-6
- COWLEY ES, KOPF SH, LARIVIERE A, et al (2015) Pediatric cystic fibrosis sputum can be chemically dynamic, anoxic, and extremely reduced due to hydrogen sulfide formation. *mBio* 6:e00767–e00767. doi: 10.1128/mBio.00767-15
- STROE MC, NETZKER T, SCHERLACH K, et al (2020) Targeted induction of a silent fungal gene cluster encoding the bacteria-specific germination inhibitor fumigermin. *eLife* 9:e52541. doi: 10.7554/eLife.52541
- DARCH SE, SIMOSKA O, FITZPATRICK M, et al (2018) Spatial determinants of quorum signaling in a *Pseudomonas aeruginosa* infection model. *Proc Natl Acad Sci U S A* 115:4779–4784. doi: 10.1073/pnas.1719317115
- DASENBROOK EC (2011) Update on methicillin-resistant *Staphylococcus aureus* in cystic fibrosis. *Curr Opin Pulm Med* 17:437–441. doi: 10.1097/MCP.0b013e32834b95ed
- DAWSON M, WIRTZ D, HANES J (2003) Enhanced viscoelasticity of human cystic fibrotic sputum correlates with increasing microheterogeneity in particle transport. *J Biol Chem* 278:50393–50401. doi: 10.1074/jbc.m309026200

- DE ARAÚJO FG, NOVAES FC, DOS SANTOS NPC, et al (2005) Prevalence of ΔF508, G551D, G542X, and R553X mutations among cystic fibrosis patients in the North of Brazil. *Brazilian J Med Biol Res* 38:11–15. doi: 10.1590/s0100-879x2005000100003
- DE VOS D, DE CHIAL M, COCHEZ C, et al (2001) Study of pyoverdine type and production by *Pseudomonas aeruginosa* isolated from cystic fibrosis patients: prevalence of type II pyoverdine isolates and accumulation of pyoverdine-negative mutations. *Arch Microbiol* 175:384–388. doi: 10.1007/s002030100278
- DE VOS MGJ, ZAGORSKI M, MCNALLY A, BOLLENBACH T (2017) Interaction networks, ecological stability, and collective antibiotic tolerance in polymicrobial infections. *Proc Natl Acad Sci U S A* 114:10666–10671. doi: 10.1073/pnas.1713372114
- DEMBITSKY VM, GLORIOZOVA TA, POROIKOV VV (2015) Naturally occurring plant isoquinoline N-oxide alkaloids: their pharmacological and SAR activities. *Phytomedicine* 22:183–202. doi: 10.1016/j.phymed.2014.11.002
- DESAI JD, BANAT IM (1997) Microbial production of surfactants and their commercial potential. *Microbiol Mol Biol Rev* 61:47–64. doi: 10.1128/.61.1.47-64.1997
- DHINGRA S, LIND AL, LIN HC, et al (2013) The fumagillin gene cluster, an example of hundreds of genes under VeA control in *Aspergillus fumigatus*. *PLoS One* 8:e77147–e77147. doi: 10.1371/journal.pone.0077147
- DIGGLE SP, WINZER K, CHABRA SR, et al (2003) The *Pseudomonas aeruginosa* quinolone signal molecule overcomes the cell density-dependency of the quorum sensing hierarchy, regulates *rhl*-dependent genes at the onset of stationary phase and can be produced in the absence of LasR. *Mol Microbiol* 50:29–43. doi: 10.1046/j.1365-2958.2003.03672.x
- DING F, OINUMA KI, SMALLEY NE, et al (2018) The *Pseudomonas aeruginosa* orphan quorum sensing signal receptor QscR regulates global quorum sensing gene expression by activating a single linked operon. *mBio* 9:e01274-18. doi: 10.1128/mBio.01274-18
- DOLAN SK, O'KEEFFE G, JONES GW, DOYLE S (2015) Resistance is not futile: gliotoxin biosynthesis, functionality and utility. *Trends Microbiol* 23:419–428. doi: 10.1016/j.tim.2015.02.005
- DU RH, LI EG, CAO Y, et al (2011) Fumigaclavine C inhibits tumor necrosis factor α production via suppression of toll-like receptor 4 and nuclear factor κ b activation in macrophages. *Life Sci* 89:235–240. doi: 10.1016/j.lfs.2011.06.015
- EHLERS T, FURNESS S, PHILIP ROBINSON T, et al (2016) Methionine aminopeptidase type-2 inhibitors targeting angiogenesis. *Curr Top Med Chem* 16:1478–1488. doi: 10.2174/1568026615666150915121204
- EICHNER A, GÜNTHER N, ARNOLD M, et al (2014) Marker genes for the metabolic adaptation of *Pseudomonas aeruginosa* to the hypoxic cystic fibrosis lung environment. *Int J Med Microbiol* 304:1050–1061. doi: 10.1016/j.ijmm.2014.07.014
- EISERICH JP, OTT SP, KADIR T, et al (2018) Quantitative assessment of cyanide in cystic fibrosis sputum and its oxidative catabolism by hypochlorous acid. *Free Radic Biol Med* 129:146–154. doi: 10.1016/j.freeradbiomed.2018.09.007
- ELIAS S, DEGTYAR E, BANIN E (2011) FvbA is required for vibriobactin utilization in *Pseudomonas aeruginosa*. *Microbiology* 157:2172–2180. doi: 10.1099/mic.0.044768-0

- ELLETT F, JORGENSEN J, FRYDMAN GH, et al (2017) Neutrophil interactions stimulate evasive hyphal branching by *Aspergillus fumigatus*. *PLoS Pathog* 13:e1006154–e1006154. doi: 10.1371/journal.ppat.1006154
- EMSERMANN J, KAUHL U, OPATZ T (2016) Marine isonitriles and their related compounds. *Mar Drugs* 14:16. doi: 10.3390/md14010016
- ENE I V, WALKER LA, SCHIAVONE M, et al (2015) Cell wall remodeling enzymes modulate fungal cell wall elasticity and osmotic stress resistance. *mBio* 6:e00986–e00986. doi: 10.1128/mBio.00986-15
- FALLON JP, REEVES EP, KAVANAGH K (2010) Inhibition of neutrophil function following exposure to the *Aspergillus fumigatus* toxin fumagillin. *J Med Microbiol* 59:625–633. doi: 10.1099/jmm.0.018192-0
- FERREIRA JAG, PENNER JC, MOSS RB, et al (2015) Inhibition of *Aspergillus fumigatus* and its biofilm by *Pseudomonas aeruginosa* is dependent on the source, phenotype and growth conditions of the bacterium. *PLoS One* 10:e0134692–e0134692. doi: 10.1371/journal.pone.0134692
- FISCHBACH MA, WALSH CT, CLARDY J (2008) The evolution of gene collectives: How natural selection drives chemical innovation. *Proc Natl Acad Sci U S A* 105:4601–4608. doi: 10.1073/pnas.0709132105
- FLAK M, KRESPACH MK, PSCHIBUL AJ, et al (2020) New avenues toward drug discovery in fungi. In: Benz P (ed) *The Mycota Vol. II: Genetics and Biotechnology*. Springer. [Accepted]
- FLIGHT WG, SMITH A, PAISEY C, et al (2015) Rapid detection of emerging pathogens and loss of microbial diversity associated with severe lung disease in cystic fibrosis. *J Clin Microbiol* 53:2022–2029. doi: 10.1128/JCM.00432-15
- FLUME PA (2003) Airway Clearance Techniques. *Semin Respir Crit Care Med* 24:727–735. doi: 10.1055/s-2004-815668
- FLUME PA (2009) Pulmonary Complications of Cystic Fibrosis. *Respir Care* 54:618–627. doi: 10.4187/aarc0443
- FLUME PA, O’SULLIVAN BP, ROBINSON KA, et al (2007) Cystic fibrosis pulmonary guidelines: Chronic medications for maintenance of lung health. *Am J Respir Crit Care Med* 176:957–969. doi: 10.1164/rccm.200705-6640C
- FODOR AA, KLEM ER, GILPIN DF, et al (2012) The adult cystic fibrosis airway microbiota is stable over time and infection type, and highly resilient to antibiotic treatment of exacerbations. *PLoS One* 7:e45001–e45001. doi: 10.1371/journal.pone.0045001
- FRIEDEN T (2013) Antibiotic resistance threats in the United States. *Centers for Disease Control and Prevention* (U.S.)
- FRIMMERSDORF E, HORATZEK S, PELNIKEVICH A, et al (2010) How *Pseudomonas aeruginosa* adapts to various environments: a metabolomic approach. *Environ Microbiol* 12:1734–1747. doi: 10.1111/j.1462-2920.2010.02253.x
- FUJIWARA A, OKUDA T, MASUDA S, et al (1982) Fermentation, isolation and characterization of isonitrile antibiotics. *Agric Biol Chem* 46:1803–1809. doi: 10.1080/00021369.1982.10865344

- GALET J, DEVEAU A, HÔTEL L, et al (2015) *Pseudomonas fluorescens* pirates both ferrioxamine and ferricoelichelin siderophores from *Streptomyces ambofaciens*. *Appl Environ Microbiol* 81:3132–3141. doi: 10.1128/AEM.03520-14
- GALLAGHER LA, MCKNIGHT SL, KUZNETSOVA MS, et al (2002) Functions required for extracellular quinolone signaling by *Pseudomonas aeruginosa*. *J Bacteriol* 184:6472–6480. doi: 10.1128/JB.184.23.6472-6480.2002
- GARSON MJ, SIMPSON JS (2004) Marine isocyanides and related natural products - structure, biosynthesis and ecology. *Nat Prod Rep* 21:164–179. doi: 10.1039/b302359c
- GELLATLY SL, HANCOCK REW (2013) *Pseudomonas aeruginosa*: New insights into pathogenesis and host defenses. *Pathog Dis* 67:159–173. doi: 10.1111/2049-632X.12033
- GIBSON DG (2011) Enzymatic assembly of overlapping DNA fragments. *Methods Enzymol* 498:349–361. doi: 10.1016/B978-0-12-385120-8.00015-2
- GIBSON DG, YOUNG L, CHUANG RY, et al (2009) Enzymatic assembly of DNA molecules up to several hundred kilobases. *Nat Methods* 6:343–345. doi: 10.1038/nmeth.1318
- GILCHRIST FJ, BELCHER J, JONES AM, et al (2015) Exhaled breath hydrogen cyanide as a marker of early *Pseudomonas aeruginosa* infection in children with cystic fibrosis. *ERJ Open Res* 1:44–2015. doi: 10.1183/23120541.00044-2015
- GLOER JB, POCH GK, SHORT DM, MCCLOSKEY D V. (1988) Structure of brassicicolin A: a novel isocyanide antibiotic from the phylloplane fungus *Alternaria brassicicola*. *J Org Chem* 53:3758–3761. doi: 10.1021/jo00251a017
- GOLDFARB WB, MARGRAF H, MOORE AM (1967) Cyanide production by *Pseudomonas aeruginosa*. *Plast Reconstr Surg* 40:100. doi: 10.1097/00006534-196707000-00027
- GONÇALVES-DE-ALBUQUERQUE CF, SILVA AR, BURTH P, et al (2016) Possible mechanisms of *Pseudomonas aeruginosa*-associated lung disease. *Int J Med Microbiol* 306:20–28. doi: 10.1016/j.ijmm.2015.11.001
- GRANILLO AR, CANALES MGM, ESPÍNDOLA MES, et al (2015) Antibiosis interaction of *Staphylococcus aureus* on *Aspergillus fumigatus* assessed *in vitro* by mixed biofilm formation. *BMC Microbiol* 15:33. doi: 10.1186/s12866-015-0363-2
- GREISER J, NIKSCH T, WEIGAND W, FREESMEYER M (2016) Investigations on the Ga(III) complex of EOB-DTPA and its ⁶⁸Ga radiolabeled analogue. *J Vis Exp* 2016:54334. doi: 10.3791/54334
- GROSS H, LOPER JE (2009) Genomics of secondary metabolite production by *Pseudomonas* spp. *Nat Prod Rep* 26:1408–1446. doi: 10.1039/b817075b
- GUINEA J, PELÁEZ T, ALCALÁ L, BOUZA E (2005) Evaluation of Czapeck agar and Sabouraud dextrose agar for the culture of airborne *Aspergillus* conidia. *Diagn Microbiol Infect Dis* 53:333–334. doi: 10.1016/j.diagmicrobio.2005.07.002
- GURUCEAGA X, EZPELETA G, MAYAYO E, et al (2018) A possible role for fumagillin in cellular damage during host infection by *Aspergillus fumigatus*. *Virulence* 9:1548–1561. doi: 10.1080/21505594.2018.1526528
- GURUCEAGA X, PEREZ-CUESTA U, DE CERIO AAD, et al (2019) Fumagillin, a mycotoxin of *Aspergillus fumigatus*: biosynthesis, biological activities, detection, and applications. *Toxins (Basel)* 12:7. doi: 10.3390/toxins12010007

- HAAS H (2012) Iron - a key nexus in the virulence of *Aspergillus fumigatus*. *Front Microbiol* 3:28. doi: 10.3389/fmicb.2012.00028
- HABA E, PINAZO A, JAUREGUI O, et al (2003) Physicochemical characterization and antimicrobial properties of rhamnolipids produced by *Pseudomonas aeruginosa* 47T2 NCBIM 40044. *Biotechnol Bioeng* 81:316–322. doi: 10.1002/bit.10474
- HANCOCK REW, SPEERT DP (2000) Antibiotic resistance in *Pseudomonas aeruginosa*: mechanisms and impact on treatment. *Drug Resist Updat* 3:247–255. doi: 10.1054/drup.2000.0152
- HARRISON F (2007) Microbial ecology of the cystic fibrosis lung. *Microbiology* 153:917–923. doi: 10.1099/mic.0.2006/004077-0
- HEEB S, HAAS D (2001) Regulatory roles of the GacS/GacA two-component system in plant-associated and other Gram-negative bacteria. *Mol Plant-Microbe Interact* 14:1351–1363. doi: 10.1094/MPMI.2001.14.12.1351
- HEINEKAMP T, THYWISSEN A, MACHELEIDT J, et al (2012) *Aspergillus fumigatus* melanins: interference with the host endocytosis pathway and impact on virulence. *Front Microbiol* 3:440. doi: 10.3389/fmicb.2012.00440
- HENKE MO, JOHN G, GERMANN M, et al (2007) MUC5AC and MUC5B mucins increase in cystic fibrosis airway secretions during pulmonary exacerbation. *Am J Respir Crit Care Med* 175:816–821. doi: 10.1164/rccm.200607-10110C
- HILL UG, FLOTO RA, HAWORTH CS (2012) Non-tuberculous mycobacteria in cystic fibrosis. *J R Soc Med* 105 Suppl 2:S14–S18. doi: 10.1258/jrsm.2012.12s003
- HISSEN AHT, CHOW JMT, PINTO LJ, MOORE MM (2004) Survival of *Aspergillus fumigatus* in serum involves removal of iron from transferrin: the role of siderophores. *Infect Immun* 72:1402–1408. doi: 10.1128/IAI.72.3.1402-1408.2004
- HMELO LR, BORLEE BR, ALMBLAD H, et al (2015) Precision-engineering the *Pseudomonas aeruginosa* genome with two-step allelic exchange. *Nat Protoc* 10:1820–1841. doi: 10.1038/nprot.2015.115
- HOFFMANN T, DORRESTEIN PC (2015) Homogeneous matrix deposition on dried agar for maldi imaging mass spectrometry of microbial cultures. *J Am Soc Mass Spectrom* 26:1959–1962. doi: 10.1007/s13361-015-1241-8
- HOGAN DA, VIK Å, KOLTER R (2004) A *Pseudomonas aeruginosa* quorum-sensing molecule influences *Candida albicans* morphology. *Mol Microbiol* 54:1212–1223. doi: 10.1111/j.1365-2958.2004.04349.x
- HOPKE A, BROWN AJP, HALL RA, WHEELER RT (2018) Dynamic fungal cell wall architecture in stress adaptation and immune evasion. *Trends Microbiol* 26:284–295. doi: 10.1016/j.tim.2018.01.007
- HUANG W, WILKS A (2017) A rapid seamless method for gene knockout in *Pseudomonas aeruginosa*. *BMC Microbiol* 17:199. doi: 10.1186/s12866-017-1112-5
- HUNTER RC, ASFOUR F, DINGEMANS J, et al (2013) Ferrous iron is a significant component of bioavailable iron in cystic fibrosis airways. *mBio* 4:e00557-13. doi: 10.1128/mBio.00557-13

- INGHAMA CJ, KALISMAND O, FINKELSHTEIND A, BEN-JACOB E (2011) Mutually facilitated dispersal between the nonmotile fungus *Aspergillus fumigatus* and the swarming bacterium *Paenibacillus vortex*. *Proc Natl Acad Sci U S A* 108:19731–19736. doi: 10.1073/pnas.1102097108
- INGLIS DO, BINKLEY J, SKRZYPEK MS, et al (2013) Comprehensive annotation of secondary metabolite biosynthetic genes and gene clusters of *Aspergillus nidulans*, *A. fumigatus*, *A. niger* and *A. oryzae*. *BMC Microbiol* 13:91. doi: 10.1186/1471-2180-13-91
- ISHIKAWA M, NINOMIYA T, AKABANE H, et al (2009) Pseurotin A and its analogues as inhibitors of immunoglobuline E production. *Bioorganic Med Chem Lett* 19:1457–1460. doi: 10.1016/j.bmcl.2009.01.029
- ITOH S, HONDA H, TOMITA F, SUZUKI T (1971) Rhamnolipids produced by *Pseudomonas aeruginosa* grown on n-paraffin (mixture of c12, c13 and c14 fractions). *J Antibiot (Tokyo)* 24:855–859. doi: 10.7164/antibiotics.24.855
- JANDER G, RAHME LG, AUSUBEL FM (2000) Positive correlation between virulence of *Pseudomonas aeruginosa* mutants in mice and insects. *J Bacteriol* 182:3843–3845. doi: 10.1128/JB.182.13.3843-3845.2000
- JANDHYALA DM, WILLSON RC, SEWELL BT, BENEDIK MJ (2005) Comparison of cyanide-degrading nitrilases. *Appl Microbiol Biotechnol* 68:327–335. doi: 10.1007/s00253-005-1903-8
- JENKE-KODAMA H, BÖRNER T, DITTMANN E (2006) Natural biocombinatorics in the polyketide synthase genes of the actinobacterium *Streptomyces avermitilis*. *PLoS Comput Biol* 2:1210–1218. doi: 10.1371/journal.pcbi.0020132
- JERRY REEN F, PHELAN JP, WOODS DF, et al (2016) Harnessing bacterial signals for suppression of biofilm formation in the nosocomial fungal pathogen *Aspergillus fumigatus*. *Front Microbiol* 7:2074. doi: 10.3389/fmicb.2016.02074
- JOMORI T, SHIBUTANI T, AHMADI P, et al (2015) A new isocyanosesquiterpene from the nudibranch *Phyllidiella pustulosa*. *Nat Prod Commun* 10:1913–1914. doi: 10.1177/1934578x1501001126
- JORTH PA, VAILLANCOURT M, NADEAU S, CALDERA JR (2020) Antibiotic resistant *Pseudomonas aeruginosa* upregulate iron piracy genes during macrophage infection and evade killing. *J Immunol* 204:231.34 LP-231.34
- JUNG A, SCHÜRMAN T, SCHWARZ C, et al (2017) Non-ABPA *Aspergillus bronchitis* in cystic fibrosis. *Cyst. Fibros.* PA1347
- KANG D, SON GH, PARK HM, et al (2013) Culture condition-dependent metabolite profiling of *Aspergillus fumigatus* with antifungal activity. *Fungal Biol* 117:211–219. doi: 10.1016/j.funbio.2013.01.009
- KANG D, REVTOVICH A V., CHEN Q, et al (2019) Pyoverdine-dependent virulence of *Pseudomonas aeruginosa* isolates from cystic fibrosis patients. *Front Microbiol* 10:2048. doi: 10.3389/fmicb.2019.02048
- KAPLAN CD, KAPLAN J (2009) Iron acquisition and transcriptional regulation. *Chem Rev* 109:4536–4552. doi: 10.1021/cr9001676

- KAUR J, PETHANI BP, KUMAR S, et al (2015) *Pseudomonas aeruginosa* inhibits the growth of *Scedosporium aurantiacum*, an opportunistic fungal pathogen isolated from the lungs of cystic fibrosis patients. *Front Microbiol* 6:866. doi: 10.3389/fmicb.2015.00866
- KAWAGUCHI T, YUNG PC, NORMAN RS, DECHO AW (2008) Rapid screening of quorum-sensing signal N-acyl homoserine lactones by an in vitro cell-free assay. *Appl Environ Microbiol* 74:3667–3671. doi: 10.1128/AEM.02869-07
- KELLER NP (2019) Fungal secondary metabolism: regulation, function and drug discovery. *Nat Rev Microbiol* 17:167–180. doi: 10.1038/s41579-018-0121-1
- KELLER S (2014) Interaktion der humanpathogenen Mikroorganismen *Aspergillus fumigatus* und *Pseudomonas aeruginosa*. PhD thesis, Friedrich-Schiller-Universität Jena.
- KEOGH RH, SZCZESNIAK R, TAYLOR-ROBINSON D, BILTON D (2018) Up-to-date and projected estimates of survival for people with cystic fibrosis using baseline characteristics: a longitudinal study using UK patient registry data. *J Cyst Fibros* 17:218–227. doi: 10.1016/j.jcf.2017.11.019
- KIM H, LANTVIT D, HWANG CH, et al (2012) Indole alkaloids from two cultured cyanobacteria, *Westiellopsis* sp. and *Fischerella muscicola*. *Bioorganic Med Chem* 20:5290–5295. doi: 10.1016/j.bmc.2012.06.030
- KING J, BRUNEL SF, WARRIS A (2016) *Aspergillus* infections in cystic fibrosis. *J Infect* 72:S50–S55. doi: 10.1016/j.jinf.2016.04.022
- KIRCHNER S, FOTHERGILL JL, WRIGHT EA, et al (2012) Use of artificial sputum medium to test antibiotic efficacy against *Pseudomonas aeruginosa* in conditions more relevant to the cystic fibrosis lung. *J Vis Exp* 1–8. doi: 10.3791/3857
- KNUTSEN AP (2017) Allergic bronchopulmonary aspergillosis in asthma. *Expert Rev Clin Immunol* 13:11–14. doi: 10.1080/1744666X.2017.1232620
- KOBAYASHI M, SHIMIZU S (1994) Versatile nitrilases: nitrile-hydrolysing enzymes. *FEMS Microbiol Lett* 120:217–223. doi: 10.1111/j.1574-6968.1994.tb07036.x
- KOCHAN I (1973) The role of iron in bacterial infections, with special consideration of host-tubercle bacillus interaction. *Curr Top Microbiol Immunol* 60:1–30
- KOLWIJCK E, VAN DE VEERDONK FL (2014) The potential impact of the pulmonary microbiome on immunopathogenesis of *Aspergillus*-related lung disease. *Eur J Immunol* 44:3156–3165. doi: 10.1002/eji.201344404
- KONG FD, HUANG XL, MA QY, et al (2018) Helvolic acid derivatives with antibacterial activities against *Streptococcus agalactiae* from the marine-derived fungus *Aspergillus fumigatus* HNMF0047. *J Nat Prod* 81:1869–1876. doi: 10.1021/acs.jnatprod.8b00382
- KÖNIG CC, SCHERLACH K, SCHROECKH V, et al (2013) Bacterium induces cryptic meroterpenoid pathway in the pathogenic fungus *Aspergillus fumigatus*. *ChemBioChem* 14:938–942. doi: 10.1002/cbic.201300070
- KRAMER J, ÖZKAYA Ö, KÜMMERLI R (2020) Bacterial siderophores in community and host interactions. *Nat Rev Microbiol* 18:152–163. doi: 10.1038/s41579-019-0284-4
- KRONSTAD JW, CAZA M (2013) Shared and distinct mechanisms of iron acquisition by bacterial and fungal pathogens of humans. *Front Cell Infect Microbiol* 4. doi: 10.3389/fcimb.2013.00080

- LAMBIASE A, CATANIA MR, ROSSANO F (2010) Anaerobic bacteria infection in cystic fibrosis airway disease. *New Microbiol.* 33:185–194
- LAMONT IL, KONINGS AF, REID DW (2009) Iron acquisition by *Pseudomonas aeruginosa* in the lungs of patients with cystic fibrosis. *BioMetals* 22:53–60. doi: 10.1007/s10534-008-9197-9
- LANGFELDER K, JAHN B, GEHRINGER H, et al (1998) Identification of a polyketide synthase gene (pksP) of *Aspergillus fumigatus* involved in conidial pigment biosynthesis and virulence. *Med Microbiol Immunol* 187:79–89. doi: 10.1007/s004300050077
- LARSEN TO, SMEDSGAARD J, NIELSEN KF, et al (2007) Production of mycotoxins by *Aspergillus lentulus* and other medically important and closely related species in section Fumigati. *Med Mycol* 45:225–232. doi: 10.1080/13693780601185939
- LATGÉ JP (1999) *Aspergillus fumigatus* and Aspergillosis. *Clin. Microbiol. Rev.* 12:310–350
- LATGÉ JP, CHAMILOS G (2020) *Aspergillus fumigatus* and aspergillosis in 2019. *Clin Microbiol Rev* 33:e00140-18. doi: 10.1128/CMR.00140-18
- LAU GW, HASSETT DJ, RAN H, KONG F (2004) The role of pyocyanin in *Pseudomonas aeruginosa* infection. *Trends Mol Med* 10:599–606. doi: 10.1016/j.molmed.2004.10.002
- LAVILLE J, BLUMER C, VON SCHROETTER C, et al (1998) Characterization of the *hcnABC* gene cluster encoding hydrogen cyanide synthase and anaerobic regulation by ANR in the strictly aerobic biocontrol agent *Pseudomonas fluorescens* CHA0. *J Bacteriol* 180:3187–3196. doi: 10.1128/jb.180.12.3187-3196.1998
- LEE J, ZHANG L (2014) The hierarchy quorum sensing network in *Pseudomonas aeruginosa*. *Protein Cell* 6:26–41. doi: 10.1007/s13238-014-0100-x
- LETHEM MI, JAMES SL, MARRIOTT C, BURKE JF (1990) The origin of DNA associated with mucus glycoproteins in cystic fibrosis sputum. *Eur Respir J* 3(1):19-23.
- LI S, CALVO AM, YUEN GY, et al (2009) Induction of cell wall thickening by the antifungal compound dihydromaltophilin disrupts fungal growth and is mediated by sphingolipid biosynthesis. *J Eukaryot Microbiol* 56:182–187. doi: 10.1111/j.1550-7408.2008.00384.x
- LIEBMANN B, MÜLLER M, BRAUN A, BRAKHAGE AA (2004) The cyclic AMP-dependent protein kinase A network regulates development and virulence in *Aspergillus fumigatus*. *Infect Immun* 72:5193–5203. doi: 10.1128/IAI.72.9.5193-5203.2004
- LIGHTLY TJ, PHUNG RR, SORENSEN JL, CARDONA ST (2017) Synthetic cystic fibrosis sputum medium diminishes *Burkholderia cenocepacia* antifungal activity against *Aspergillus fumigatus* independently of phenylacetic acid production. *Can J Microbiol* 63:427–438. doi: 10.1139/cjm-2016-0705
- LIM FY, WON TH, RAFFA N, et al (2018) Fungal isocyanide synthases and xanthocillin biosynthesis in *Aspergillus fumigatus*. *mBio* 9:e00785-18. doi: 10.1128/mBio.00785-18
- LIND AL, LIM FY, SOUKUP AA, et al (2018) An LaeA- and BrlA-dependent cellular network governs tissue-specific secondary metabolism in the human pathogen *Aspergillus fumigatus*. *mSphere* 3(2)::e00050-18. doi: 10.1128/mSphere.00050-18
- LIPUMA JJ (2010) The changing microbial epidemiology in cystic fibrosis. *Clin Microbiol Rev* 23:299–323. doi: 10.1128/CMR.00068-09

- LIU JC, MODHA DE, GAILLARD EA (2013) What is the clinical significance of filamentous fungi positive sputum cultures in patients with cystic fibrosis? *J Cyst Fibros* 12:187–193. doi: 10.1016/j.jcf.2013.02.003
- LIZEWSKI SE, LUNDBERG DS, SCHURR MJ (2002) The transcriptional regulator AlgR is essential for *Pseudomonas aeruginosa* pathogenesis. *Infect Immun* 70:6083–6093. doi: 10.1128/IAI.70.11.6083-6093.2002
- LIZEWSKI SE, SCHURR JR, JACKSON DW, et al (2004) Identification of AlgR-regulated genes in *Pseudomonas aeruginosa* by use of microarray analysis. *J Bacteriol* 186:5672–5684. doi: 10.1128/JB.186.17.5672-5684.2004
- LOPEZ-MEDINA E, FAN D, COUGHLIN LA, et al (2015) *Candida albicans* inhibits *Pseudomonas aeruginosa* virulence through suppression of pyochelin and pyoverdine biosynthesis. *PLoS Pathog* 11:e1005129–e1005129. doi: 10.1371/journal.ppat.1005129
- LV JM, HU D, GAO H, et al (2017) Biosynthesis of helvolic acid and identification of an unusual C-4-demethylation process distinct from sterol biosynthesis. *Nat Commun* 8:1644. doi: 10.1038/s41467-017-01813-9
- LYCZAK JB, CANNON CL, PIER GB (2002) Lung infections associated with cystic fibrosis. *Clin Microbiol Rev* 15:194–222. doi: 10.1128/CMR.15.2.194-222.2002
- MACHELEIDT J, MATTERN DJ, FISCHER J, et al (2016) Regulation and role of fungal secondary metabolites. *Annu Rev Genet* 50:371–392. doi: 10.1146/annurev-genet-120215-035203
- MANAVATHU EK (2015) Effects of antimicrobial combinations on *Pseudomonas aeruginosa-Aspergillus fumigatus* mixed microbial biofilm. *J Microbiol Exp* 2. doi: 10.15406/jmen.2015.02.00057
- MANAVATHU EK, VAGER DL, VAZQUEZ JA (2014) Development and antimicrobial susceptibility studies of in vitro monomicrobial and polymicrobial biofilm models with *Aspergillus fumigatus* and *Pseudomonas aeruginosa*. *BMC Microbiol* 14. doi: 10.1186/1471-2180-14-53
- MARCHLER-BAUER A, BO Y, HAN L, et al (2017) CDD/SPARCLE: Functional classification of proteins via subfamily domain architectures. *Nucleic Acids Res* 45:D200–D203. doi: 10.1093/nar/gkw1129
- MARTIN LW, REID DW, SHARPLES KJ, LAMONT IL (2011) *Pseudomonas* siderophores in the sputum of patients with cystic fibrosis. *BioMetals* 24:1059–1067. doi: 10.1007/s10534-011-9464-z
- MATHEE K, NARASIMHAN G, VALDES C, et al (2008) Dynamics of *Pseudomonas aeruginosa* genome evolution. *Proc Natl Acad Sci U S A* 105:3100–3105. doi: 10.1073/pnas.0711982105
- MATTHAIYOU EI, SASS G, STEVENS DA, HSU JL (2018) Iron: an essential nutrient for *Aspergillus fumigatus* and a fulcrum for pathogenesis. *Curr Opin Infect Dis* 31:506–511. doi: 10.1097/QCO.0000000000000487
- MATURU VN, AGARWAL R (2015) Prevalence of *Aspergillus* sensitization and allergic bronchopulmonary aspergillosis in cystic fibrosis: systematic review and meta-analysis. *Clin Exp Allergy* 45:1765–1778. doi: 10.1111/cea.12595

- MAVRODI D V., BLANKENFELDT W, THOMASHOW LS (2006) Phenazine compounds in fluorescent *Pseudomonas* spp. biosynthesis and regulation. *Annu Rev Phytopathol* 44:417–445. doi: 10.1146/annurev.phyto.44.013106.145710
- MAVRODI D V., PAULSEN IT, REN Q, LOPER JE (2007) Genomics of *Pseudomonas fluorescens* Pf-5. *Pseudomonas* 5:3–30.
- MEHTA A (2005) CFTR: More than just a chloride channel. *Pediatr Pulmonol* 39:292–298. doi: 10.1002/ppul.20147
- MELLOUL E, LUIGGI S, ANNAÏS L, et al (2016) Characteristics of *Aspergillus fumigatus* in association with *Stenotrophomonas maltophilia* in an in vitro model of mixed biofilm. *PLoS One* 11:e0166325–e0166325. doi: 10.1371/journal.pone.0166325
- MELLOUL E, ROISIN L, DURIEUX MF, et al (2018) Interactions of *Aspergillus fumigatus* and *Stenotrophomonas maltophilia* in an in vitro mixed biofilm model: Does the strain matter? *Front Microbiol* 9:2850. doi: 10.3389/fmicb.2018.02850
- MINANDRI F, IMPERI F, FRANGIPANI E, et al (2016) Role of iron uptake systems in *Pseudomonas aeruginosa* virulence and airway infection. *Infect Immun* 84:2324–2335. doi: 10.1128/IAI.00098-16
- MIRANDA-CASOLUENGO AA, STAUNTON PM, DINAN AM, et al (2016) Functional characterization of the *Mycobacterium abscessus* genome coupled with condition specific transcriptomics reveals conserved molecular strategies for host adaptation and persistence. *BMC Genomics* 17:553. doi: 10.1186/s12864-016-2868-y
- MISSLINGER M, LECHNER BE, BACHER K, HAAS H (2018) Iron-sensing is governed by mitochondrial, not by cytosolic iron-sulfur cluster biogenesis in *Aspergillus fumigatus*. *Metallomics* 10:1687–1700. doi: 10.1039/c8mt00263k
- MOMANY M, LINDSEY R, HILL TW, et al (2004) The *Aspergillus fumigatus* cell wall is organized in domains that are remodelled during polarity establishment. *Microbiology* 150:3261–3268. doi: 10.1099/mic.0.27318-0
- MOMANY M, KANG SE (2013) Sporulation environment drives phenotypic variation in the pathogen *Aspergillus fumigatus*. *J Chem Inf Model* 53:1689–1699
- MONTGOMERY ST, MALL MA, KICIC A, STICK SM (2017) Hypoxia and sterile inflammation in cystic fibrosis airways: mechanisms and potential therapies. *Eur Respir J* 49:1600903. doi: 10.1183/13993003.00903-2016
- MORADALI MF, GHODS S, REHM BHA (2017) *Pseudomonas aeruginosa* lifestyle: a paradigm for adaptation, survival, and persistence. *Front Cell Infect Microbiol* 7:39. doi: 10.3389/fcimb.2017.00039
- MORALES DK, JACOBS NJ, RAJAMANI S, et al (2010) Antifungal mechanisms by which a novel *Pseudomonas aeruginosa* phenazine toxin kills *Candida albicans* in biofilms. *Mol Microbiol* 78:1379–1392. doi: 10.1111/j.1365-2958.2010.07414.x
- MOREE WJ, PHELAN V V., WU CH, et al (2012) Interkingdom metabolic transformations captured by microbial imaging mass spectrometry. *Proc Natl Acad Sci U S A* 109:13811–13816. doi: 10.1073/pnas.1206855109
- MORGAN BG, WARREN P, MEWIS RE, RIVETT DW (2020) Bacterial dominance is due to effective utilisation of secondary metabolites produced by competitors. *Sci Rep* 10:2316. doi: 10.1038/s41598-020-59048-6

- MOWAT E, RAJENDRAN R, WILLIAMS C, et al (2010) *Pseudomonas aeruginosa* and their small diffusible extracellular molecules inhibit *Aspergillus fumigatus* biofilm formation. *FEMS Microbiol Lett* 313:96–102. doi: 10.1111/j.1574-6968.2010.02130.x
- MULLIGAN CN (2005) Environmental applications for biosurfactants. *Environ Pollut* 133:183–198. doi: 10.1016/j.envpol.2004.06.009
- MUND A, DIGGLE SP, HARRISON F (2017) The fitness of *Pseudomonas aeruginosa* quorum sensing signal cheats is influenced by the diffusivity of the environment. *mBio* 8:e00353-17. doi: 10.1128/mBio.00353-17
- MUÑOZ-ELÍAS EJ, MCKINNEY JD (2006) Carbon metabolism of intracellular bacteria. *Cell Microbiol* 8:10–22. doi: 10.1111/j.1462-5822.2005.00648.x
- NATHWANI D, RAMAN G, SULHAM K, et al (2014) Clinical and economic consequences of hospital-acquired resistant and multidrug-resistant *Pseudomonas aeruginosa* infections: a systematic review and meta-analysis. *Antimicrob Resist Infect Control* 3:32. doi: 10.1186/2047-2994-3-32
- NEERINCX AH, MANDON J, VAN INGEN J, et al (2015) Real-time monitoring of hydrogen cyanide (HCN) and ammonia (NH₃) emitted by *Pseudomonas aeruginosa*. *J Breath Res* 9:27102. doi: 10.1088/1752-7155/9/2/027102
- NETZKER T, FLAK M, KRESPACH MK, et al (2018) Microbial interactions trigger the production of antibiotics. *Curr Opin Microbiol* 45:117–123. doi: 10.1016/j.mib.2018.04.002
- NOGUEIRA F, SHARGHI S, KUCHLER K, LION T (2019) Pathogenetic impact of bacterial–fungal interactions. *Microorganisms* 7:459. doi: 10.3390/microorganisms7100459
- NORRANDER J, KEMPE T, MESSING J (1983) Construction of improved M13 vectors using oligodeoxynucleotide-directed mutagenesis. *Gene* 26:101–106. doi: 10.1016/0378-1119(83)90040-9
- NOVOHRADSKÁ S, FERLING I, HILLMANN F (2017) Exploring virulence determinants of filamentous fungal pathogens through interactions with soil amoebae. *Front Cell Infect Microbiol* 7:497. doi: 10.3389/fcimb.2017.00497
- O’SULLIVAN BP, FREEDMAN SD (2009) Cystic fibrosis. *Lancet* 373:1891–1904. doi: 10.1016/S0140-6736(09)60327-5
- OCHSNER UA, JOHNSON Z, VASIL ML (2000) Genetics and regulation of two distinct haem-uptake systems, *phu* and *has*, in *Pseudomonas aeruginosa*. *Microbiology* 146:185–198. doi: 10.1099/00221287-146-1-185
- OKKOTSU Y, LITTLE AS, SCHURR MJ (2014) The *Pseudomonas aeruginosa* AlgZR two-component system coordinates multiple phenotypes. *Front Cell Infect Microbiol* 4:82. doi: 10.3389/fcimb.2014.00082
- OMURA S, TOMODA H, KIM YK, NISHIDA H (1993) Pyripyropenes, highly potent inhibitors of acyl-Coa: cholesterol acyltransferase produced by *Aspergillus fumigatus*. *J Antibiot (Tokyo)* 46:1168–1169. doi: 10.7164/antibiotics.46.1168
- PALMER KL, AYE LM, WHITELEY M (2007) Nutritional cues control *Pseudomonas aeruginosa* multicellular behavior in cystic fibrosis sputum. *J Bacteriol* 189:8079–8087. doi: 10.1128/JB.01138-07

- PALMER KL, MASHBURN LM, SINGH PK, WHITELEY M (2005) Cystic fibrosis sputum supports growth and cues key aspects of *Pseudomonas aeruginosa* physiology. *J Bacteriol* 187:5267–5277. doi: 10.1128/JB.187.15.5267-5277.2005
- PANACCIONE DG, ARNOLD SL (2017) Ergot alkaloids contribute to virulence in an insect model of invasive aspergillosis. *Sci Rep* 7:8930. doi: 10.1038/s41598-017-09107-2
- PESSI G, HAAS D (2000) Transcriptional control of the hydrogen cyanide biosynthetic genes *hcnABC* by the anaerobic regulator ANR and the quorum-sensing regulators LasR and RhIR in *Pseudomonas aeruginosa*. *J Bacteriol* 182:6940–6949. doi: 10.1128/JB.182.24.6940-6949.2000
- PETERS BM, JABRA-RIZK MA, O'MAY GA, et al (2012) Polymicrobial interactions: Impact on pathogenesis and human disease. *Clin Microbiol Rev* 25:193–213. doi: 10.1128/CMR.00013-11
- PETRIK M, FRANSEN GM, HAAS H, et al (2012) Preclinical evaluation of two ⁶⁸Ga-siderophores as potential radiopharmaceuticals for *Aspergillus fumigatus* infection imaging. *Eur J Nucl Med Mol Imaging* 39:1175–1183. doi: 10.1007/s00259-012-2110-3
- PETRIK M, HAAS H, DOBROZEMSKY G, et al (2010) ⁶⁸Ga-siderophores for PET imaging of invasive pulmonary aspergillosis: proof of principle. *J Nucl Med* 51:639–645. doi: 10.2967/jnumed.109.072462
- PETRIK M, HAAS H, LAVERMAN P, et al (2014) ⁶⁸Ga-triacetylfusarinine C and ⁶⁸Ga-ferrioxamine e for *Aspergillus* infection imaging: uptake specificity in various microorganisms. *Mol Imaging Biol* 16:102–108. doi: 10.1007/s11307-013-0654-7
- PIHET M, CARRERE J, CIMON B, et al (2009) Occurrence and relevance of filamentous fungi in respiratory secretions of patients with cystic fibrosis - a review. *Med Mycol* 47:387–397. doi: 10.1080/13693780802609604
- PINHEIRO EAA, CARVALHO JM, DOS SANTOS DCP, et al (2013) Antibacterial activity of alkaloids produced by endophytic fungus *Aspergillus* sp. EJC08 isolated from medical plant *Bauhinia guianensis*. *Nat Prod Res* 27:1633–1638. doi: 10.1080/14786419.2012.750316
- PONTECORVO G, ROPER JA, CHEMMONS LM, et al (1953) The genetics of *Aspergillus nidulans*. *Adv Genet* 5:141–238. doi: 10.1016/S0065-2660(08)60408-3
- POOLE K (2011) *Pseudomonas aeruginosa*: resistance to the max. *Front Microbiol* 2:65. doi: 10.3389/fmicb.2011.00065
- POULTON JE (1990) Cyanogenesis in plants. *Plant Physiol* 94:401–405. doi: 10.1104/pp.94.2.401
- PRIEBE S, LINDE J, ALBRECHT D, et al (2011) FungiFun: A web-based application for functional categorization of fungal genes and proteins. *Fungal Genet Biol* 48:353–358. doi: 10.1016/j.fgb.2010.11.001
- QUINN RA, WHITESON K, LIM YW, et al (2016) Ecological networking of cystic fibrosis lung infections. *Biofilms Microbiomes* 2:4. doi: 10.1038/s41522-016-0002-1
- RAETZ CRH, WHITFIELD C (2002) Lipopolysaccharide endotoxins. *Annu Rev Biochem* 71:635–700. doi: 10.1146/annurev.biochem.71.110601.135414

- RAFEEQ MM, MURAD HAS (2017) Cystic fibrosis: current therapeutic targets and future approaches. *J Transl Med* 15:84. doi: 10.1186/s12967-017-1193-9
- RAFFA N, KELLER NP (2019) A call to arms: mustering secondary metabolites for success and survival of an opportunistic pathogen. *PLoS Pathog* 15:e1007606–e1007606. doi: 10.1371/journal.ppat.1007606
- RATNAWEERA PB, WILLIAMS DE, DE SILVA ED, et al (2014) Helvolic acid, an antibacterial nortriterpenoid from a fungal endophyte, *Xylaria* sp. of orchid *Anoectochilus setaceus* endemic to Sri Lanka. *Mycology* 5:23–28. doi: 10.1080/21501203.2014.892905
- RAYMOND-BOUCHARD I, CARROLL CS, NESBITT JR, et al (2012) Structural requirements for the activity of the MirB ferrisiderophore transporter of *Aspergillus fumigatus*. *Eukaryot Cell* 11:1333–1344. doi: 10.1128/EC.00159-12
- REECE E, RENWICK J, SEGURADO R, et al (2017) Co-colonisation of the cystic fibrosis airways with *A. fumigatus* and *P. aeruginosa* is associated with poorer health: an Irish registry analysis. *J Cyst Fibros* 16:S101. doi: 10.1016/s1569-1993(17)30504-0
- REECE E, DOYLE S, GREALLY P, et al (2018) *Aspergillus fumigatus* inhibits *Pseudomonas aeruginosa* in co-culture: implications of a mutually antagonistic relationship on virulence and inflammation in the CF airway. *Front Microbiol* 9:1205. doi: 10.3389/fmicb.2018.01205
- RHODES JC (2006) *Aspergillus fumigatus*: growth and virulence. *Med Mycol* 44:77–81. doi: 10.1080/13693780600779419
- RIETSCH A, WOLFGANG MC, MEKALANOS JJ (2004) Effect of metabolic imbalance on expression of type III secretion genes in *Pseudomonas aeruginosa*. *Infect Immun* 72:1383–1390. doi: 10.1128/IAI.72.3.1383-1390.2004
- RIETSCH A, VALLET-GELY I, DOVE SL, MEKALANOS JJ (2005) ExsE, a secreted regulator of type III secretion genes in *Pseudomonas aeruginosa*. *Proc Natl Acad Sci U S A* 102:8006–8011. doi: 10.1073/pnas.0503005102
- RISCILI BP, WOOD KL (2009) Noninvasive pulmonary *Aspergillus* infections. *Clin Chest Med* 30:315–335. doi: 10.1016/j.ccm.2009.02.008
- ROGERS GB, HART CA, MASON JR, et al (2003) Bacterial diversity in cases of lung infection in cystic fibrosis patients: 16S ribosomal DNA (rDNA) length heterogeneity PCR and 16S rDNA terminal restriction fragment length polymorphism profiling. *J Clin Microbiol* 41:3548–3558. doi: 10.1128/JCM.41.8.3548-3558.2003
- ROSENTHAL VD, BIJIE H, MAKI DG, et al (2012) International Nosocomial Infection Control Consortium (INICC) report, data summary of 36 countries, for 2004-2009. *Am J Infect Control* 40:396–407. doi: 10.1016/j.ajic.2011.05.020
- ROTHER W (1954) Das neue Antibiotikum Xanthocillin. *Deutsche Medizinische Wochenschrift* 79:1080–1081. doi: 10.1055/s-0028-1119307
- RUBIN BK (2009) Mucus, phlegm, and sputum in cystic fibrosis. *Respir Care* 54:726–732. doi: 10.4187/002013209790983269
- RUEPING M (2007) Complex indole alkaloids from cyanobacteria. *ChemInform* 38:. doi: 10.1002/chin.200743268

- RYALL B, DAVIES JC, WILSON R, et al (2008) *Pseudomonas aeruginosa*, cyanide accumulation and lung function in CF and non-CF bronchiectasis patients. *Eur Respir J* 32:740–747. doi: 10.1183/09031936.00159607
- RYALL B, LEE X, ZLOSNIK JEA, et al (2008) Bacteria of the *Burkholderia cepacia* complex are cyanogenic under biofilm and colonial growth conditions. *BMC Microbiol* 8:108. doi: 10.1186/1471-2180-8-108
- SAMBROOK J, FRITSCH EF, MANIATIS T (1989) Molecular Cloning: A Laboratory Manual, second edition. *Cold Spring Harbor, Cold Spring Harbor Laboratory Press*.
- SANDERS NN, DE SMEDT SC, VAN ROMPAEY E, et al (2000) Cystic fibrosis sputum: a barrier to the transport of nanospheres. *Am J Respir Crit Care Med* 162:1905–1911. doi: 10.1164/ajrccm.162.5.9909009
- SANDERSON K, WESCOMBE L, KIROV SM, et al (2008) Bacterial cyanogenesis occurs in the cystic fibrosis lung. *Eur Respir J* 32:329–333. doi: 10.1183/09031936.00152407
- SANTOS AS, SAMPAIO APW, VASQUEZ GS, et al (2002) Evaluation of different carbon and nitrogen sources in production of rhamnolipids by a strain of *Pseudomonas aeruginosa*. *Appl Biochem Biotechnol - Part A Enzym Eng Biotechnol* 98–100:1025–1035. doi: 10.1385/ABAB:98-100:1-9:1025
- SASS G, ANSARI SR, DIETL AM, et al (2019) Intermicrobial interaction: *Aspergillus fumigatus* siderophores protect against competition by *Pseudomonas aeruginosa*. *PLoS One* 14:e0216085. doi: 10.1371/journal.pone.0216085
- SASS G, NAZIK H, PENNER J, et al (2019) *Aspergillus-Pseudomonas* interaction, relevant to competition in airways. *Med. Mycol.* 57:S228–S232
- SASS G, NAZIK H, PENNER J, et al (2018) Studies of *Pseudomonas aeruginosa* mutants indicate pyoverdine as the central factor in inhibition of *Aspergillus fumigatus* biofilm. *J Bacteriol* 200:e00345-17. doi: 10.1128/JB.00345-17
- SCHALK IJ, GUILLON L (2013) Fate of ferrisiderophores after import across bacterial outer membranes: different iron release strategies are observed in the cytoplasm or periplasm depending on the siderophore pathways. *Amino Acids* 44:1267–1277. doi: 10.1007/s00726-013-1468-2
- SCHARF DH, HEINEKAMP T, REMME N, et al (2012) Biosynthesis and function of gliotoxin in *Aspergillus fumigatus*. *Appl Microbiol Biotechnol* 93:467–472. doi: 10.1007/s00253-011-3689-1
- SCHMEDA-HIRSCHMANN G, HORMAZABAL E, RODRIGUEZ JA, THEODULOZ C (2008) Cycloaspeptide A and pseurotin A from the endophytic fungus *Penicillium janczewskii*. *Zeitschrift fur Naturforsch - Sect C J Biosci* 63:383–388. doi: 10.1515/znc-2008-5-612
- SCHRETTL M, BIGNELL E, KRAGL C, et al (2004) Siderophore biosynthesis but not reductive iron assimilation is essential for *Aspergillus fumigatus* virulence. *J Exp Med* 200:1213–1219. doi: 10.1084/jem.20041242
- SCHRETTL M, BIGNELL E, KRAGL C, et al (2007) Distinct roles for intra- and extracellular siderophores during *Aspergillus fumigatus* infection. *PLoS Pathog* 3:1195–1207. doi: 10.1371/journal.ppat.0030128

- SCHROECKH V, SCHERLACH K, NÜTZMANN HW, et al (2009) Intimate bacterial-fungal interaction triggers biosynthesis of archetypal polyketides in *Aspergillus nidulans*. *Proc Natl Acad Sci U S A* 106:14558–14563. doi: 10.1073/pnas.0901870106
- SEGAL BH (2009) Aspergillosis. *N Engl J Med* 360:1870–1884. doi: 10.1056/NEJMra0808853
- SESTOK AE, LINKOUS RO, SMITH AT (2018) Toward a mechanistic understanding of Feo-mediated ferrous iron uptake. *Metallomics* 10:887–898. doi: 10.1039/c8mt00097b
- SEXTON AC, HOWLETT BJ (2000) Characterisation of a cyanide hydratase gene in the phytopathogenic fungus *Leptosphaeria maculans*. *Mol Gen Genet* 263:463–470. doi: 10.1007/s004380051190
- SHELDON JR, LAAKSO HA, HEINRICHS DE (2016) Iron acquisition strategies of bacterial pathogens. *Virulence Mech. Bact. Pathog.* 43–85
- SHINER EK, TARENTYEV D, BRYAN A, ET AL (2006) *Pseudomonas aeruginosa* autoinducer modulates host cell responses through calcium signalling. *Cell Microbiol* 8:1601–1610. doi: 10.1111/j.1462-5822.2006.00734.x
- SHORT FL, MURDOCH SL, RYAN RP (2014) Polybacterial human disease: the ills of social networking. *Trends Microbiol* 22:508–516. doi: 10.1016/j.tim.2014.05.007
- SHOSEYOV D, BROWNLEE KG, CONWAY SP, KEREM E (2006) *Aspergillus* bronchitis in cystic fibrosis. *Chest* 130:222–226. doi: 10.1378/chest.130.1.222
- SHROUT JD, CHOPP DL, JUST CL, et al (2006) The impact of quorum sensing and swarming motility on *Pseudomonas aeruginosa* biofilm formation is nutritionally conditional. *Mol Microbiol* 62:1264–1277. doi: 10.1111/j.1365-2958.2006.05421.x
- SIBLEY CD, PARKINS MD, RABIN HR, et al (2008) A polymicrobial perspective of pulmonary infections exposes an enigmatic pathogen in cystic fibrosis patients. *Proc Natl Acad Sci U S A* 105:15070–15075. doi: 10.1073/pnas.0804326105
- SIN N, MENG L, WANG MQW, et al (1997) The anti-angiogenic agent fumagillin covalently binds and inhibits the methionine aminopeptidase, MetAP-2. *Proc Natl Acad Sci U S A* 94:6099–6103. doi: 10.1073/pnas.94.12.6099
- SONAWANE A, JYOT J, DURING R, RAMPHAL R (2006) Neutrophil elastase, an innate immunity effector molecule, represses flagellin transcription in *Pseudomonas aeruginosa*. *Infect Immun* 74:6682–6689. doi: 10.1128/IAI.00922-06
- SORET P, VANDENBORGHT LE, FRANCIS F, et al (2020) Respiratory mycobiome and suggestion of inter-kingdom network during acute pulmonary exacerbation in cystic fibrosis. *Sci Rep* 10:3589. doi: 10.1038/s41598-020-60015-4
- SPIKES S, XU R, NGUYEN CK, et al (2008) Gliotoxin production in *Aspergillus fumigatus* contributes to host-specific differences in virulence. *J Infect Dis* 197:479–486. doi: 10.1086/525044
- SRIRAMULU DD, LÜNSDORF H, LAM JS, RÖMLING U (2005) Microcolony formation: a novel biofilm model of *Pseudomonas aeruginosa* for the cystic fibrosis lung. *J Med Microbiol* 54:667–676. doi: 10.1099/jmm.0.45969-0

- STAUDINGER BJ, MULLER JF, HALLDÓRSSON S, et al (2014) Conditions associated with the cystic fibrosis defect promote chronic *Pseudomonas aeruginosa* infection. *Am J Respir Crit Care Med* 189:812–824. doi: 10.1164/rccm.201312-2142OC
- STELMASZYŃSKA T (1985) Formation of HCN by human phagocytosing neutrophils - 1. Chlorination of *Staphylococcus epidermidis* as a source of HCN. *Int J Biochem* 17:373–379. doi: 10.1016/0020-711X(85)90213-7
- STELMASZYŃSKA T (1986) Formation of HCN and its chlorination to ClCN- by stimulated human neutrophils - 2. Oxidation of thiocyanate as a source of HCN. *Int J Biochem* 18:1107–1114. doi: 10.1016/0020-711X(86)90084-4
- STEVENS DA, MOSS RB, et al (2003) Allergic bronchopulmonary aspergillosis in cystic fibrosis—state of the art: cystic fibrosis foundation consensus conference. *Clin Infect Dis* 37:S225–S264. doi: 10.1086/376525
- STICK SM (2014) Early cystic fibrosis lung disease. *Eur Respir Monogr* 64:77–87
- STINTZI A, EVANS K, MEYER JM, POOLE K (1998) Quorum-sensing and siderophore biosynthesis in *Pseudomonas aeruginosa*: lasR/lasI mutants exhibit reduced pyoverdine biosynthesis. *FEMS Microbiol Lett* 166:341–345. doi: 10.1111/j.1574-6968.1998.tb13910.X
- STOCKMAN JA (2013) A CFTR potentiator in patients with cystic fibrosis and the G551D mutation. *Yearb Pediatr* 2013:556–557. doi: 10.1016/j.yped.2011.12.014
- SURETTE MG (2014) The cystic fibrosis lung microbiome. *Ann Am Thorac Soc* 11:S61–S65. doi: 10.1513/AnnalsATS.201306-159MG
- SVAHN KS, GÖRANSSON U, CHRYSANTHOU E, et al (2014) Induction of gliotoxin secretion in *Aspergillus fumigatus* by bacteria-associated molecules. *PLoS One* 9:e93685–e93685. doi: 10.1371/journal.pone.0093685
- TAKASE H, NITANAI H, HOSHINO K, OTANI T (2000) Requirement of the *Pseudomonas aeruginosa tonB* gene for high-affinity iron acquisition and infection. *Infect Immun* 68:4498–4504. doi: 10.1128/IAI.68.8.4498-4504.2000
- TAKESHITA N (2019) Fungal-bacterial mutualistic mechanism; fungal highway and bacterial toll. In: *Asian Mycological Congress, 2019*.
- TALWALKAR JS, MURRAY TS (2016) The approach to *Pseudomonas aeruginosa* in cystic fibrosis. *Clin Chest Med* 37:69–81. doi: 10.1016/j.ccm.2015.10.004
- TAYLOR-COUSAR J, NIKNIAN M, GILMARTIN G, PILEWSKI JM (2016) Effect of ivacaftor in patients with advanced cystic fibrosis and a G551D-CFTR mutation: safety and efficacy in an expanded access program in the United States. *J Cyst Fibros* 15:116–122. doi: 10.1016/j.jcf.2015.01.008
- TRAXLER MF, SEYEDSAYAMDOST MR, CLARDY J, KOLTER R (2012) Interspecies modulation of bacterial development through iron competition and siderophore piracy. *Mol Microbiol* 86:628–644. doi: 10.1111/mmi.12008
- TSENG CF, BURGER A, MISLIN GLA, et al (2006) Bacterial siderophores: The solution stoichiometry and coordination of the Fe(III) complexes of pyochelin and related compounds. *J Biol Inorg Chem* 11:419–432. doi: 10.1007/s00775-006-0088-7

- TSUNAKAWA M, KOBARU S, MURATA S, et al (1993) Bu-4704, a new member of the xanthocillin class. *J Antibiot (Tokyo)* 46:687–688. doi: 10.7164/antibiotics.46.687
- TÜMMLER B, KLOCKGETHER J (2017) Recent advances in understanding *Pseudomonas aeruginosa* as a pathogen. *F1000 Research* 6:1261. doi: 10.12688/f1000research.10506.1
- TURNER KH, WESSEL AK, PALMER GC, et al (2015) Essential genome of *Pseudomonas aeruginosa* in cystic fibrosis sputum. *Proc Natl Acad Sci U S A* 112:4110–4115. doi: 10.1073/pnas.1419677112
- VALENZA G, TAPPE D, TURNWALD D, et al (2008) Prevalence and antimicrobial susceptibility of microorganisms isolated from sputa of patients with cystic fibrosis. *J Cyst Fibros* 7:123–127. doi: 10.1016/j.jcf.2007.06.006
- VALIANTE V, MACHELEIDT J, FÖGE M, BRAKHAGE AA (2015) The *Aspergillus fumigatus* cell wall integrity signalling pathway: drug target, compensatory pathways and virulence. *Front Microbiol* 6:325. doi: 10.3389/fmicb.2015.00325
- VAN GENNIP M, CHRISTENSEN LD, ALHEDE M, et al (2009) Inactivation of the *rhlA* gene in *Pseudomonas aeruginosa* prevents rhamnolipid production, disabling the protection against polymorphonuclear leukocytes. *Apmis* 117:537–546. doi: 10.1111/j.1600-0463.2009.02466.x
- VANKEERBERGHEN A, CUPPENS H, CASSIMAN JJ (2002) The cystic fibrosis transmembrane conductance regulator: an intriguing protein with pleiotropic functions. *J Cyst Fibros* 1:13–29. doi: 10.1016/S1569-1993(01)00003-0
- VELTEN R, STEGLICH W, ANKE H (1995) Darlucins A and B, new isocyanide antibiotics from *Sphaerellopsis filum* (*Darluca filum*). *J Antibiot (Tokyo)* 48:36–41. doi: 10.7164/antibiotics.48.36
- VERKMAN AS, SONG Y, THIAGARAJAH JR (2003) Role of airway surface liquid and submucosal glands in cystic fibrosis lung disease. *Am J Physiol - Cell Physiol* 284:C2–C15. doi: 10.1152/ajpcell.00417.2002
- VISCA P, IMPERI F, LAMONT IL (2007) Pyoverdine siderophores: from biogenesis to biosignificance. *Trends Microbiol* 15:22–30. doi: 10.1016/j.tim.2006.11.004
- VÖDISCH M, SCHERLACH K, WINKLER R, et al (2011) Analysis of the *Aspergillus fumigatus* proteome reveals metabolic changes and the activation of the pseurotin A biosynthesis gene cluster in response to hypoxia. *J Proteome Res* 10:2508–2524. doi: 10.1021/pr1012812
- WAGNER GP, KIN K, LYNCH VJ (2012) Measurement of mRNA abundance using RNA-seq data: RPKM measure is inconsistent among samples. *Theory Biosci* 131:281–285. doi: 10.1007/s12064-012-0162-3
- WAKEFIELD J, HASSAN HM, JASPARS M, et al (2017) Dual induction of new microbial secondary metabolites by fungal bacterial co-cultivation. *Front Microbiol* 8:1284. doi: 10.3389/fmicb.2017.01284
- WANG J, PANTOPOULOS K (2011) Regulation of cellular iron metabolism. *Biochem J* 434:365–381. doi: 10.1042/BJ20101825
- WANG L, ZHU M, ZHANG Q, et al (2017) Diisonitrile natural product SF2768 functions as a chalkophore that mediates copper acquisition in *Streptomyces thioluteus*. *ACS Chem Biol* 12:3067–3075. doi: 10.1021/acscchembio.7b00897

- WANG P, VANETTEN HD (1992) Cloning and properties of a cyanide hydratase gene from the phytopathogenic fungus *Gloeocercospora sorghi*. *Biochem Biophys Res Commun* 187:1048–1054. doi: 10.1016/0006-291X(92)91303-8
- WANG Y, WILKS JC, DANHORN T, et al (2011) Phenazine-1-carboxylic acid promotes bacterial biofilm development via ferrous iron acquisition. *J Bacteriol* 193:3606–3617. doi: 10.1128/JB.00396-11
- WATANABE A, YANO K, IKEBUKURO K, KARUBE I (1998) Cloning and expression of a gene encoding cyanidase from *Pseudomonas stutzeri* AK61. *Appl Microbiol Biotechnol* 50:93–97. doi: 10.1007/s002530051261
- WEI X, HUANG X, TANG L, et al (2013) Global control of GacA in secondary metabolism, primary metabolism, secretion systems, and motility in the rhizobacterium *Pseudomonas aeruginosa* M18. *J Bacteriol* 195:3387–3400. doi: 10.1128/JB.00214-13
- WELSH MA, BLACKWELL HE (2016) chemical genetics reveals environment-specific roles for quorum sensing circuits in *Pseudomonas aeruginosa*. *Cell Chem Biol* 23:361–369. doi: 10.1016/j.chembiol.2016.01.006
- WERNER E, ROE F, BUGNICOURT A, et al (2004) Stratified growth in *Pseudomonas aeruginosa* biofilms. *Appl Environ Microbiol* 70:6188–6196. doi: 10.1128/AEM.70.10.6188-6196.2004
- WESSEL D, FLÜGGE UI (1984) A method for the quantitative recovery of protein in dilute solution in the presence of detergents and lipids. *Anal Biochem* 138:141–143. doi: 10.1016/0003-2697(84)90782-6
- WIEMANN P, GUO CJ, PALMER JM, et al (2013) Prototype of an intertwined secondary metabolite supercluster. *Proc Natl Acad Sci U S A* 110:17065–17070. doi: 10.1073/pnas.1313258110
- WILLSEY GG, ECKSTROM K, LABAUVE AE, et al (2019) *Stenotrophomonas maltophilia* differential gene expression in synthetic cystic fibrosis sputum reveals shared and cystic fibrosis strain-specific responses to the sputum environment. *J Bacteriol* 201:e00074-19. doi: 10.1128/JB.00074-19
- WILSON R, SYKES DA, WATSON D, et al (1988) Measurement of *Pseudomonas aeruginosa* phenazine pigments in sputum and assessment of their contribution to sputum sol toxicity for respiratory epithelium. *Infect Immun* 56:2515–2517. doi: 10.1128/iai.56.9.2515-2517.1988
- WISSING F (1975) Cyanide production from glycine by a homogenate from a *Pseudomonas species*. *J Bacteriol* 121:695–699. doi: 10.1128/jb.121.2.695-699.1975
- WORLITZSCH D, TARRAN R, ULRICH M, et al (2002) Effects of reduced mucus oxygen concentration in airway *Pseudomonas* infections of cystic fibrosis patients. *J Clin Invest* 109:317–325. doi: 10.1172/JCI0213870
- YOUARD ZA, WENNER N, REIMMANN C (2011) Iron acquisition with the natural siderophore enantiomers pyochelin and enantio-pyochelin in *Pseudomonas* species. *BioMetals* 24:513–522. doi: 10.1007/s10534-010-9399-9
- ZHENG H, KELLER N, WANG Y (2015) Establishing a biofilm co-culture of *Pseudomonas* and *Aspergillus* for metabolite extraction. *Bio-Protocol* 5:e1667. doi: 10.21769/bioprotoc.1667

ZHENG H, KIM J, LIEW M, et al (2015) Redox metabolites signal polymicrobial biofilm development via the napa oxidative stress cascade in *Aspergillus*. *Curr Biol* 25:29–37. doi: 10.1016/j.cub.2014.11.018

ZLOSNIK JEA, WILLIAMS HD (2004) Methods for assaying cyanide in bacterial culture supernatant. *Lett Appl Microbiol* 38:360–365. doi: 10.1111/j.1472-765X.2004.01489.x

ZUCK KM, SHIPLEY S, NEWMAN DJ (2011) Induced production of N-formyl alkaloids from *Aspergillus fumigatus* by co-culture with *Streptomyces peucetius*. *J Nat Prod* 74:1653–1657. doi: 10.1021/np200255f

ZULIANELLO L, CANARD C, KÖHLER T, et al (2006) Rhamnolipids are virulence factors that promote early infiltration of primary human airway epithelia by *Pseudomonas aeruginosa*. *Infect Immun* 74:3134–3147. doi: 10.1128/IAI.01772-05

List of Tables

Table 1. Bacterial strains used in this study	16
Table 2. Fungal strains used in this study	16
Table 3. Plasmids used in this study	17
Table 4. PCR primers used in this study	17
Table 5. qRT-PCR primers used in this study	18
Table 6. Media used for cultivation of microorganisms	20
Table 7. Medium supplements used for cultivation of bacteria and fungi	22
Table 8. qRT-PCR reaction mixture	27
Table 9. List of selected genes from the 280 most highly upregulated genes of <i>A. fumigatus</i> CEA17 Δ<i>akuB</i> co-cultured with <i>P. aeruginosa</i>	28
Table 10. List of selected genes from the 280 most highly downregulated genes of <i>A. fumigatus</i> CEA17 Δ<i>akuB</i> co-cultured with <i>P. aeruginosa</i>	42
Table 11. Most highly upregulated proteins in co-culture of <i>A. fumigatus</i> and <i>P. aeruginosa</i> carried out in SCFM2 medium; change expressed as fold change of abundance ratio Af + PsA/Af	63
Table 12. Most highly downregulated proteins in co-culture of <i>A. fumigatus</i> and <i>P. aeruginosa</i> carried out in SCFM2 medium; change expressed as fold change of abundance ratio Af + PsA/Af	64
Table 13. Most highly abundant co-isolated proteins of <i>P. aeruginosa</i> present in supernatant of co-culture of <i>A. fumigatus</i> and <i>P. aeruginosa</i> carried out in SCFM2 medium	66

List of figures

Figure 1. Synthesis of cyanide in <i>P. aeruginosa</i> from glycine by oxidative decarboxylation, via the HcnABC operon	9
Figure 2. Enzymatic degradation of cyanide	11
Figure 3. Currently documented interactions of <i>A. fumigatus</i> and <i>P. aeruginosa</i>	12
Figure 4. Growth of <i>P. aeruginosa</i> and <i>A. fumigatus</i> CEA17 Δ akuB and CF10 on SCFM2 solid medium	35
Figure 5. Phenotypic characteristics of <i>A. fumigatus</i> CEA17 Δ akuB and CF10 grown in liquid SCFM2	36
Figure 6. SCFM2 supports a balanced growth of <i>A. fumigatus</i> and <i>P. aeruginosa</i> alike	36
Figure 7. <i>Pseudomonas aeruginosa</i> passively adheres to the hyphae of <i>Aspergillus fumigatus</i> .	37
Figure 8. Growth of <i>Pseudomonas aeruginosa</i> and <i>Aspergillus fumigatus</i> on SFM2 agar under hypoxic conditions.	37
Figure 9. FungiFun analysis of 277 most upregulated genes of <i>A. fumigatus</i> in co-cultivation with <i>P. aeruginosa</i>	39
Figure 10. FungiFun analysis of 280 most downregulated genes of <i>A. fumigatus</i> in co-cultivation with <i>P. aeruginosa</i>	42
Figure 11. LC-MS-based analysis of secondary metabolites of <i>A. fumigatus</i> in co-culture with <i>P. aeruginosa</i>	45
Figure 12. Fumagillin and pseurotin-producing supercluster on chromosome 8 and its expression pattern in <i>A. fumigatus</i> CEA17 Δ akuB and CF10 in co-culture with <i>P. aeruginosa</i>	46
Figure 13. A novel peak appears in the LC-MS analysis of the organic extract of <i>A. fumigatus</i> CF10 and <i>P. aeruginosa</i> co-culture	48
Figure 14. BU-4704, an isonitrile alkaloid, is the novel compound produced by <i>A. fumigatus</i> CF10	48
Figure 15. A previously unidentified compound, BU-4704B, is produced by <i>A. fumigatus</i> CF10 alongside BU-4704	49
Figure 16. First two steps of the proposed biosynthesis pathway of paerucumarin	50
Figure 17. Conserved domain analysis of the DNA sequence of CF10_04996, a suspected isonitrile synthase	50
Figure 18. Gene composition and expression pattern of the BU-4704-producing biosynthetic gene cluster	51
Figure 19. Generation of <i>A. fumigatus</i> Δ CF10_04996 mutant	51
Figure 20. BU-4704 and BU-4704B are not produced by <i>A. fumigatus</i> CF10 Δ CF10_04996	52
Figure 21. BU-4704 and BU-4704B triggered by <i>P. aeruginosa</i> do not confer a selective advantage in interaction on the producing <i>A. fumigatus</i> CF10 strain	53
Figure 22. Inactive PKS biosynthetic gene cluster in <i>A. fumigatus</i>	53

Figure 23. Layout of the samples used fo MALDI-IMS	55
Figure 24. Rhamnolipids produced by <i>P. aeruginosa</i> alone and in co-culture with <i>A. fumigatus</i>	56
Figure 25. Abundance and distribution of pyoverdine produced by <i>P. aeruginosa</i> in monoculture and co-culture with the fungus	56
Figure 26. MALDI-IMS revealed the production of unknown strain-specific metabolites triggered by the co-culture	57
Figure 27. Quorum sensing of <i>P. aeruginosa</i> in SCFM2-based co-culture with <i>A. fumigatus</i>	58
Figure 28. Growth of <i>P. aeruginosa</i> PAO1 and a siderophore-deficient mutant Δ<i>pvdA</i>Δ<i>pchEF</i> in minimal medium with ferric TAFC as the sole iron source	60
Figure 29. TLC-based analysis of radiochemical purity of ^{68}Ga-TACF	61
Figure 30. Radioactivity measured within <i>P. aeruginosa</i> caused by ^{68}Ga-TACF internalisation	61
Figure 31. Cyanide hydratase of <i>A. fumigatus</i>	68
Figure 32. Expression profile of <i>chtA</i> (AFUB_033190) in response to exogenous HCN in the culture	69
Figure 33. Deletion of <i>chtA</i> (AFUB_033190) in <i>A. fumigatus</i> CEA17 Δ<i>akuB</i>	70
Figure 34. Biomass formation of <i>A. fumigatus</i> grown in presence of 300 μM HCN	70
Figure 35. Cyanide detoxication by <i>A. fumigatus</i>	71
Figure 36. Construction of an acyanogenic Δ<i>hcnB</i> mutant	72
Figure 37. Interaction of <i>P. aeruginosa</i> and <i>A. fumigatus</i> cyanide-producing and -degrading mutants grown on SCFM2 agar.	72
Figure 38. Expression profile of <i>hcnA</i> in <i>P. aeruginosa</i> PAO1 in co-cultivation with <i>A. fumigatus</i> wild type and Δ<i>chtA</i> mutant	73
Figure 39. Analysis of antiproliferative effects exhibited by extracts of <i>P. aeruginosa</i> and <i>A. fumigatus</i> co-cultures carried out in SCFM2	73
Figure 40. Interactions between <i>A. fumigatus</i> and <i>P. aeruginosa</i> described in the present work	87

Abbreviations

AMM	<i>Aspergillus</i> minimal medium
() ^R	resistance
°C	degree Celsius
A	adenine
Af	<i>Aspergillus fumigatus</i>
Amp	ampicillin
BLAST	Basic Local Alignment Search Tool
bp	base pair(s)
C	cytosine
Cb	carbenicillin
cDNA	complementary DNA
CLSM	confocal laser scanning microscopy
DMAT	dimethylallyl tryptophan synthase
DMSO	dimethylsulfoxide
DNA	deoxyribonucleic acid
dNTP	deoxynucleotide
DTPA	diethylenetriaminepentaacetic acid
EIC	extracted ion chromatogram
et al.	<i>et alii</i> (lat. 'and others')
G	guanine
Gm	gentamicin
HRESI-MS	high resolution electrospray ionisation mass spectrometry
IAA	iodoacetamide
IMS	imaging mass spectrometry
ISE	ion-selective electrode
LB	lysogeny broth
LC	liquid chromatography
LC-MS	liquid chromatography-mass spectrometry
MALDI	matrix-assisted laser desorption ionisation
MeCN	acetonitrile
MOPS	3-(<i>N</i> -morpholino)propanesulphonic acid
MS	mass spectrometry
NRPS	non-ribosomal peptide synthetase

NSLB	no-salt lysogeny broth
PCR	polymerase chain reaction
PKS	polyketide synthase
PsA	<i>Pseudomonas aeruginosa</i>
Pt	pyrithiamine
qRT-PCR	quantitative real-time PCR
RNA	ribonucleic acid
rpm	revolutions per minute
RT	retention time
SCFM2	synthetic cystic fibrosis sputum medium
SPE	solid phase extraction
T	thymine
TAFC	N'N''N'''-triacetylfusarinine
TCEP	tris(2-carboxyethyl)phosphine
TEAB	triethylammonium bicarbonate
TFA	trifluoroacetic acid
TFE	trifluoroethanol
TIC	total ion chromatogram
TOF	time-of-flight
TPM	transcripts per million
v/v	volume per volume
VBMM	Vogel-Bonner minimal medium
w/v	weight per volume
Δ	deletion

Curriculum vitae

Personal data

Name

Michal Flak

**Date and place of
birth**

11th May 1991, Martin, Slovakia

Scientific publications

Netzker T, Schroeckh V, Gregory MA, **Flak M**, Krespach MK, Leadley P, Brakhage AA (2016) An efficient method to generate gene deletion mutants of the rapamycin-producing bacterium *Streptomyces iranensis* HM 35. *Applied and Environmental Microbiology* 8(12):3481-3492.

Netzker T, **Flak M**, Krespach MK, Stroe MC, Weber J, Schroeckh V, Brakhage AA (2018) Microbial interactions trigger the production of antibiotics. *Current Opinion in Microbiology* 45, 117-123 (review).

Flak M, Krespach MK, Pschibul AJ, Schroeckh V, Brakhage AA (2020) New avenues towards drug discovery in fungi. In: Benz P (ed.) *The Mycota: Genetics and Biotechnology, vol. II*. Springer (review; accepted).

Krespach MK, García-Altare Pérez M, **Flak M**, Schoeler H, Scherlach K, Netzker T, Schmalzl A, Mattern DJ, Schroeckh V, Komor A, Mittag M, Hertweck C, Brakhage A. (2020) Lichen-like association of *Chlamydomonas reinhardtii* and *Aspergillus nidulans* protects algal cells from bacteria, in revision.

Flak M, Krüger T, Brakhage AA (2020) A functional cyanide hydratase of *Aspergillus fumigatus* could be implicated in an interkingdom interaction with *Pseudomonas aeruginosa*, in preparation.

Acknowledgements

First and foremost, I would like to extend my gratitude to Prof. Dr. Axel A. Brakhage for offering the doctoral position in his lab, and accompanying and guiding me throughout the process. Although things did not always look optimistic with individual projects, I am profoundly thankful to Prof. Brakhage for providing advice and support when they were needed, as well as challenging me to try ever harder, reach for further insights, and proffering his expert opinion and space for valuable discussion. I am also grateful for his forthcoming attitude and prompt, concise feedback when putting together my dissertation.

Secondly, I would like to thank Dr. Volker Schroeckh for fruitful discussions and guidance in many instances along my doctoral journey. I could always count on Volker to provide a viewpoint that was different from mine and put things in a different perspective.

Thirdly, I would like to thank all the past and present members of the Natural Products and Microbial Communication work group for the safe environment we have created for ourselves, where ideas could be shared and mutual support was guaranteed. In particular, Dr. Maria Stroe has shared the journey with me from the get-go, always been supportive and helpful, and has become a close friend along the way. Dr. Tina Netzker and Dr. Juliane Fischer helped me get acquainted with the field of microbial communication, and often also the unfathomable depths of German bureaucracy.

I owe a large debt of gratitude to Carmen Schult and Christina Täumer who always took care of the day-to-day running of the labs I worked at, and were invaluable in helping me with the practical work, as well as with improving my German language skills. Out of the lab, Daniela Wagner was always most helpful when the seemingly unceasing administrative questions and requests ensued.

I would also like to thank several (former) scientists from the HKI, including Dr. Pierre Stallforth, Dr. Maria García-Altare Pérez, and Dr. Kirstin Scherlach, for their help, advice, open attitude, and fruitful discussions. These conversations were often instrumental to my progress. I also appreciate the help that Andrea Perner and Dr. Hans-Martin Dahse provided with analysing my samples, frequently without much prior notice.

Moreover, I would like to thank my colleagues and friends from the HKI, who made my stay at the institute as enjoyable as it was. I'll keep fond memories of the laughs, lunches, coffee breaks, and little celebrations that meant a lot. Many of you have helped me become who I am today.

Last but not least, I owe a massive thank you to my (bio)logical family and who have always been there for me, and who don't understand the science, yet have an uncanny sense about what's going on at work. I couldn't have done half of it without my mum, dad, sis, and R., as well as many others who are not named here.

Ehrenwörtliche Erklärung

Die geltende Promotionsordnung der Fakultät für Biowissenschaften der Friedrich-Schiller-Universität Jena ist mir bekannt. Die vorliegende Dissertation habe ich selbständig verfasst und dabei weder Textabschnitte aus einer eigenen Prüfungsarbeit oder von dritten ohne Kennzeichnung übernommen. Es wurden keine anderen als die von mir angegebenen Quellen, persönliche Mitteilungen und Hilfsmittel verwendet. Ich versichere, dass die aufgelisteten Publikationen und Manuskripte, ausschließlich auf Ergebnissen beruhen, die während meiner Promotion generiert wurden.

Bei der Auswahl und Auswertung des Materials, wie auch bei der Herstellung der Manuskripte haben mich die in der Danksagung meiner Dissertation genannten Personen unterstützt. Personen, die bei der Anfertigung der Publikationen und Manuskripte beteiligt waren, sowie deren Eigenanteil sind gekennzeichnet. Die Hilfe eines kommerziellen Promotionsberaters wurde nicht in Anspruch genommen. Auch haben Dritte weder unmittelbar noch mittelbar geldwerte Leistungen, die im Zusammenhang mit dem Inhalt der vorliegenden Dissertation stehen, erhalten.

Ich habe die Dissertation noch nicht als Prüfungsarbeit für eine staatliche oder andere wissenschaftliche Prüfung eingereicht. Ferner habe ich nicht versucht, diese Arbeit oder eine in wesentlichen Teilen ähnliche oder eine andere Abhandlung bei einer anderen Hochschule als Dissertation einzureichen.

Jena, den 23.06.2020

Michal Flak